Ph.D. Thesis

The role of mitochondria in reactive nitrogen species production and in restoring energy levels of oxidatively injured cells

Eszter Pankotai

Semmelweis University, PhD School for Medical Sciences
Institute of Human Physiology and Clinical Experimental Research
Budapest, Hungary
2010

Supervisor: Zsombor Lacza, MD, PhD

Committee members:

László Virág M.D., Ph.D., D.Sc.

Zsolt Radák M. Sc., Ph.D., D. Sc

Violetta Kékesi M.D., Ph.D.

Reviewers: Eszter Farkas PhD

István Szokodi MD, PhD

CONTENTS

LIST OF ABBREVATIONS

3-NPA	3-nitropropionic acid
AhpC	Peroxiredoxin alkyl hydroperoxide reductase
AIF	Apoptosis inducing factor
AMI	Acut myocardial infarctus
ATP	Adenosine triphosphate
BM	Bone marrow
BOOST	Bone Marrow Transfer to Enhance ST-Elevation Infarct Regeneration
CAT	Catalase
CM	Cardiomyocytes
CPH	1-hydroxy-3-carboxypyrrolidine
CPz	3-carboxy-proxyl radical
CuSOD	Copper superoxide dismutase
DAF	Diaminofluorescein
DCPIP	2,6-dichlorophenolindophenol
DLDH	Dihydrolipoamide dehydrogenase
EDTA	Ethylene diamine tetraacetic acid
EGTA	Ethylene glycol tetraacetic acid
eNOS	Endothelial nitric oxide synthase
EPC	Endothelial progenitor cells
EPR	Electron paramagnetic resonance
ESC	Embryonic stem cells
EtBr	Ethidium bromide
FAD	Flavin adenine dinucleotid
FCCP	Carbonyl cyanide 4 (trifluoromethoxy) phenylhydrazone
FeTPPS	5,10,15,20-tetrakis (4-sulfonatophenyl) porphyrinato iron (III) chloride

FP15	Tetrakis 2- triethylene glycol monomethyl ether (pyridil porphyrin (2-T(PEG3)- PyP)
G-CSF	Granulocyte colony stimulating factor
GFP	Green fluorescent protein
GSH	Glutathione
GSNO	S-nitroso-glutathione
GSSG	Glutathione disulfide
GTN	Glyceryl trinitrate
H_2O_2	Hydrogen peroxide
HEK	Human embryonic kidney cells
HEPES	2-[4-(2-hydroxyethyl)piperazin-1]-ethanesulfonic acid
hMSC	Human mesenchymal stem cell
HNE	4-hydroxy-2-nonenal
IgG-HRP	Immunoglobulin-G conjugated horseradish peroxidase
IMS	Intermembrane space
iNOS	Inducible nitric oxide synthase
K_2HPO_4	Potassium hydrogen phosphate
K_{ATP}	ATP-dependent K^+ channels
KCl	Potassium chloride
KCN	Potassium cyanide
KGDH	Ketoglutarate dehydrogenase
L-NA	N-nitro-L-arginine
L-NAME	L-nitroarginine-methyl-esther
L-NMMA	L-N-methylarginine
LVEF	Left ventricular ejection fraction
MAGIC	Myoblast Autologous Grafting in Ischemic Cardiomyopathy
MDA	Malondialdehyde
MDCK	Madin-Darby canine kidney cells
$MgCl_2$	Magnesium chloride
MICA	5-methoxyindole-2-carboxylic acid
MnSOD	Manganase superoxide dismutase
MPT	Mitochondrial permeability transition

MSCs	Mesenchymal stem cells
mtALDH	Mitochondrial aldehyde-dehydrogenase
mtNOS	Mitochondrial nitric oxide synthase
NAD^+	Nicotinamid adenine dinucleotide
NADP	Nicotinamid adenine dinucleotide phosphate
$NaHPO_4$	Sodium phosphate
NFκB	Nuclear factor of kappa light polypeptide gene enhancer in B-cells
nNOS	Neuronal nitric oxide synthase
NO	Nitric oxide
NOS	Nitric oxide synthase
OGD	Oxygen and glucose deprivation
PARP	Poly (ADP-ribose) polymerase
PAR	Poly (ADP-ribose)
PARylated	Poly (ADP-ribosyl)ated
PARylation	Poly (ADP-ribosyl)ation
PC12	Pheochromocytoma cell
PCI	Percutaneous coronary intervention
PDH	Pyruvate dehydrogenase
PSD	Post source decay
RFP	Red fluorescent protein
RNS	Reactive nitrogen species
ROS	Reactive oxygen species
RSH	Thiols
RSNO	S-nitrosothiols
SCF-1	Stem cell factor 1
SDS-PAGE	Sodium dodecyl sulphate polyacrilamide gel electrophoresis
SMC	Smooth muscle cell
SNAP	S-nitroso-N-acetylpenicillamine
SNP	Sodium nitroprusside
SOD	Superoxide dismutase
TBS	TRIS buffered saline

THD	NADH transhydrogenase
TNF-alpha	Tumor necrosis factor alpha
TNT	Tunneling nanotubes
TOPCARE-AMI	Transplantation of Progenitor Cells and Regeneration Enhancement in Acute Myocardial Infarction
TPx	Thioredoxin peroxidase
TR	Thioredoxin reductase
TRx^{ox}	Oxidized thioredoxin
TRx^{red}	Reduced thioredoxin

1. INTRODUCTION

1.1. Cell Therapies

Cardiovascular diseases are the leading cause of hospitalization and death in the industrialized world. Despite significant advances in the last decades, current therapeutic methods are not sufficient to decrease the incidence and prevalence of heart failure. The critical loss of cardiomyocytes following myocardial infarction can only be partially complemented by natural regeneration of cardiomyocytes in adult hearts (1), thus, new approaches such as cell-transplantation therapies are the target of cardiac research. Several studies reported improved regional and global cardiac function following cell transplantation after myocardial injury (2), (3), (4). Despite the wide range of literature available on the beneficial effects of cardiac cell transplantation after myocardial injury, little is known about the mechanism underlying the regeneration process. Some studies showed separation and isolation of the graft from the host by scar tissue, others reported the release of growth factors that support the regeneration of the host tissue and also some reports mention direct cell – to – cell interactions that may help active contraction of the graft (5).

1.1.1. Diseases treated with cell therapies

Cell therapy is the application of new, healthy cells to damaged tissues in order to regenerate the injured cells, and to treat different diseases. There are a wide range of diseases where cell therapies were introduced including Parkinson's disease, Huntington's disease, Alzheimer's disease, , stroke, spinal cord injury, brain tumor, muscular dystrophy (6), (7). Several clinical trials have been already completed for treating osteoporosis, hematological malignancies and acute myocardial infarction according to the U.S. National Institute of Health database (http://www.clinicaltrials.gov).

Latest observations point to the stem cell reservoir of the heart that helps tissue regeneration; however, this pool of self stem cells is not enough to protect against the irreversible injuries during myocardial infarction (8). Cell therapies of the heart are aimed to assist these regenerative processes to reduce infarct size and to improve cardiac function. Several studies proved the usefulness of different cell therapies in myocardial infarction, cardiovascular diseases and ischemic heart disease (9), (10), (11), (12). Human clinical studies using bone marrow derived stem cells or circulating progenitor cells after acute myocardial infarction are detailed in Chapter 1.1.7.

1.1.2. Cell types used

Many different cell types; for example skeletal myoblasts, smooth muscle cells, bone marrow stem cells, embryonic stem cells are used in animal studies. Several studies reported improved regional and global cardiac function following cell transplantation after myocardial injury. However, attention turned toward using fetal, neonatal or adult cardiomyocytes in cellular cardiomyoplasty. Roell et al showed that embryonic ventricular cardiomyocyte transplantation improved heart function and increased survival after cryoinjury of the left ventricular wall in mice (13). A study by Li et al also reported improved heart function upon the transplantation of fetal cardiomyocytes after cardiac injury (14). The use of fetal cardiomyocytes is limited in clinical utilization because they are subject to rejection and the use of human fetal cardiomyocytes faces ethical problems. Autologous adult heart cells could be ideal source for transplantation, as they are available from biopsy samples and their number can be upscaled in vitro in cell cultures. Sakai et al harvested and cultured cells from rat left atrial appendages and injected them to a transmural scar in the left ventricular free wall of adult rats. The transplantation of autologous adult heart cells limited scar thinning and dilation and improved myocardial function (15).

All of the used cell types have their advantages and disadvantages (Table 1.). Skeletal myoblasts are autologous and easily cultured, but they are not able to transdifferentiate into cardiomyocytes and they may cause arrhythmias. Bone marrow stem cells are easily accessible, but they may form other tissue types, and there is not enough evidence on their transdifferentiation. Primary cardiomyocytes have

morphological representation and preserve cardiac function but they are not able to proliferate and self-renew, and they have a short life in cell culture (16). In spite of the controversies, there are already preclinical and clinical studies using cell transplantation that report modest improvements in cardiac function (17), (18). Above all, there is no agreement on the type of the most suitable cell, on the dose of cells implanted and on the optimal timing of cell transplantation.

Donor cells	Advantages	Limitations
Embryonic stem cells	Undoubted pluripotency, unlimited proliferation	Immunosuppression is required, ethical debate, lack of availability, tumor potential
Fetal cardiomyocytes	Definitive cardiac structures and functions	Immunosuppression is required, ethical debate, lack of availability, short-term survival
Endothelial progenitor cells	Lack of immunogenicity, autologous transplantation, definitive angiogenic capacity, possible cardiomyogenic capacity	Need for expansion
Mesenchymal stem cells	Lack of immunogenicity, autologous transplantation	Need for expansion and aspiration from bone marrow
Hematopoietic stem cells	Lack of immunogenicity, autologous transplantation	Potential to transdifferentiate into cardiac myocytes is doubted
Bone marrow – or peripherial blood-derived mononuclear cells	Lack of immunogenicity, autologous transplantation, abundant of a number of progenitor cells	Aspiration from bone marrow is required
Skeletal myoblasts	Lack of immunogenicity, autologous transplantation, fatigue-resistant, slow twitch-fibers	Arrhytmogenic effects and lack of gap junction with host cardiac cells
Resident cardiac stem cells	Undoubted cardiomyogenic differentiation and lack of immunogenicity	Lack of availability
Umbilical cord blood- or vein-derived stem cells	Similar phenotype to bone marrow-derived MSCs, abundant of many kinds of progenitor cells	Immunosuppression is required, ethical debate, lack of availability

Table 1. Advantages and limitations of donor cells in cellular cardiomyoplasty. Many different cell types are autologous and easy to access, but they are either not able or may not transdifferentiate into cardiomyocytes. Other cells that would be ideal source for cell transplantation therapies are not easily accessible or their use face ethical problems (19).

1.1.3. Modes of cell delivery

Currently used implementation strategies aim to deliver the ideal concentration of cells needed for the regeneration of the affected myocardial area with the lowest risk to patients. Cells can be delivered through coronary arteries, coronary veins, or peripheral veins. Direct intramyocardial injection can be performed using a surgical, transendocardial, or transvenous approach. Mobilization of stem cells from the bone marrow using cytokine therapy is also a delivery strategy, with or without peripheral harvesting. Main delivery strategies are introduced below (20).

1.1.3.1. Cell mobilization, selection, enrichment

In myocardial ischemia stem cells emerge from the bone marrow and travel trough the blood system to reach the injured myocardium. This endogen repair process can be influenced by the pharmacological mobilization of the cells. Different cytokines and growth factors are used to beneficially improve the regeneration process, including granulocyte colony stimulating factor (G-CSF). Cytokines can be combined with stem cell factor (SCF-1) to avoid side effects. SCF-1 is expressed on the surface of marrow stromal cell, fibroblasts, endothel cells; and they are essential for the survival, proliferation, migration and differentiation of stem cells (21). This method was used in the Myoblast Autologous Grafting in Ischaemic Cardiomyopathy (MAGIC) clinical study, when G-CSF was administered before coronary intervention, but resulted in restenosis in a high percentage of the cases. Later studies eliminated this side effect by using sirolimus and paclitaxel releasing stents (22).

1.1.3.2. Intravascular cell delivery

The easiest and most convenient but least effective method is the peripheral intravenous infusion of the cells. Most of the cells are filtered by the lungs, liver or

spleen. In this case less than 1% of the cells reach the target location. Cells reaching the circulation can also cause microembolization and the impairment of the affected tissue (23). Peripherally infused stem cells home to infarcted areas only when injected within a few days of AMI, thus this delivery strategy is less useful for treating chronic myocardial ischemia.

A different cell delivery strategy is the infusion of cells through the coronary venous system. In this model an angioplasty balloon is placed into the selected cardiac vein and inflated to stop blood flow in the coronary venous system. Cells are delivered to the affected area through the lumen of the balloon catheter under high pressure. Although this method is suitable for the delivery of large amount of cells, accessing certain myocardial veins can be difficult or impossible, because of the variability of the coronary venous system (24).

The intracoronary infusion of the cells involves the "over-the-wire" positioning of an angioplasty balloon in one of the coronary arteries. When coronary blood flow is stopped, cells are infused under pressure, which enhances the contact between the cells and the microcirculation of the affected artery. Intracoronary infusion is a popular mode of delivery in the clinics, mostly used 4-9 days after AMI; however, strong evidence regarding safety and efficacy is still missing (20).

1.1.3.3. Intramyocardial injection

Intramyocardial injection is another way of application of cells straight to the myocardium transepicardially, transendocardially or through coronary vein (25). This delivery method is mainly performed in chronic myocardial ischemia and in clinical settings that results in weaker homing signals, such as chronic congestive heart failure (26), (27). During intramyocardial injection cells are applied to the myocardium through a hollow needle under pressure. This method is the most suitable for delivering large cells that could plug capillaries, such as skeletal myoblasts and mesenchymal stem cells.

1.1.4. Modes of action

Despite the wide range of literature available on the beneficial effects of cardiac cell transplantation after myocardial injury, little is known about the mechanism underlying the regeneration process. Although several studies reported improved cardiac function after different types of cell transplantation, it is not clear how these grafts can incorporate into the cardiac tissue, how they can contract in synchron with the host tissue, how many grafted cells survive on the long run after transplantation. Some studies showed separation and isolation of the graft from the host by scar tissue, for example van Laake et al. found that human embryonic stem cell-derived cardiomyocytes (hESC-CM) are embedded in collagens, laminin and fibronectin when cultured in vitro and also continue secreting collagens and fibronectin when transplanted into the mouse heart (28). They also showed that the co-transplantation of hESC-CM with endothelial cells improve the engraftment of the cells. Others studies reported the beneficial effects of the release of growth factors that support the regeneration of the host tissue and also some reports mention direct cell – to – cell interactions that may help active contraction of the graft (5). Paracrine factors, transdifferentiation, cell fusion and direct cell – to – cell interactions together play an important role in the regeneration processes, but still there are controversial opinions about them, and still their therapeutic effects have not been clearly defined (Figure 1.).

1.1.4.1. Transdifferentiation, cell fusion

Several animal and preliminary human studies of stem cell therapy after AMI show overall improvement of cardiac function. This improvement first was thought to result from the transdifferentiaton of the grafted cells or fusion of the grafted cells with the host cells. Several studies reported that bone marrow (BM)-derived stem cells are able to home in the heart and transdifferentiate into cardiomyocytes (29), (30). Resident cardiac stem cells and mesenchymal stem cells (MSCs) were shown to regenerate cardiac tissue by functionally integrating into the myocardium (31), (32), (33), (34). However, the question of functional engraftment of the stem cells still remains, and the low number of newly generated cardiomyocytes, either by transdifferentiation or cell fusion, seems to be too low to explain the significant cardiac improvement. Thus, a new

hypothesis arose: transplanted stem cells release soluble factors that, acting in a paracrine fashion, contribute to cardiac repair and regeneration.

1.1.4.2. Paracrine effects

Growing evidence supports the hypothesis that paracrine mechanisms mediated by factors released by stem cells play an essential role in the reparative process observed after stem cell mobilization or injection into infarcted hearts. Stem cells produce and secrete cytokines, chemokines, and growth factors that may potentially be involved in cardiac repair; and hypoxic stress increases the production of several of these factors (35), (36). Singla et al noted that although 80-90% of transplanted embryonic stem cells (ESCs) die, there is still an improvement of cardiac function. In search for the mechanisms behind this regeneration process they showed that H_2O_2 induced apoptosis of H9c2 cells can be prevented by the addition of cell culture media from ESCs (37). ESCs released anti-apoptotic factors into the cell culture media, and this media was sufficient to defend H9c2 cells from H_2O_2 induced apoptosis.

1.1.4.3. Direct cell – to – cell interactions

On the contrary, there are several studies that emphasize the role of direct cell – to – cell interactions in the regeneration process. Cells can communicate via different mechanisms, such as synapses, gap junctions and also through long distance membrane connections. The presence of these membrane bridges between cells has been observed in many different cell types, including bone marrow derived mesenchymal stem cells, macrophages, dendritic cells, Jurkat T cells. Koyanagi et al showed the formation of nanotubes between endothelial progenitor cells and cardiomyocytes (38). Various research groups reported that direct cell – to – cell contact between graft and host cells is required for bone marrow stromal cells and mesenchymal stem cells to express cardiogenic phenotype (39), (40), (41). Wang et al isolated MSCs from rat bone marrow, amplified them in vitro and cultured them with rat cardiomyocytes in direct co-

culture – when cells were grown together –, or in indirect co-culture – when cells were separated by an insert in the culture dish – or in conditioned culture – when MSCs were fed for one week with the media collected from the direct co-culture. One week later they performed immunofluorescence staining against alpha-actin, desmin and cardiac troponin T. Immunofluorescence staining was positive against alpha-actin, desmin and cardiac troponin T only in the direct co-culture, but not in the indirect co-culture, nor in the conditioned culture group. They concluded that direct cell-to-cell contact between MSCs and adult cardiomyocytes, but not the soluble signaling molecules are obligatory in the differentiation of MSCs into cardiomyocytes or smooth muscle cells (SMCs) (42). Not only was the existence of these nanotubes proved but also the flow of mitochondria in them. Mesenchymal stem cells and cardiomyocytes also develop nanotubes and MSCs can donate mitochondria to cardiomyocytes restoring their energetic state (43), (44). Driesen et al also showed partial cell fusion between cardiomyocytes and fibroblasts. The phenomenon of this intercellular communication presumes short cell – to – cell interactions, during which neighboring cells exchange membrane- and organelle particles, such as mitochondria or other cytoplasmic components (45).

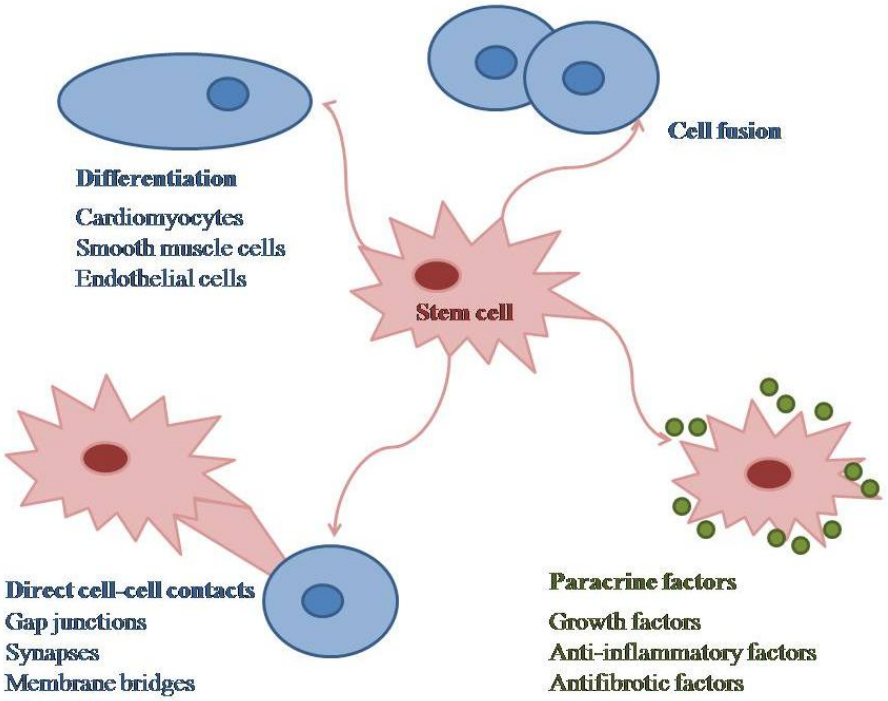

Figure 1. Possible concepts for the mechanism underlying the regeneration process. Transplanted cells can differentiate into; or fuse with host cells. They can also release paracrine factors, which may help the regeneration process of the surrounding host tissue; or establish direct cell-to-cell contacts through membrane bridges that can play a role in restoring energy levels of the neighboring host cells.

1.1.5. Role of mitochondria in cell therapies

Mitochondria are essential organelles in plant and animal cells and play a key role in processes such as oxidative phosphorylation, aerobic metabolism of glucose and fat, calcium signaling, and apoptosis (46), (47). Current theory indicates that mitochondria were obtained 1.5 billion years ago from an ancient prokaryote. The mitochondria provided the capacity for aerobic respiration, the creation of the eukaryotic cell, and eventually complex multicellular organisms. Recent reports have found that mitochondria play essential roles in aging and determining lifespan. A variety of heritable and acquired diseases are linked to mitochondrial dysfunction. Jeffrey L. Spees et al reported in 2005 that mitochondria are more dynamic than previously considered: mitochondria or mtDNA can move between cells (48). The active transfer from adult stem cells and somatic cells can rescue aerobic respiration in mammalian cells with nonfunctional mitochondria. They used cells that were pretreated with ethidium bromide so that the mtDNA became mutated and depleted and the cells became incapable of aerobic respiration and growth (A549 ρ° cells), except in a permissive medium containing uridine and pyruvate to supplement anaerobic glycolysis (49), (50). The A549 ρ° cells were co-cultured with either adult nonhematopoietic stem/progenitor cells from human bone marrow (hMSCs) or with skin fibroblasts. The co-cultures produced clones of rescued A549 ρ° cells with functional mitochondria. In the same year Koyanagi et al showed the formation of nanotubes between endothelial progenitor cells and cardiomyocytes (38). They investigated the formation of intercellular connections, which may allow the transport of macromolecular structures between labeled adult human endothelial progenitor cells (EPCs) and green fluorescent protein (GFP) - expressing neonatal rat cardiomyocytes (CM) in a co-culture system. To determine whether the nanotubular structures allowed the transport of organelles, they labeled CM with a mitochondrial live tracker (MitoTracker). Using time lapse video

microscopy, they observed the transport of stained complexes between CM and EPC resulting in the uptake of MitoTracker-positive structures in EPC. Mesenchymal stem cells and cardiomyocytes also develop nanotubes and MSCs can donate mitochondria to cardiomyocytes restoring their energetic state (44). Light and fluorescence microscopy as well as scanning electron microscopy revealed that after co-cultivation, cells formed intercellular contacts and transient exchange of cytosolic elements could be observed. The transport of cytosolic entity had no specific direction. Noticeably, mitochondria were also transferred to the recipient cells in a unidirectional fashion (towards cardiomyocytes only). Transmission electron microscopy revealed significant variability in both the diameter of intercellular contacting tubes and their shape. Inside of these nanotubes mitochondria-resembling structures were identified.

1.1.6. Tunneling membrane bridges

Cell-to-cell communication is a crucial prerequisite for the development and maintenance of multicellular organisms. Animal cells evolved diverse mechanisms of intercellular exchange of signaling molecules. This includes the secretion and receptor – mediated binding of diffusible messengers like hormones and growth factors, the transport of small molecules trough gap junctions (51), (52), (53) as well as the release of membrane carriers such as exosomes (54). In 2004 a new route of cell-to-cell communication was discovered between rat pheochromocytoma (PC12) cells (55). These structures called tunneling nanotubes (TNT) form *de novo* between PC12 cells and have a diameter of 50-200 nm and a length of up to several cell diameters. TNTs stretch between interconnected cells attached at their nearest distance and they do not connect to the substrate and hover in the medium. These structures are fragile when exposed to light, shearing force or chemical fixation. TNTs facilitate the intercellular transfer of vesicles of endocytic origin as well as of membrane components and cytoplasmic components. Based on the morphological criteria defined for PC12 cells, similar TNT-like connections were subsequently identified for several permanent cell lines and primary cultures (Table 2.), (56), (57).

Cell type	Cytoskeletal components	Cargo
PC12 cells	F-actin, myosin Va	Endosome-related organelles, lipid-anchored proteins
Between neonatal rat cardiomyocytes and adult human endothelial progenitors	ND	Mitochondria, soluble proteins (GFP)
Primary rat astrocytes	F-actin, myosin Va	ND
Human monocyte-derived macrophages	F-actin, microtubules	Mitochondria, endosome-related organelles, lysosomes
Jurkat T cells	F-actin	HIV-1 protein Gag

Table 2. TNT-like structures in vitro. TNT formation occurs between many different cell types. These membrane bridges contain cytoskeletal components and are able to transfer various proteins; and also organelles such as mitochondria between the connected cells. ND: not defined (57).

An advantage of establishing direct bridges between cells is an improvement in selective communication even over long distances. In agreement with this assumption, the common feature of all TNT-like structures is the transfer of cargo between connected cells (Figure 2.). Direct evidence for the intercellular exchange of cargo via TNT-like structures was obtained by video-microscopic studies. By employing fluorescent dyes, organelles belonging to the endosomal/lysosomal system (55), (Gurke, S., Gerdes, H.-H., unpublished data) as well as mitochondria (38) were shown to traffic uni-directionally along TNT-like structures between cells over long distances. The transferred endocytic vesicles are able to fuse with their counterparts in the target cells (55), and provide signaling information from the single cell to a larger community. In addition to the transfer of organelles, plasma membrane components such as lipid-anchored proteins can laterally transfer along the TNT-like bridge into the plasma membrane of connected cells (Figure 2.).

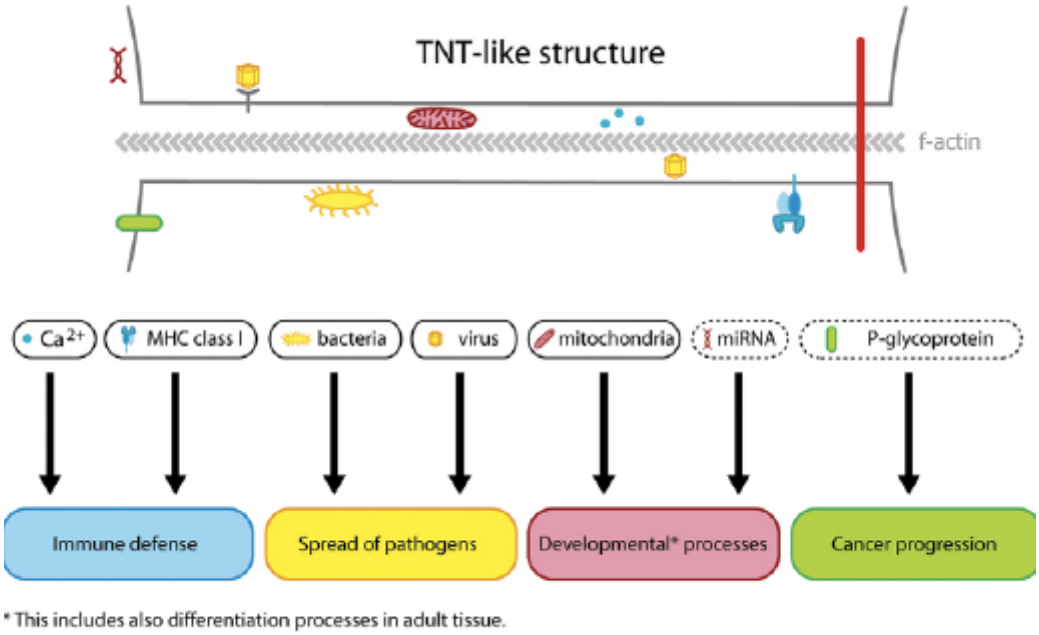

Figure 2. Schematic representation of cargo transported along a TNT-like structure and proposed physiological implications. The travel of mitochondria, Ca^{2+} flux and viruses have been identified in TNTs (shown in boxes with continuous lines). P-glycoprotein and miRNA have been proposed to travel along these membrane bridges (shown in boxes with broken lines) (58).

1.1.7. Clinical Studies

TOPCARE-AMI stands for Transplantation of Progenitor Cells and Regeneration Enhancement in Acute Myocardial Infarction. The study was carried out in patients with reperfused acute myocardial infarction (AMI) to receive intracoronary infusion of either bone marrow–derived cells (BMCs) or circulating blood–derived progenitor cells into the infarct artery 4.3±1.5 days after AMI (59). At 4 months follow up coronary blood flow reserve was significantly increased in the infarct artery and they observed a significant increase in myocardial viability in the infarct zone (60). The improvement in left ventricular ejection fraction (LVEF) was also maintained after 12 months follow-up. The same group investigated the clinical outcome after 2 years and they found that the administration of cells is associated with a significant reduction of the occurrence of major adverse cardiovascular events and that functional improvements after BMC therapy persist for at least 2 years (61).

In the MAGIC (Myoblast Autologous Grafting in Ischemic Cardiomyopathy) study the effect of the intracoronary infusion of circulating peripheral stem cells obtained by Granulocyte stimulating factor (G-CSF) mobilization was analyzed. Patients with myocardial infarction and percutaneous coronary intervention (PCI) were divided into three groups. Control group, cell therapy group, and a group that only received G-CSF treatment without cell infusion. Patients received peripherial blood-derived stem cells right after PCI through an 'over-the-wire' balloon catheter. 6 months later only the group with cell therapy treatment had significantly increased ejection fraction. Regarding the high occurrence of restenosis in the G-CSF treated group the study was terminated (62).

In the BOOST (Bone Marrow Transfer to Enhance ST-Elevation Infarct Regeneration) study after PCI for acute ST-segment elevation myocardial infarction patients either received optimum postinfarction medical treatment, or received autologous bone-marrow cells 4.8 (SD 1.3) days after PCI through an 'over-the-wire' balloon catheter. 6 months later the LVEF was significantly increased in the bone marrow treated group, however, there was no significant improvement in LVEF after 18 months, thus the long life of the grafted cells is still questionable (63).

In a Hungarian study patients received CD34+ stem cells 9-12 days after PCI. CD34 positivity is a widely used marker of hematopoietic stem cells, but also a feature of capillary endothel cells and bone marrow stromal cells. 6 months later LVEF was significantly increased, left ventricular wall thickness decreased, perfusion was improved in the cell treated group compared to the control. The improvement of these parameters started after 3 months. The therapy proved to be safe after the 6 months follow up, no restenosis was observed (64).

In a meta analyses Dimmeler et al. analyzed 18 studies with nearly a thousand patients who received either bone marrow derived stem cells or circulating peripheral stem cells after myocardial infarction. Cell transplantation increased the ventricular ejection fraction with 3.66% and decreased the size of the scar tissue with 5.49% compared to the control group. They also observed that patients with severe infarct benefit better from cell therapy and that it is not useful to apply cells immediately, but between 4-14 days after the infarction (65). The outcome of these clinical studies varies between wide ranges because of the different cell transplantation techniques, different

transplanted cell types, different timing of transplantation, different follow up times, and because of the differences in data analysis methods (Table 3.). TOPCARE-AMI recorded 6-9 % increase of LVEF in the cell transplanted group that is maintained after 12 months. Another study by Thiele et al. showed the positive effects of cell transplantation even after 15 months follow up (66). On the contrary; the beneficial effects of cell transplantation at 6 months in the BOOST study were diminished after 18 months. Scientists agree on the urgent need for a comprehensive, standardized clinical study with a large number of patients and long term follow up.

Study	Cell type	Days after 1st surgery	Follow up (months)
TOPCARE-AMI	Circulating blood-derived progenitor cells	4.3 (SD1.5)	4-12
MAGIC	Circulating peripheral stem cells	Same day	6
BOOST	Autologous bone marrow cells	4.8 (SD 1.3)	6-18
HUNGARIAN	Bone marrow-derived CD34+ stem cells	9-12	6

Table 3. Clinical studies use various cell types at different time points after first surgery. The outcome of these studies varies on a wide scale because of the differences between the applied cell types and timing of transplantation.

1.2. Cell signaling in oxidative and nitrosative stress

Reactive oxygen species (ROS) and reactive nitrogen species (RNS) formation increases in oxidative injury. Nitric oxide (NO) is involved in several signaling pathways related to a diverse array of cell functions. In the myocardium, NO is produced by the enzyme nitric oxide synthase (NOS), which is present in three isoforms: neuronal NOS (nNOS), inducible NOS (iNOS), and endothelial NOS (eNOS) (67). Several studies raised the possibility that a distinct mitochondrial NO synthase enzyme (mtNOS) exists, although this theory was challenged recently and skepticism regarding its existence, origin, as well as functional role has remained (68), (69), (70).

Excess production of reactive oxygen species (ROS) results in the overactivation of the nuclear enzyme poly (ADP-ribose) polymerase (PARP), which leads to

mitochondrial dysfunction and cell death (71). PARP, residing in the nucleus, builds up poly (ADP-ribose) polymers on different proteins, such as histones, and on PARP itself, regulating enzyme activity. Some studies described (ADP-ribosyl)ation of proteins in mitochondria either via an enzymatic pathway or via the non-enzymatic transfer of nicotinamid adenine dinucleotide (NAD^+) - glycohydrolase liberated ADP-ribose onto acceptor proteins (72), (73). In spite of the presence of different (ADP-ribosyl) transferases and free ADP-ribose moieties in mitochondria, very limited information is available on the acceptor proteins, as well as on the nature of the enzymes catalyzing intra-mitochondrial poly (ADP-ribosyl)ation (PARylation) reactions. Furthermore, the contribution of oxidative and nitrosative stress to mitochondrial poly (ADP-ribose) (PAR) formation is not yet understood. Du et al showed PARP-1 activity in mitochondria of primary cortical neurons and fibroblasts (74). Nevertheless, the existence of a genuine PARP enzyme in the mitochondrial matrix is still subject to debate (75).

1.2.1. Oxidative and nitrosative stress

1.2.1.1. Reactive oxygen species in mitochondria

Mitochondria are the major site of ROS production and also the target of free radicals in the cells. The mitochondrial respiratory chain produces superoxide and H_2O_2 at Complex I and Complex III, which can be enhanced by inhibition of the respiratory chain owing to a lack of oxygen (Figure 3.). H_2O_2 then reacts with iron to form hydroxyl radicals (76). The main targets of ROS in mitochondria are the protein component of the membranes, especially the respiratory chain proteins containing Fe-S centers (77) and the polyunsaturated fatty acids (78). Oxidants increase the release of calcium from mitochondria, thus stimulating calcium-dependent enzymes such as proteases, nucleases and phospholipases. The absence of mitochondrial DNA-protecting proteins, the low efficiency reparation mechanisms and the proximity of the respiration chain, makes mtDNA a privileged target for ROS (79). H_2O_2 causes the disruption of mitochondrial membrane potential and the release of cytochrome-c (80), and cause upregulation of Fas/FasL system and modulation of transcription factors such as NFκB

resulting in altered gene expression (81). Furthermore, H_2O_2 suppresses both the activation and activity of caspases, possibly through modulation of the redox status of the cell and the oxidation of cystein-residues (82). In the presence of transition metals such as copper and iron, H_2O_2 is converted to a highly reactive species, hydroxyl radical (83).

Cells developed a complex antioxidant defense system to fight oxidative damage, that include enzymatic activities (superoxide dismutase (SOD), catalase, glutathione peroxidase) and free radical scavengers (glutathione, thioredoxine, vitamin C and E), (84). However, free radical production overwhelms endogenous protective mechanisms after oxidative injury. Cytoplasmic copper superoxide dismutase (CuSOD) and mitochondrial manganese superoxide dismutase (MnSOD) catalyze the dismutation of superoxide to H_2O_2, which then converted to water and oxygen by catalase and glutathione (GSH) peroxidase.

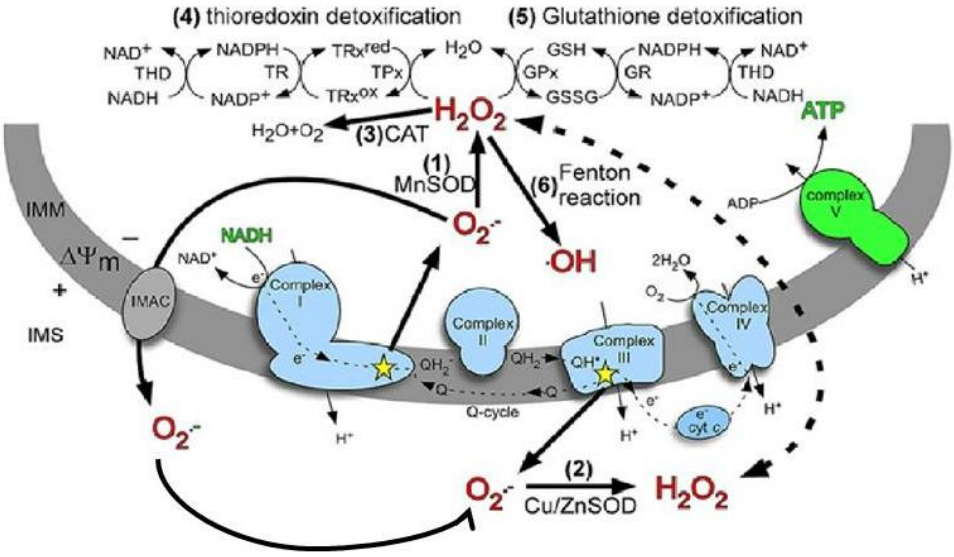

Figure 3. ROS production and antioxidant defense in mitochondria. Superoxide ($O_2^{\cdot-}$) generated at complex I and at complex III can spontaneously dismute to H_2O_2 or is enzymatically dismuted by MnSOD (*1*) or Cu/ZnSOD (*2*) in the intermembrane space (IMS) or cytosol. H_2O_2 can be detoxified by catalase (CAT) (*3*), or by the thioredoxin/thioredoxin peroxidase system (*4*), or by the glutathione/glutathione peroxidase system (*5*) in the matrix. H_2O_2 can also react with metal ions to generate the highly reactive hydroxyl radical ($^{\cdot}OH$) via Fenton chemistry (*6*). THD: NADH transhydrogenase; TR: thioredoxin reductase; TPx: thioredoxin peroxidase; TRx^{red}: reduced thioredoxin; TRx^{ox}: oxidized thioredoxin; GSH: glutathione; GSSG: glutathione disulfide, GPx: glutathione peroxidase (85).

1.2.1.2. Reactive nitrogen species in mitochondria

NO and its derivatives $ONOO^-$, and nitrogen dioxide inhibit mitochondrial respiration by distinct mechanisms. Low amounts of NO reversibly inhibit cytochrome oxidase, by binding to either of the two metals of the oxygen-binding site of the enzyme. Both forms of inhibition are rapid and reversible (86), (87). When high concentrations of NO are present, RNS – such as ONOO-, NO_2, N_2O_3 and S-nitrosothiols – are formed. These RNS then cause slow, non-selective but irreversible inhibition of other respiratory chain enzymes, in fact $ONOO^-$ itself is able to inhibit all of the respiratory chain complexes (88). Figure 4 shows the interactions of NO, RNS, ROS and the mitochondrial respiratory chain complexes.

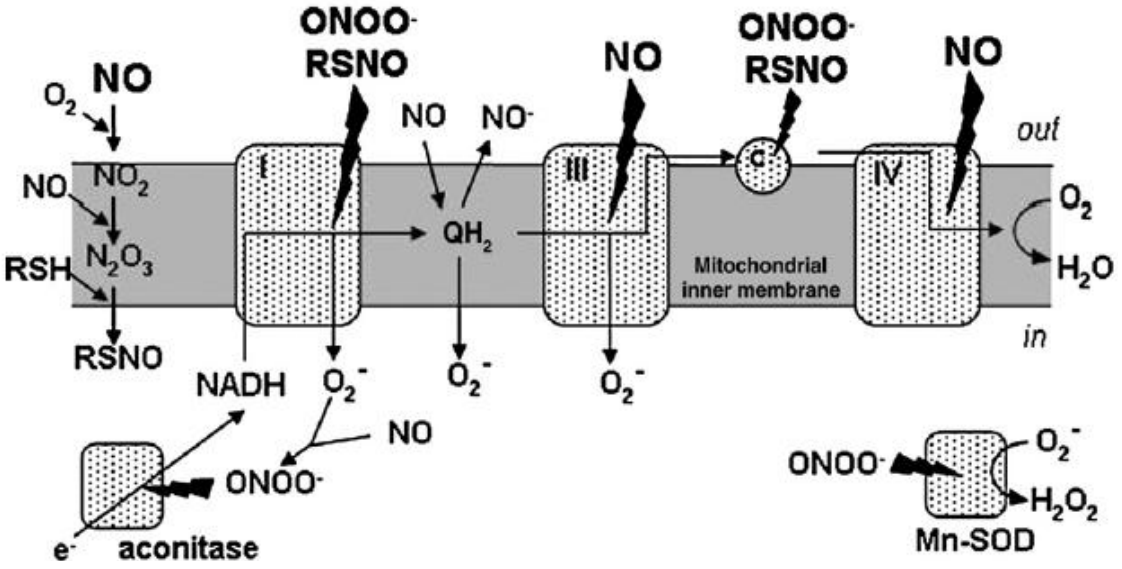

Figure 4. Formation of RNS and ROS on the mitochondrial respiratory chain. NO reacts with oxygen producing NO_2 and N_2O_3, which then reacts with thiols (RSH) to form S-nitrosothiols (RSNO). NO specifically and reversibly inhibits Complex IV, while RNS inactivates Complex I by S-nitrosation, and aconitase of the Krebs-cycle and Complex II, due to removal of iron from the iron-sulfur centers of the enzymes. Peroxynitrite itself can inhibit Complex I-V, aconitase and Mn-SOD and also cytochrome c, which undergoes S-nitrosation (89).

NO and RNS can also influence mitochondrial energy production by inhibiting aconitase, creatine kinase and SOD, stimulating further ROS production. $ONOO^-$ and S-nitrosothiols can cause mitochondrial membrane permeabilisation, increased proton leak

through the membrane, finally leading to the opening of the mitochondrial permeability transition (MPT) pore (90), (91). Opening of the MPT pore either can lead to mitochondrial depolarization, decreased ATP synthesis and necrosis, or to the release of cytochrom-c, activation of caspases and apoptosis.

1.2.1.3. Nitric oxide synthase in mitochondria

New discoveries in the last decade significantly altered our view on mitochondria. They are no longer viewed as energy-making slaves but rather individual cells-within-the-cell. In particular, it has been suggested that many important cellular mechanisms involving specific enzymes and ion channels, such as nitric oxide synthase (NOS), ATP-dependent K^+ (K_{ATP}) channels, and poly (ADP-ribose) polymerase (PARP); have a distinct, mitochondrial variant. The possibility that mitochondria are significant sources of nitric oxide via a unique mitochondrial NOS variant has attracted intense interest among research groups. Extra-mitochondrial sources of NO include the three recognized isoforms of NOS, including inducible (iNOS), endothelial NOS (eNOS), and neuronal NOS (nNOS). These enzymes convert L-arginine to NO and L-citrulline. NO can diffuse into mitochondria from the surrounding cellular space but can also be produced in mitochondria by other pathways not involving metabolism of L-arginine by NOS. In particular, the possible existence and chemical structure of a distinct NOS variant in the mitochondrion (mtNOS) are subjects of intense debate.

The known NOS isoforms are encoded in the nuclear genes and mitochondrial DNA does not contain any of the conventional NOS genes. However, nuclear NOS genes do not possess the necessary transport sequences to pass through the inner mitochondrial membrane. Various studies found eNOS-like and iNOS-like immunoreactivity in mitochondria preparations, and also functional activity of mtNOS with electron microscopy by detecting NADPH diaphorase activity in mitochondria (92), (93), (94), (95), (96), (97), (98), (99). Several studies detected NOS positive protein bands in mitochondria preparations using various anti-NOS antibodies (70); however, it is also possible that one or more of the cellular NOS proteins are attached to the outer surface of the mitochondria and they represent NOS protein bands in mitochondrial preparations (100), (101), (102). Another fact against the existence of an

mtNOS enzyme is that the mitochondrial matrix contains several abundant L-arginine-consuming enzymes, which can effectively compete with the hypothetical mtNOS for its substrate. L-arginine is converted to ornithine and citrulline by urea cycle enzymes, and these metabolites are then converted back to arginine in the cytosol. An alternative fate for L-arginine may involve its conversion to NO and L-citrulline by mtNOS (Figure 5.). However, the kinetics of these two pathways favors the urea cycle even under conditions optimized for NOS activity and in the presence of arginase inhibitors. Mitochondria also contain arginine-decarboxylase, which converts arginine to agmatine (103). Agmatine is a known NOS inhibitor, making the mitochondrial matrix an even less favorable environment for a hypothetical mtNOS (104), (105). In search for the putative mtNOS in a recent study Venkatakrishnan et al. analyzed pure mitochondria fractions with nano-HPLC-coupled linear ion trap-mass spectrometry. They found that rat liver mitochondria and submitochondrial particles do not contain any peptide from any NOS isoforms; and calmodulin, which is required for NOS activity was also absent in mitochondria (106).

Using extensive positive and negative controls we were able to exclude all known conventional mammalian NOS proteins as candidates for the proposed mtNOS, concomitant with the findings of three independent laboratories that provide strong evidence that NOS activity in mitochondria is either nonexistent or falls below the threshold needed to induce physiological responses (107), (108), (109).

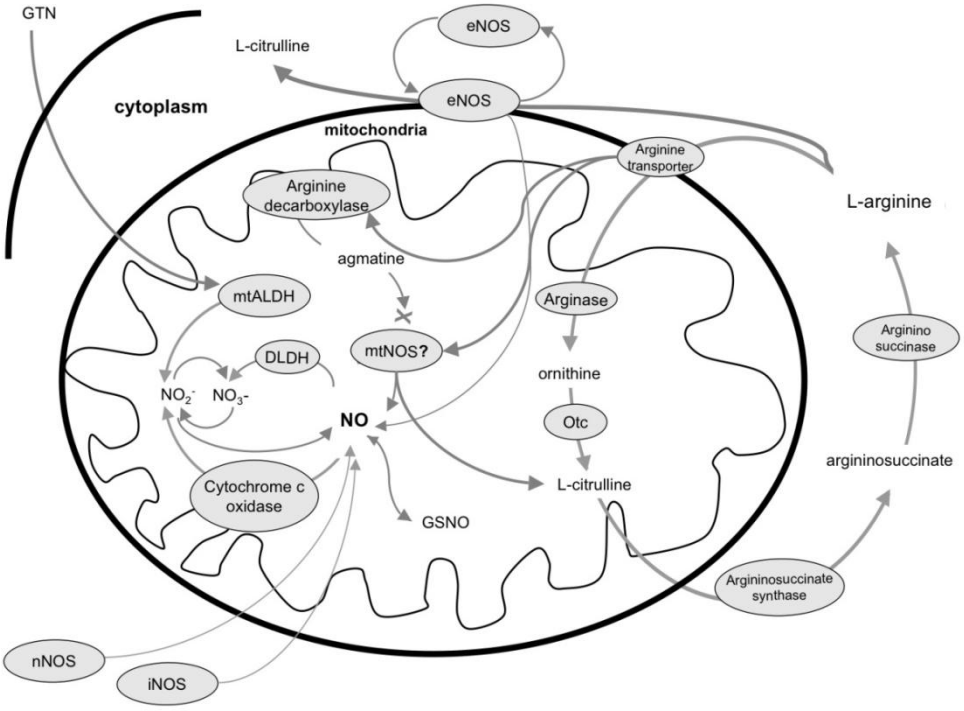

Figure 5. NO sources and NO metabolism in mitochondria. NO, produced by the conventional NOS isoforms can easily diffuse to mitochondria from the cytoplasm, but NO can also originate from the respiratory chain enzymes. Mitochondrial aldehyde-dehydrogenase (mtALDH) is also able to denitrate glyceryl trinitrate (GTN) – used in the treatment of acute myocardial infarction or angina – to form NO. Cytochrome c oxidase forms NO_2^- from NO, while the dihydrolipoamide dehydrogenase (DLDH) converts it to NO_3^- (105).

1.2.2. Poly (ADP-ribose) polymerase

1.2.2.1. The poly (ADP-ribose) polymerase enzyme

PARP-1 is a highly conserved 116 kDa nuclear enzyme. It is the first identified member of the superfamily of PARP enzymes. Poly (ADP-ribosyl)ation is a post-translational modification, affecting several proteins in the nucleus. PARP-1 is responsible for the majority of PARylation in the nucleus. PARP-1 consists of three main domains: the N-terminal DNA-binding domain containing two zinc fingers, the automodification domain, and the C-terminal catalytic domain. The primary structure of the enzyme is highly conserved in eukaryotes. PARP-1 primarily functions as a DNA damage sensor in the nucleus. PARP-1 binds mainly to single stranded DNA breaks,

which can develop as a response to free radical and oxidant cell injury. Active PARP-1 forms homodimers and catalyzes the cleavage of NAD^+ into nicotinamid and ADP-ribose. The size of the branched polymer varies from a few to 200 ADP-ribose units. Because of its high negative charge, the covalently attached ADP-ribose polymer dramatically affects the function of target proteins. In vivo, the most abundantly poly (ADP-ribosyl)ated protein is PARP-1 itself, and auto-poly (ADP-ribosyl)ation represents a major regulatory mechanism for PARP-1 resulting in the down-regulation of the enzyme. Histones are also major acceptors of poly (ADP-ribose) (110). Poly (ADP-ribosyl)ation confers negative charge to histones, leading to electrostatic repulsion between DNA and histones. This process has been implicated in chromatin remodeling, DNA repair, and transcriptional regulation. Poly (ADP-ribosyl)ation is a dynamic process, indicated by the short (<1 min) in vivo half-life of the polymer (111). Two enzymes – poly (ADP-ribose) glycohydrolase (PARG) and ADP-ribosyl protein lyase – are involved in the catabolism of poly (ADP)-ribose (112). Overactivation of PARP-1 uses the NAD^+ and ATP resources of the cell that leads to cell dysfunction, slowing the rate of glycolysis and mitochondrial respiration and finally leads to cell death. The regulation of PARP-1 activity is established through different mechanisms. The best characterized mechanism is the down-regulation of enzyme activity through auto-poly (ADP-ribosyl)ation (113). Furthermore, nicotinamid, the smaller cleavage product of NAD^+, also exerts inhibitory effect on PARP-1, allowing negative feedback regulation. The biological role of PARP-1 is complex and involves DNA repair and maintenance of genomic integrity, regulation of the expression of various proteins at the transcriptional level, regulation of replication and differentiation. Poly (ADP-ribose) polymer can serve as an emergency source of energy used by the base excision machinery to synthetize ATP (114) and may also serve as a signal for protein degradation in oxidatively injured cells (115).

1.2.2.2. The role of PARP in cell death

During apoptosis, caspase-7 and caspase-3 cleave PARP-1 into two fragments separating the DNA binding domain from the catalytic domain, resulting in the inactivation of the enzyme (116). Depletion of PARP-1 by antisense RNA expression or

genetic ablation of PARP-1 gene in PARP-$1^{-/-}$ fibroblasts blocked poly (ADP-ribosyl)ation and also inhibited Fas-induced apoptosis (117). These data indicate that PARP-1-mediated poly (ADP-ribosyl)ation of nuclear proteins is required for apoptosis. A further evidence for the involvement of PARylation in cell death is provided by the observation that PARP is required for the translocation of the apoptosis inducing factor (AIF) protein from mitochondria to the nucleus with the consequent activation of a caspase independent apoptotic pathway (75). Molecular mechanisms triggering the release of AIF are still unclear, but the existence of an intramitochondrial PARP could explain its direct effect on AIF (118). However, a series of experiments with PARP -/- cell lines showed that wild type and knock-out cells are sensitive to apoptosis inducing agents to the same extent. ATP and NAD^+ are important determinants of the mode of cell death, especially in oxidatively injured cells (119). In case PARP is in a caspase-uncleavable form in fibroblasts, tumor necrosis factor - alpha (TNF-α) treatment leads to NAD^+ depletion and necrosis (120). It was hypothesized that PARP as a NAD^+-catabolizing enzyme may serve as a molecular switch between apoptosis and necrosis. Szabó et al used thymocytes from PARP-$1^{+/+}$ and PARP-$1^{-/-}$ mice and compared their responses to peroxynitrite and hydrogen peroxide (DNA-damaging stimuli) as well as dexamethasone and anti-Fas treatment (non-DNA-damaging agents). While nongenotoxic stimuli triggered equal apoptotic responses in wild-type and PARP-1-deficient thymocytes, marked differences could be observed with DNA-damaging oxidative agents. They observed apoptotic cell death in both PARP-$1^{+/+}$ and PARP-$1^{-/-}$ cells when treated with low concentrations of peroxynitrite and hydrogen peroxide and 3-aminobenzamide had no effect on the responses. At higher concentrations of the oxidants cells underwent necrotic cell death that could be prevented by 3-aminobenzamide, indicating that PARP activation was responsible for the apoptosis-to-necrosis switch in severely damaged cells. Other groups also reported protection from cell death by PARP inhibitors; and also the dual role of PARP in apoptotic and necrotic cell death (121), (122), (123). Moroni et al. also showed the role of PARP as a cell death switch in an oxygen-glucose deprivation model in cerebral ischemia (124). Besides NAD^+ depletion and mitochondrial dysfunction, PARP activation also causes cell acidification that can be related to necrotic cell death. Upon oxidative stress or upon treatment with DNA-damaging agents cells can undergo different ways of cell death

depending on the intensity of stimulus. In case of severe DNA damage caspases inactivate PARP-1 and cells die in an apoptotic way. Extensive DNA breakage that is usually triggered by a massive degree of oxidative or nitrosative stress (hydroxyl radical, peroxynitrite, nitroxyl anion) leads to the overactivation of PARP that uses the NAD^+ and ATP stores leaving cells to undergo necrosis.

1.2.2.3. PARP in myocardial oxidative injury

Oxidative and nitrosative stress triggers the activation of PARP in cardiovascular diseases, such as myocardial infarction, ischemia-reperfusion and heart failure (125), (126). The extent of tissue and cell damage in the heart depends mainly on the duration of ischemia (127). Under oxidative conditions cells fail to maintain normal ATP levels, cell membrane permeability is increased, and the K^+, Ca^{2+}, Na^+ ion flux is altered. Increased intracellular Ca^{2+} levels activate proteases, influences mitochondrial respiration causing increased ROS production (128). These reactive oxygen species are the superoxide anion radical ($O_2^{-\cdot}$), the hydroxyl radical ($OH^{\cdot}$), hydrogen peroxide (H_2O_2), and peroxynitrite ($ONOO^-$) formed from superoxide and NO. Free radicals cause DNA-damage that activates PARP. PARP overactivation leads to rapid decline in cellular NAD^+ and ATP levels leading cells to an energy crisis that results in cellular dysfunction, and finally cell death either by apoptosis or necrosis, depending on the amount of available ATP (Figure 6.). In reperfusion neutrophils accumulate and H_2O_2 is converted to $OH^{\cdot}$ spontaneously or converted to hypochlorous acid by myeloperoxidase. Under hypoxia ATP is degraded to AMP and hypoxanthine, which is converted to uric acid and $O_2^{-\cdot}$ by xanthine oxidase, when oxygen supplies are restored during reperfusion. ROS produced during both ischemia and reperfusion then can react with proteins, membrane lipids, and DNA resulting in a misbalance between ROS-producing and ROS-eliminating reactions.

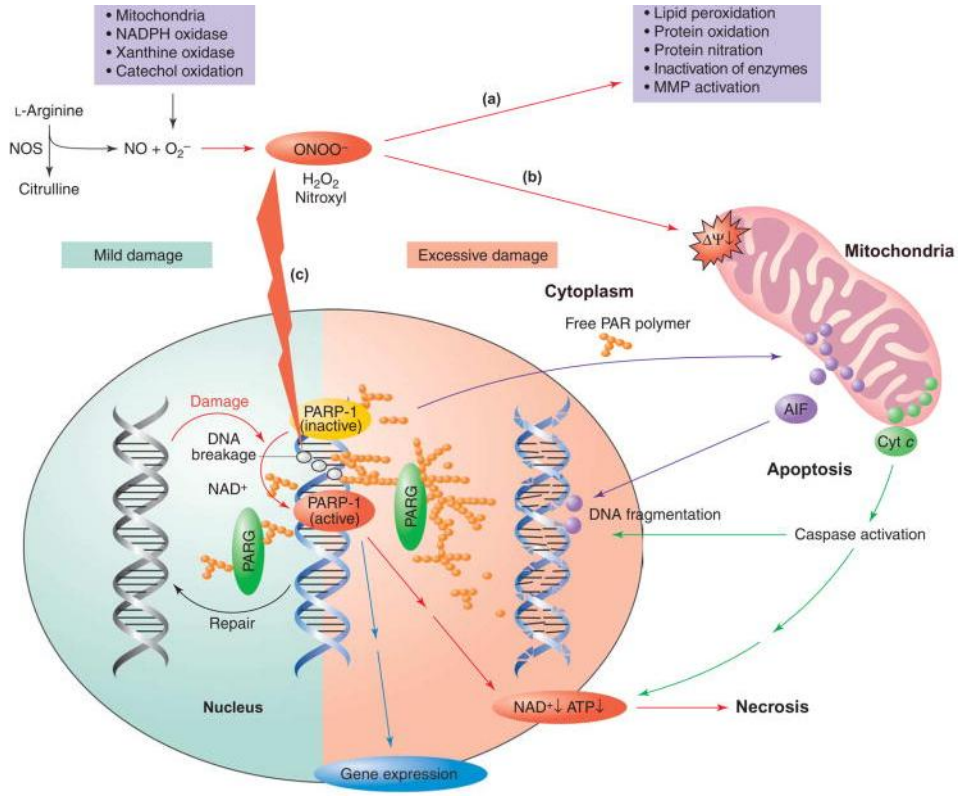

Figure 6. Cellular and molecular changes after oxidative injury. In oxidative and nitrosative stress free radicals – NO, superoxide and $ONOO^-$ - damage proteins and membrane lipids, inactivate enzymes, slowing down transmembrane ion transports, and decreasing mitochondrial membrane potential. These free radicals induce DNA strand breaks, but as long as PARP can repair DNA damage, cells will survive. The high occurrence of DNA strand breaks in excessive damage overactivates PARP, using up the NAD^+ stores, leading to ATP level decrease. Free PAR polymers cleaved by PARG and mitochondrial membrane depolarization leads to the release of AIF and cytochrome c from mitochondria. Cells can undergo caspase-dependent, caspase-independent apoptotic, or necrotic cell death depending on the amount of available ATP and on the seriousness of the oxidative injury (129).

The beneficial effect of PARP inhibitors have been implicated in several diseases, such as heart failure, reperfusion injury after heart transplantation or transient focal cerebral ischemia (130), (131), (132). Recent work from Bartha et al. proved that PARP inhibition favorably influences the signaling pathways related to oxidative stress, and they also showed that PARP inhibition prevents remodeling, preserves systolic function, delays the transition of hypertensive cardiomyopathy to heart failure in spontaneously hypertensive rats (133), (134).

1.2.2.4. Poly (ADP-ribosyl)ation in mitochondria

PARP is a nuclear enzyme, but PARP activation also has a role in mitochondrial dysfunction under oxidative stress. Several lines of evidence pointed to a cross-talk between the nucleus and the mitochondria, and demonstrated that increased PAR formation plays a crucial role in this process, leading to the release of stress signals, such as cytochrome c and AIF from the mitochondrion. However, how exactly mitochondria play their role in this process is not well understood, and how PARP transfers information to the mitochondria is unclear. In vitro studies using PARP-1 deficient myocytes showed that H_2O_2 induced oxidative stress results in a better maintenance of mitochondrial membrane potential, mitochondrial respiration and cellular NAD^+ levels in PARP-1 deficient myocytes compared to the wild type cells. Release of cytochrome c and AIF was also attenuated in knock out cells (135), Mitochondrial enzymes that play role in ADP-ribosylation were identified earlier, such as ADP-ribosyltransferases, ADP-ribosyl cyclases or cyclic ADP-ribose hydrolases (73); and Kun et al identified a poly (ADP-ribosyl)ated protein around 100kDa in mitochondria as early as the 1970's (136). Further studies in rat liver, brain and testis mitochondria showed the transfer of single or oligo-ADP-ribose to mitochondrial proteins (137), (138). Some studies indicated that PARP-1 is present in the mitochondria (74) and besides playing a role in repairing the mitochondrial DNA (139), (140) it can also PARylate mitochondrial proteins. A recent study showed that PAR polymers are able to transfer a signal to the mitochondria and stimulate AIF translocation from the mitochondrion to the nucleus (141). Lai et al found several poly (ADP-ribosyl)ated proteins in vitro and in vivo in rat brain after traumatic brain injury, including mitochondrial stress proteins, and the electron transport chain components F_1F_0 ATPase, cytochrome c oxidase, and cytochrome c reductase (142). A recent study also shown that PARG, which is responsible for the catabolism of PAR polymers is localized to the mitochondria (143). In spite all these findings the presence and location of a mitochondrial PARP and its role remain controversial (144), (75). Thus, in this study we tried to find poly (ADP-ribosyl)ated proteins in mitochondria following oxidative and nitrosative stress, and candidate mitochondrial proteins with a possible poly (ADP-ribosyl)ating enzymatic activity.

1.3. Dihydrolipoamide dehydrogenase and α-ketoglutarate dehydrogenase

Dihydrolipoamide dehydrogenase (DLDH) is a subunit of the α-ketoglutarate dehydrogenase (KGDH) and the pyruvate-dehydrogenase (PDH) complexes. These enzymes are central players in a sequence of mitochondrial events in oxidative and nitrosative stress. The presence of excessive reactive nitrogen and reactive oxygen species influences the activity of DLDH, KGDH and PDH. PDH produces acetyl-CoA from pyruvate for the Krebs-cycle; while KGDH converts α-ketoglutarate to succinyl-CoA, both enzymes using NAD^+ as a cofactor. Malfunction of these enzymes during oxidative stress alters mitochondrial metabolism and can lead to serious bioenergetic deficit (145).

1.3.1. Structure and function of the enzymes

Dihydrolipoamide dehydrogenase (DLDH, EC 1.8.1.4, also known as dihydrolipoyl dehydrogenase) was discovered by Straub, F.B. in the late 1930's. (144), (146). The greatest proportion of DLDH activity (90%) is in mitochondria, where it serves as the E3 component of pyruvate dehydrogenase, alpha-ketoglutarate dehydrogenase and glycine decarboxylase complexes (Figure 7.). DLDH regenerates the dihydrolipoic acceptors covalently attached to ε-amino groups of lysine residues on the swinging arms of the E2 succinyl-transferase subunit of the complexes (147). DLDH is a dimeric flavoprotein with broad specificity for electron acceptors. It has diaphorase activity, transferring electrons from NAD(P)H to oxygen. DLDH can use cytochrome c as electron acceptor or artificial electron acceptors such as methylene blue, 2,6-dichlorophenolindophenol (DCPIP), ferricyanide or quinones. The enzyme has two centers that can bind two electrons each: a flavin adenine dinucleotid (FAD) and an enzymic disulfide. In the two-electron-reduced state (EH2), the disulfide is reduced and FAD is oxidized; and in the four-electron-reduced state (EH4) both disulfide and FAD are reduced (146), (148), (149).

Alpha-ketoglutarate dehydrogenase (EC 1.2.4.2, KGDH, also known as 2-oxoglutarate dehydrogenase) is a Krebs cycle enzyme that has three subunits:

oxoglutarate-dehydrogenase (E1), dihydrolipoyl-succinyltransferase (E2), dihydrolipoyl-dehydrogenase (E3), (Table 4.). KGDH catalyses the non-equilibrium reaction, converting α–ketoglutarate, coenzyme A and NAD^+ to succinyl-CoA, NADH and CO_2; providing electrons for the respiratory chain in mitochondria (Figure 7.).

Subunit	EC Number	Name	Cofactors
E1	EC 1.2.4.2	oxoglutarate-dehydrogenase	thiamine pyrophosphate
E2	EC 2.3.1.61	dihydrolipoyl-succinyltransferase	lipoic acid, CoASH
E3	EC 1.8.1.4.	dihydrolipoyl-dehydrogenase	FAD, NAD^+

Table 4. Subunit composition of KGDH and the cofactors used by the enzymes. KGDH has three subunits and uses five different cofactors to convert α–ketoglutarate to succinyl-CoA, while providing electrons for the mitochondrial electron transport chain.

KGDH is highly regulated and is the primary site of control of the metabolic flux through the Krebs cycle. It is inhibited by its end products, succinyl-CoA and NADH and is also inhibited by high energy charges in the cell. Regulation of KGDH is complex involving ATP/ADP ratio, $NADH/NAD^+$ ratio, calcium and the substrate availability in mitochondria. Calcium plays a key role in activating KGDH in the 0.1–10 mM range; however, high concentrations of calcium in pathological conditions can inhibit the enzyme (150).

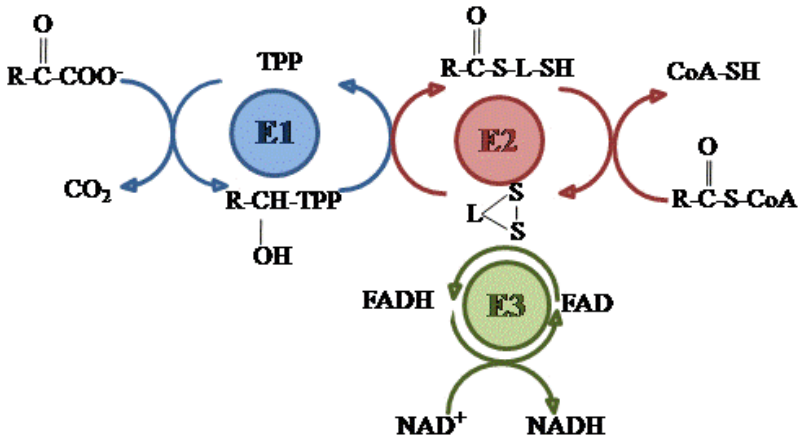

Figure 7. The role of DLDH as a part of KGDH and PDH. PDH using NAD^+ converts pyruvate - arriving from glycolysis- to acetyl-CoA that then enters the Krebs cycle. KGDH is responsible for the transformation of alpha-ketoglutarate into succinyl-CoA also using NAD^+. The role of DLDH as the E3 subunit of KGDH and PDH is to reoxygenize lipoic acid, and subsequently NAD^+ is reduced. R-CO-COO^-: pyruvate or alpha-ketoglutarate, TPP: thiamine pyrophosphate, R-CO-S-CoA: succinyl-CoA or acetyl-CoA.

1.3.2. Role of the enzymes in oxidative and nitrosative stress

NO and peroxynitrite – formed from the reaction of NO with superoxide – are the main reactive nitrogen species that are responsible for nitrosative stress in tissues. Some bacteria and yeast use flavohemoglobins to detoxify NO, while animals use hexacoordinate hemoglobins to modulate NO levels in their cells. Igamberdiev et al reported that DLDH has NO scavenging activity in mammalian heart mitochondria and it is able to convert NO to nitrate using NADH, even when NO concentration is higher than in normal conditions (151). NO reversibly inhibits cytochrome c oxidase that converts NO to nitrite in mitochondria. This study by Igamberdiev suggests that because of the abundance of DLDH in mitochondria and its high reactivity it can readily compete with the cytochrome c oxidase interaction with NO. Another study by Bryk et al also suggests that DLDH plays a role in the antioxidant defense of Mycobacterium upon oxidative and nitrosative stress (152). They found that peroxiredoxin alkyl hydroperoxide reductase (AhpC) which is a nonheme peroxidase that protects cells against oxidative and nitrosative stress both in bacteria and human (153) is linked to DLDH and also to succinyl-transferase – the other component of the KGDH complex.

Mitochondrial matrix maintains a pH gradient that is more alkaline than the cytosol. This balance is interrupted when the mitochondrial membrane potential changes during ischemia and results in matrix acidification (154). DLDH is sensitive to intracellular pH and it switches between its different activities and oligomeric states during changes in cellular pH. Mitochondrial matrix acidification during oxidative stress is sufficient to influence DLDH specificity, reducing mitochondrial defenses, leading to mitochondrial dysfunction, further oxidative damage and cellular injury (155). At the same time it is also known that both KGDH and PDH activities are reduced following oxidative stress both in the heart and in the brain (156), (157). Various studies showed that the mobilization of intracellular Zn^{2+} is important in cellular toxicity after ischemia-reperfusion (158), (159). Zn^{2+} at submicromolar concentrations inhibits DLDH purified from the heart, and inhibits KGDH-dependent respiration in liver mitochondria (160). DLDH catalyzes the transfer of electrons from dihydrolipoate to a thiol pair, then the FAD moiety transfers electrons to NAD^{+}. This reaction is strongly inhibited by Zn^{2+} in both directions, because Zn^{2+} competes with the oxidized lipoamide for the two-electron reduced enzyme.

KGDH is an important regulatory point in the mitochondrial metabolism, and as it is sensitive to ROS; the inhibition of the enzyme in oxidative stress could be critical leading to bioenergetic deficit. In brain the amount of KGDH present in the mitochondria is the lowest of all Krebs cycle enzymes, thus it could be a rate –limiting factor regulating the flux through the cycle. KGDH is inhibited or has decreased activity in various tissues - such as brain, muscle, heart, liver - following oxidative or nitrosative stress (161), (162). KGDH is mainly vulnerable to H_2O_2, but it also has decreased activity by lipid peroxidation products, superoxide donors, peroxynitrite, and NO itself. It was shown that the target of 4-hydroxy-2-nonenal, the fragmentation product of lipid peroxidation, is the DLDH subunit of KGDH in cardiac mitochondria (161). Andersson showed that superoxide inhibits KGDH in soleus muscle, but NO alone had no effect (163). In contrast, peroxynitrite generated from superoxide and NO was more effective than superoxide alone. Addition to this, NO alone was effective to inactivate KGDH in microglia and in the isolated KGDH enzyme (164). Aconitase, another Krebs cycle enzyme is even more sensitive to H_2O_2 than KGDH; however, when aconitase is 100% inhibited by H_2O_2 NADH production is still maintained. In contrast, after complete

aconitase inhibition, when also KGDH is inhibited at higher concentrations of H_2O_2, NADH level falls rapidly, pointing to the fact that KGDH is the key regulator enzyme which limits NADH generation in the Krebs cycle under acute exposure to oxidative stress (145). As a consequence, Krebs cycle cannot provide enough NADH for Complex I, mitochondrial respiration decreases, ATP level decreases, and mitochondrial membrane potential collapse (150). In an earlier study it was shown that the overuse of NAD^+ pools following oxidative stress leads to the blockade of glycolysis at glyceraldehyde-3-phosphate dehydrogenase (165). The blockade at this step influences the amount of glucose carbon that enters the Krebs cycle. Ying and colleagues showed that addition of Krebs cycle substrates – such as alpha-ketoglutarate or pyruvate - can prevent cell death after treatment with a DNA alkylating agent (166).

2. OBJECTIVES

The main objective of the present thesis was to further elucidate the role of mitochondria in oxidative and nitrosative stress and in the regeneration of cardiac muscle after ischemic injury.

2.1. Role of mitochondria in restoring energy levels of oxidatively injured cardiomyocytes in an *in vitro* ischemia model

Previous studies have proved the beneficial effects of cell transplantation in cardiac muscle regeneration after ischemic injuries. Various cell types are used and the most suitable cell delivery technique is still questionable. Cells can either transdifferentiate, fuse with host cells or release paracrine factors to improve the regeneration of the surrounding cardiac muscle. Previous studies by our research group using mesenchymal stem cells in co-culture with cardiomyocytes excluded the possibility of positive paracrine effects (43). In the present study we concentrated on direct cell-cell interactions between healthy and oxidatively injured cardiomyocytes and on the role of mitochondrial traffic on cell survival after hypoxia.

Our aim was to identify direct cell-to-cell crosstalk between cardiomyocytes and to prove the role of intact mitochondria in rescuing oxidatively injured cells.

2.2. Oxidative stress induces poly(ADP-ribosyl)ation of mitochondrial proteins

PARP overactivation and PARP induced AIF release from mitochondria plays an important role in cell death after oxidative stress. PARP resides in the nucleus, repairs DNA-single strand breaks, using NAD^+ and ATP supplied by mitochondria. In spite that earlier studies have found poly (ADP-ribosyl)ated proteins not only in the nucleus, but also in the mitochondrion; and also showed the presence of PARP-1 inside the organelle; there are several unidentified poly(ADP-ribosyl)ated proteins in the mitochondrion; and little is known about how PARP reaches the mitochondrion as it does not have a mitochondrial target sequence.

Our aim was to identify poly (ADP-ribosyl)ated proteins in mitochondria and to investigate their role in oxidative and nitrosative stress. We also searched for enzymes in the mitochondria which – along with the putative mitochondrial PARP-1– may have poly(ADP-ribosyl)ating activities.

2.3. The mitochondrial nitric oxide synthase and other possible sources of mitochondrial reactive nitrogen species

Mitochondria are the major sources and also the target of reactive oxygen and nitrogen species. The respiratory chain complexes I. and III., and also xanthine-oxidase, NADPH-oxidase are potential sites of superoxide production in mitochondria. Nitric oxide originates from the conversion of L-arginine to L-citrulline by one of the known nitric oxide synthase enzymes; nNOS, eNOS or iNOS. Peroxynitrite is formed from NO and superoxide; and causes DNA strand breaks and decreases mitochondrial membrane potential. The existence of a mitochondrial NOS enzyme is in the center of intensive scientific argument, and it was first mentioned about a decade ago. Since then several evidence was published either supporting or questioning the role and the existence of a mitochondrial NOS enzyme.

Using different methods - such as Western blotting, flow cytometry, electron paramagnetic resonance measurements, gas-phase chemiluminescent technique to quantify NO – we searched for the possible sources of NO in mitochondria, and tried to identify the putative mtNOS enzyme.

3. MATERIALS AND METHODS

3.1. In vitro cell culture experiments

3.1.1. Cell types

H9c2 rat cardiac myoblasts were obtained from ATCC (Wesel, Germany). The H9c2 myoblast cell line is derived from embryonic rat heart; and it is used as an in vitro model for both skeletal and cardiac muscle (167). These cells are able to differentiate from mononucleated myoblasts to myotubes upon reduction of serum concentration. During the differentiation process, cells retain several elements of the electrical and hormonal signaling pathway of cardiac cells, and have therefore become an accepted in vitro model to study the effects of ischemia and diabetes on the heart. The human embryonic kidney cells (HEK), and Madin-Darby canine kidney cells (MDCK) cells were the courtesy of Professor Emília Madarász.

3.1.2. Oxygen and glucose deprivation

H9c2 cells were grown in high glucose (4.5 g/L) DMEM containing 10% fetal bovine serum, 4 mM L-glutamine, 100 U/ml penicillin and 100 μg/ml streptomycin. These cells were labeled with the fluorescent dye: Vybrant DiO. Oxygen glucose deprivation (OGD) was performed by omitting oxygen and glucose from the culture media of cardiomyocytes in vitro. The cells were incubated in glucose-free DMEM in an atmosphere of 0.5% O_2 and 99.5% N_2 for 2.5 h. Following OGD glucose-free DMEM was replaced with the original, fresh high-glucose media and oxygen was added back to the system. After 30 min of reoxygenation, Vybrant DiD-labeled various cell types were added to the culture. These cell types were as follows: healthy H9c2 cells, mitochondria-damaged H9c2 cells, healthy HEK cells or healthy MDCK cells. Mitochondrial dysfunction was achieved with EtBr or F16 treatment to prove that the presence of intact mitochondria is essential to rescue oxidatively injured cardiomyocytes, as described later. These Vybrant DiD-labeled cells were co-cultured with the OGD treated, Vybrant DiO-labeled H9c2 cells for 24 h (Figure 8.).

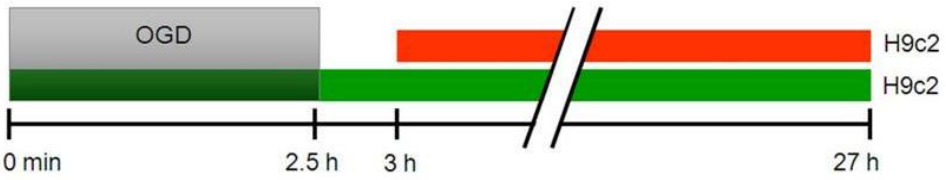

Figure 8. Experimental protocol. Vybrant-DiO-labeled (green) H9c2 cells were treated with 2.5 hours OGD, followed by 30 minutes reoxygenation. Cells then were co-cultured with Vybrant-DiD-labeled (red) healthy or mitochondria-damaged H9c2 cells. Pictures were taken with a confocal microscope at 0, 2.5 and 27 hours.

3.1.3. Fluorescent labeling

Cells were labeled with the membrane dye Vybrant DiO in a dilution of 1:200 for 30 minutes at 37°C before OGD. Additional rescue cells were labeled separately with Vybrant DiD in the same dilution. The absorption/emission maxima are 484/501 nm for Vybrant DiO, and 644/665 nm for Vybrant DiD. To follow the movement of mitochondria all cells were stained with MitoTracker Red in a dilution of 1:2000 for 10 minutes at 37°C, which is a mitochondrion-selective stain and accumulates in active mitochondria. The absorption/emission maxima for MitoTracker Red is 579/599 nm.

3.1.4. Green and red fluorescent protein labeling

Green fluorescent protein (GFP) and red fluorescent protein (RFP) labeling was carried out using cells, which were transfected with plasmid DNA coding 2MTS-EGFP or 2MTS-mRFP. These constructs use the N-terminal target sequence of the human cytochrome c oxidase subunit 8A (MSVLTPLLLRGLTGSARRLPVPRAKIHSL) in duplicate fused to the N terminus of the fluorescent proteins through a short linker (KLRILQSTVPRARDPPVAT). Cells were transfected with the indicated constructs using the Neon Transfection System (from Invitrogen) according to the manufacturer's instructions. Briefly $3x10^6$ cells were transfected with 4 μg of DNA in 100 μl Neon tips, using the following conditions: 1150 V, 30 ms, 2 pulses.

3.1.5. Ethidium bromide and F16 treatment

H9c2 cells were treated with 50ng/ml ethidium bromide (EtBr) in the cell culture media for 2 months. EtBr affects only mitochondrial DNA at this concentration. EtBr inhibits the replication and transcription of mtDNA, and the presence of the drug for about three cell division cycles reduces mtDNA content 10-fold (168). EtBr treatment results in slower proliferation of the cells reduced oxygen consumption and reduced cytochrome c oxidase activity. We tested the effects of another mitochondria-damaging agent, F16. F16 is a small, lipophilic cation that inhibits oxidative phosphorylation. We treated H9c2 cells with F16 in different concentrations: 137.5μM, 275μM, 550μM. Cells were labeled with the nuclear dye Hoechst and the mitochondrial dye MitoTracker Red. The intensity of the fluorescent signals, and the cell number was followed at the different concentrations of F16 treatment to determine the most suitable F16 concentration for our experiments. Finally, F16 was applied in the cell culture media for 48 h, in 200μM concentration.

3.1.6. Confocal microscopy

Cells were seeded on glass coverslips and their movement and the formation of tunneling membrane tubes was observed overnight using a Zeiss LSM 510 META confocal microscope. Pictures were taken every 15 minutes at high resolution, with a 63x objective.

Cells were grown in 12-well plates for calculating the live cell number after EtBr and F16 treatment. Seeded cell number was always 15 000 in each well. 2x2 tile scan pictures were taken from two different locations from each well. Using the ImageJ cell counter software dead cardiomyocytes, live cardiomyocytes and healthy rescue cells were labeled with different colors and counted.

3.2. Proteomic analysis experiments

In search or PARP-like enzymes in the mitochondria and poly(ADP ribosyl)ated proteins, we isolated mitochondria from rat liver. Fresh, respiring mitochondria were

treated with H_2O_2 or various NO-donors for 30 minutes to induce oxidative or nitrosative stress. Proteins were isolated from these mitochondrial preparations and analyzed with Western blot using anti-PARP and anti-PAR antibodies. Two-dimensional gel electrophoresis was also carried out in the control and H_2O_2 treated groups for better separation of the proteins. Four PAR-positive protein bands from the H_2O_2 treated group; and one PAR-positive protein band from the NO-donor treated group were isolated from the silver stained gels and analyzed with mass spectrometry. The PARP-like enzymatic activity of one of the identified proteins – namely dihydrolipoamide dehydrogenase – was tested via two different enzyme activity assays.

3.2.1. Isolation of mitochondria

Mitochondria were prepared from the liver of male Wistar rats using the discontinuous Percoll gradient method as described previously (94). The protocol was carried out for the H_2O_2 and two dimensional gel electrophoresis experiments. Mitochondria were isolated using ice-cold sucrose isolation buffer (0.25M sucrose, 0.5mM EDTA, 5mM TRIS, pH 7.2) according to a modified protocol of Kozlov (169) for the experiments with NO-donors and DLDH.

3.2.2. Treatment of mitochondria samples

The isolated mitochondria groups were either treated with H_2O_2 or NO-donors (S-nitroso glutathione: GSNO or S-nitroso-N-acetylpenicillamine: SNAP to induce oxidative and nitrosative stress. NO donors, such as GSNO was shown to induce S-glutathionylation and S-nitrosylation of important proteins during cellular nitrosative stress both *in vitro* and under cellular conditions. Nitrosative stress was shown to induce the S-glutathionylation of metallothioneins, glyceraldehydes-3-phosphate dehydrogenase, and S-nitrosylation of several proteins that accumulate in the mitochondria. Literature data varies on the concentration of applied GSNO in the 0.5-5 mM range, but the most effective concentration range is between 1-4 mM (170), (171), (172). To check that dihydrolipoamide dehydrogenase is responsible for the poly (ADP-ribosyl)ation of mitochondrial proteins in the NO-donor treated group, we tested the

effect of the specific dihydrolipoamide dehydrogenase inhibitor 5-methoxyindole-2-carboxylic acid (MICA). The groups received the following treatments: 1: Control, no treatment, 2: 3mM GSNO for 30 minutes on ice (+/- 5mM MICA as pretreatment for 30 minutes), 3: 3mM SNAP for 30 minutes on ice (+/- 5mM MICA as pretreatment for 30 minutes), 4: 3mM H_2O_2 for 30 minutes on ice (+/- 5mM MICA as pretreatment for 30 minutes), 5: 10μg of recombinant DLDH enzyme in 100μl mitochondria sample.

3.2.3. Immunoblotting

Proteins were extracted from the samples using hot lysis buffer (0.5% Tris, 0.5% SDS) followed by sonication. Protein concentration was measured using the Bio-Rad Protein Assay Kit, according to the manufacturer's instructions. 10μg protein was loaded from each sample onto 4-12% Bis-Tris Invitrogen mini gels. Proteins were transferred to Invitrogen nitrocellulose membranes. Membranes were blocked in 10% non-fat dry milk in TBS containing 0.05% Tween for 1 hour at room temperature, and then washed 3 times for 5 minutes in TBS-Tween. Membranes were incubated with anti-PAR rabbit polyclonal primary antibody in the dilution of 1: 5000 (Calbiochem) or anti-PARP rabbit polyclonal primary antibody in the dilution of 1: 4000 (Calbiochem) overnight at 4^0C, followed by 3 times 5 minutes washing steps, then incubation with anti-rabbit IgG-HRP secondary antibody in the dilution of 1: 2000 (Cell Signaling) for 1 hour at room temperature. After washing the membrane 4 times 5 minutes in TBS-Tween, Amersham ECL detection kit was used to visualize protein bands.

3.2.4. Two-dimensional gel electrophoresis

Two-dimensional gel electrophoresis was carried out according to the Invitrogen ZOOM IPG Runner System protocol. 25-40μg protein was loaded from each sample onto ZOOM IPG strips. Isoelectric focusing steps were as follows: 50V for 90 minutes, 200V for 20 minutes, 450V for 15 minutes, 750V for 15 minutes 1000V for 6 hours, 2000V for 1 hour using a Bio-Rad PowerPac 3000 power supply. Strips were equilibrated in two steps each for 15 minutes: 1; in 1X NuPAGE LDS sample buffer containing 10% NuPAGE sample reducing agent, 2; in 125 mM alkylating solution

containing fresh iodoacetamide. ZOOM IPG strips were placed in ZOOM IPG 4-12% Bis-Tris gels and covered with 0.5% agarose solution. SDS-PAGE was performed at 200V for 50 minutes. Gels were either stained using the SilverQuest Silver staining kit (Invitrogen) according to the manufacturer's protocol or blotted to nitrocellulose membranes. Membranes were immunoblotted as described above in the Immunoblotting section.

3.2.5. Enzyme activity assays

Enzyme activity assays were performed to test the possible PARP-like activity of the DLDH and KGDH enzymes. Two different assays were carried out.

3.2.5.1. Modified protocol of Igamberdiev

In order to measure the PARylation effects of DLDH and KGDH, we carried out Western blot analyses of the recombinant enzymes with anti-PAR antibody. The enzymes were preincubated with their cofactors NADH and FAD^+ and optimal pH for their proper function was attained by $NaHPO_4$ in the incubation buffer mix. To mimic oxidative stress H_2O_2 was added to the same buffer mix. The assay buffer mixture was as follows: 100µl of 50mM $NaHPO_4$, 10µl of 10mM NADH, 10µl of 20mM FAD^+, +/- 20µl of 30% H_2O_2, and 125µl of KGDH (Sigma, MO, USA) or 100µl of DLDH (Sigma, MO, USA). We followed the modified protocol of Igamberdiev et al (151).

3.2.5.2. Colorimetric PARP assay

The commercially available PARP Colorimetric Assay Kit (Trevigen) was used to measure enzyme activity. The kit uses histone coated 96 well plates to measure the incorporation of biotinylated PAR in the presence of activated DNA and PARP buffer. We have followed the assay manual in our procedures and used 1U PARP enzyme as positive control, and the final reaction volume was 50µl in all cases. In the negative control samples no enzyme was added to the reaction. The activity of 0.5 Unit KGDH or DLDH was tested, and the effect of the PARP inhibitor 3-aminobenzamide (2mM)

was also measured. The activity of DLDH and KGDH complexes was measured on the same plate, in the same volume, and 50mM NaHPO4, at pH 7.5 was added to the reaction according to a modified protocol of Igamberdiev et al (151).

3.2.6. Mass spectrometry of the identified proteins

Mass spectrometry analysis was carried out by the Proteomics Research Group at the University of Szeged (http://www.szbk.u-szeged.hu/mslab/) according to the following protocol: http://ms-facility.ucsf.edu/ingel.html). Protein spots were analyzed on a Reflex III matrix assisted laser desorption/ionization, time of flight mass spectrometer (MALDI TOF MS, Bruker, Germany). 2,5-dihidroxy-benzoic acid was used as the matrix. All spectra were acquired in positive reflectron mode using trypsin autolysis products as internal calibration. A database search was performed in the National Center for Biotechnology Information nonredundant (NCBInr) database using ProteinProspector. To obtain sequence information post source decay (PSD) analysis of selected components were performed. Mass accuracy considered was 50 ppm for monoisotopic MS data and 1500 ppm for average mass PSD fragments. Protein masses in the database differ from the masses on the gel, but we expected a wide range of protein masses because of the different poly-ADP-ribosylation rate of the proteins. MALDI-TOF mass spectrometers allow the user to set various specific criteria regarding the post-translational modifications of the analyzed proteins. Post-translational modifications, such as phosphorylation, glycolysation, acetylation, methylation can be characterized by mass spectrometry. Cleavage fragments that contain modifications can be identified by characteristic mass shifts; and also the location of the modification can be determined from mass shifts in the tandem mass spectrum (173). MALDI-TOF combined with post source decay (PSD) analysis has been widely applied in peptide sequencing, because of its high sensitivity and because of its high tolerance of sample impurities and sample inhomogeneity. In our experiments MALDI-TOF spectrometer and also PSD analyses was applied in all cases because of its main advance, which is its compatibility with post-translational modifications.

3.3. NO measurement experiments

Mitochondria were isolated from the liver, heart and brain of C57/BL6 mouse. In one set of experiments, to find the source of NO production in mitochondria, samples were treated with different NOS inhibitors (either incubated with the mitochondria samples or added previously for 3 days in the drinking water of the animals). NO and RNS production was measured using diaminofluorescein (DAF). To check whether the presence of $ONOO^-$ also increases DAF-FM signals, mitochondria samples received two different types of $ONOO^-$ scavengers. To rule out the role of superoxide and H_2O_2 in the contribution to DAF-FM fluorescence a superoxide dismutase mimetic (M40401) and catalase were also applied. In another set of experiments we measured the NO and RNS production by the respiratory chain complexes. The effect of inhibitors of each of the 5 complexes on DAF-FM fluorescence was tested.

3.3.1. Mitochondria preparation

3.3.1.1. Mitochondria preparation from mouse

Mitochondria were prepared from halothane anesthetized mouse brain, heart and liver using the discontinuous Percoll gradient method as described previously (94). Six to ten week-old male wild-type mice were used from the C57/BL6 strain (Jackson, Bar Harbor, ME). The mitochondria preparation obtained with this method had a high respiratory ratio (4.94 ± 0.46). Purity testing by Western blotting of mitochondrial and endoplasmic reticulum markers (cytochrome c oxidase and calreticulin, respectively) and electron micrographs were applied regularly to maintain comparability of the results (108), (174).

3.3.1.2. Mitochondria preparation from human tissue

All procedures were approved by the local Ethical Committee and all patients involved in the study signed a written agreement before the operation. Atrial auricula was harvested during extracorporal circulation surgery, when the auriculum is cut off in

order to introduce the aortic canulla. Papillary muscle was harvested during replacement of the mitral valve. These tissues are discarded under routine surgical practice and using them for scientific purposes does not affect the patients in any way. Heart mitochondria were isolated by Percoll gradient purification as described previously. Mitochondrial protein concentration was measured with the DC Protein Assay (Bio-Rad). Average protein concentration of mitochondria samples (n=5) was 0.0730 mg/ml (SD=0.0448).

3.3.2. Flow cytometry

Freshly isolated mitochondria were dispersed in K^+ - buffer containing 125mM KCl, 2mM K_2HPO_4, 5mM MgCl2, 10mM HEPES, 10 μM EGTA at pH 7.0. Mitochondria were energized by the addition of malate (5mM) and K-glutamate (5 mM) and the mitochondrial suspension dilution was: 1:100 v/v. The preparations were incubated for 20 min at 37 ^{0}C to energize the mitochondria. Treatments were also added to the preparations at the beginning of the incubation. Following energization, DAF–FM (7 μM) was added to the preparations and the fluorescence was measured with flow cytometry. DAF-FM is widely used for monitoring NO production; it reacts with NO to form benzotriazole that result in over a 100 fold increase in fluorescence. Forward-scatter, side-scatter and green fluorescence (FL1-H) were recorded by a BD-FacsCalibur flow cytometer from 100,000 events in each preparation. Data were evaluated by the CellQuestPro software. Special care was taken to keep the preparations and the dyes in darkness throughout the experiment to avoid photoactivation of the fluorescent probe (175). Experiments were performed in parallel in brain, heart and liver mitochondria and were reproduced at least two times. Mitochondrial fluorescence was observed under control conditions and in the presence of $ONOO^-$ scavengers tetrakis 2-triethylene glycol monomethyl ether (pyridil porphyrin (2-T(PEG3)- PyP) (FP15, 100 μM) (176), or 5,10,15,20-tetrakis (4-sulfonatophenyl) porphyrinato iron (III) chloride (FeTPPS, 100 μM). The contribution of the hypothetical mtNOS to the NO production detected by DAF was tested by supplementation of the K^+ buffer with L-arginine (1mM) and Ca^{2+}(1 μM) in the absence of EGTA, or in the presence or absence of the NOS inhibitor L-nitroarginine-methyl-esther (L-NAME, 1mM, or 10 mg/ml for 3 days in the drinking water of the animals) or L-N-methylarginine (L-NMMA, 1 mM). The

following treatments and their combinations were used to test the involvement of the mitochondrial respiratory chain: the complex I blocker rotenone (10 μM) in the absence of mitochondrial substrates malate and glutamate or in the presence of K-succinate (5mM); the succinate dehydrogenase (complex II) inhibitor 3-nitropropionic acid (3-NPA, 100 μM); the complex III inhibitor myxothiazole (10 μM), the complex IV inhibitor KCN (100 μM) and the protonophore carbonyl cyanide 4 (trifluoromethoxy) phenylhydrazone (FCCP, 10 μM). FCCP was dissolved in ethanol and the final ethanol content in the preparation was 1%. All other drugs were dissolved in H_2O and diluted to the final concentration with K^+ buffer.

3.3.3. Electron paramagnetic resonance (EPR) measurements

Mouse heart mitochondria were suspended in a buffer containing 105 mM KCl, 20mM TRIS–HCl, 1mM diethylenetriaminepentaacetic acid, 4mM KH_2PO_4, and 1 mg/ml fatty acid-free bovine serum albumin (pH 7.4, 25 ^{0}C). The final concentration of mitochondria was 0.5mg of mitochondrial protein/ml. The mitochondria were stimulated by the addition of 10mM succinate. The rate of ROS–RNS generation in heart mitochondria was detected in the presence of 250 μM of 1-hydroxy-3-carboxypyrrolidine (CPH) as described previously (177). Mitochondria were incubated for 20 min at 22 ± 1.5 ^{0}C. All measurements were carried out at room temperature, and to ensure the same temperature and the diffusion of O_2 throughout the samples, a shaking table was used to provide gentle mixing of the mitochondrial suspension with air. Mitochondrial concentration and incubation buffer were identical in all cases to guarantee equivalent pH 7.4, in all the samples. Following incubation, the samples were placed in glass capillars and EPR spectra were recorded with an X-band MiniScope 200 EPR spectrometer. The general settings were: modulation frequency 100 kHz, modulation amplitude 2.5 G; gain 700, power 5mW. Upon reaction with ROS or RNS CPH is transformed into a stable CPz radical (3-carboxy-proxyl). Calibration data were obtained in mitochondria-free buffers containing increasing concentrations of the probe 3-CP.

3.3.4. NO measurement

Nitric oxide release was measured in the head-space gas of the mitochondria preparations (108). Mitochondria were suspended in 300 µl of buffer containing glutamate and malate (5 mM each) and incubated for 45 min in 1500 µl eppendorf tubes. The NO content in the headspace gas was measured by a chemiluminescent reaction (Exhaled NO Analyzer, Logan Research, England). Sodium nitroprusside solution (SNP, 10^{-7}–10^{-3} M) was used as a positive control.

3.4. Chemicals

Vybrant DiO, DiD fluorescent dyes and MitoTracker mitochondria stain were from Invitrogen, Hungary. DAF-FM was purchased from Molecular Probes, OR, USA. FeTPPS, F16, and anti PARP/PAR antibodies were from Calbiochem, CA, USA. Secondary antibodies were purchased from Cell Signaling. Anti NOS antibodies were either from BD Pharmingen, CA, USA. The KGDH and DLDH enzymes, iodoacetamide, EtBr, FCCP, KCN, L-NAME, L-NMMA, 3-NPA, TRIS, EGTA, EDTA, NO-donors, MICA were purchased from SIGMA, MO, USA. FP15 was from Inotek Corporation, MA, USA. CPH was from Noxygen GmbH, Germany. Protein assay kit for protein concentration measurements was from Bio-Rad, Hungary or Bio-Rad, USA. All the equipment for gel electrophoresis experiments – such as gels, running buffer, transfer buffer, sample buffer, silver stain kit, IPG strips – were purchased from Invitrogen, Hungary. The colorimetric PARP assay kit was from Trevigen, MD, USA. ECL detection kit was purchased from Amersham, NJ, USA. Cell culture media, trypsin, streptomycin were purchased from Biochrom, Hungary.

3.5. Statistics

Cells were grown in 12-well plates for the EtBr and F16 treatment experiments. Seeded cell number was always 15 000 in each well. The number of experiments was 6 in each group except in the HEK and MDCK groups where 3 experiments were carried out. 2x2 tile scan pictures were taken from two different locations from each well. The ImageJ

cell counter software was used to calculate the number of live cells. The number of live cells is expressed as mean ± SEM, * $p< 0.05$ with ANOVA analysis.

One-way ANOVA followed by Tukey's multiple comparison test was carried out in the enzyme activity assay experiments. Six parallel experiments were run in each group. Optical density results are shown as mean ± SEM (*: $p < 0.05$).

4. RESULTS

4.1. In vitro cell culture experiments

4.1.1. Effects of OGD on cell survival

OGD was performed by withdrawing oxygen and glucose from the culture media of cardiomyocytes in vitro. The cells were incubated in glucose-free DMEM in an atmosphere of 0.5% O_2 and 99.5% N_2 for 2.5 h. Following OGD, glucose-free DMEM was replaced with the original, fresh high-glucose media and oxygen was added back to the system. During 2.5 h OGD, approximately 50-70% of the cells died, or suffered major changes in their shape and structure (Figure 9.).

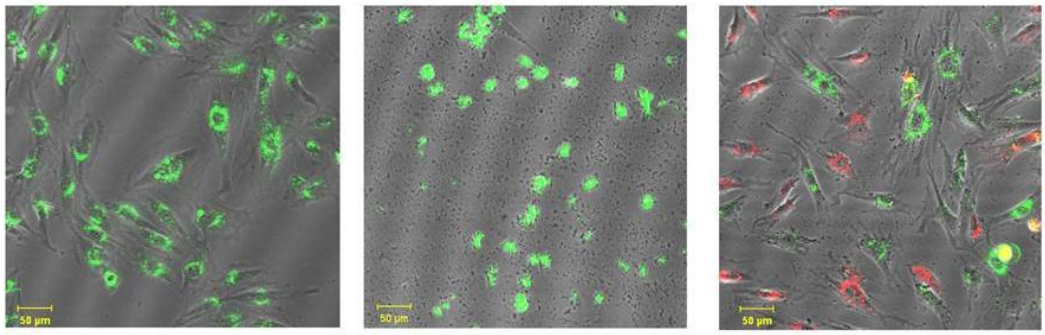

Figure 9. Cells suffer major structural changes during oxygen and glucose deprivation. Vybrant-DiO-labeled (green) H9c2 cells were treated with 2.5 hours OGD, followed by 30 minutes reoxigenation. Cells then were co-cultured with Vybrant-DiD-labeled (red) healthy or mitochondria-damaged H9c2 cells. Pictures were taken with a confocal microscope at 0, 2.5 and 27 hours. Cells are completely attached to the surface and show normal cell structure before OGD, but after 2.5 hours they lose their integrity, detach from the surface and about half of them die. Most of the cells regain their structural integrity and reattach to the surface after one day co-cultivation with healthy H9c2 cells.

4.1.2. Effects of the addition of H9c2 cells to oxidatively damaged cells

4.1.2.1. Effect of the addition of healthy or EtBr treated H9c2 cells

Healthy H9c2 cells were co-cultured with the OGD treated H9c2 cells for 24 hours. Cells attached to the surface of the culture dish and made contacts with their healthy and also with their OGD treated neighbors. During OGD 50-70 % of the cells died or suffered structural changes. Healthy H9c2 cells were able to increase the live cell number with approximately 50 % in the co-culture.

In order to investigate the role of mitochondria in this 'rescue' mechanism not only healthy H9c2 cells were added to the OGD treated cells. In a set of experiments the additional H9c2 cells were pretreated with 50ng/ml EtBr in the cell culture media for 2 months. This compound affects only mitochondrial DNA at this concentration and in this time frame (168). The statistical analyses shows the number of live cells as mean ± SEM and * $p < 0.05$. Healthy H9c2 cells were able to significantly improve the survival of their OGD treated neighbors. On the contrary, addition of EtBr treated, mitochondria-damaged H9c2 cells to the OGD treated cells, did not increase the number of the surviving cells (Figure 10.).

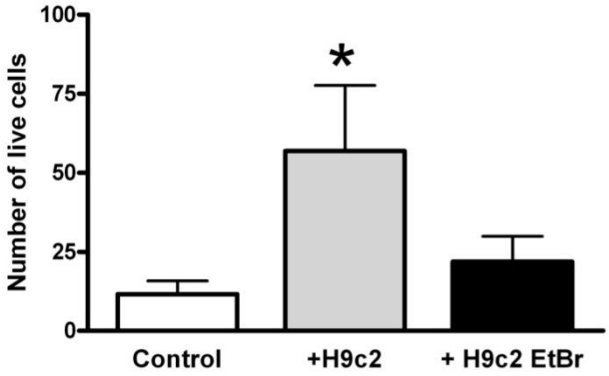

Figure 10. Mitochondria play a role in saving oxidatively injured cardiomyocytes. The diagram shows the live cell number in the control group of cells that received OGD treatment, but did not receive any additional cells. The addition and co-cultivation of healthy H9c2 cells significantly increased the live cell number. EtBr pretreatment of the additional H9c2 cells resulted in altered mitochondrial function, and these EtBr treated H9c2 cells were not able to significantly increase the live cell number in the co-culture.

4.1.2.3. Effect of the addition of F16 treated H9c2 cells

Opinions and protocols in the literature differ on the mitochondria-damaging effect of EtBr. The concentration applied in the cell culture media and the time-frame of usage are both critical points. We have tested the effect of another mitochondrial toxin to overcome these controversies. F16 is a small, liophilic cation that binds to mitochondrial membranes and inhibits oxidative phosphorylation. F16 can be easily visualized and monitored by its fluorescent properties. We have showed that F16 decreases the number of live cells in a dose dependent manner. The two higher concentrations (275 μM and 550 μM) significantly lowered the number of live cells in the culture (Figure 11.).

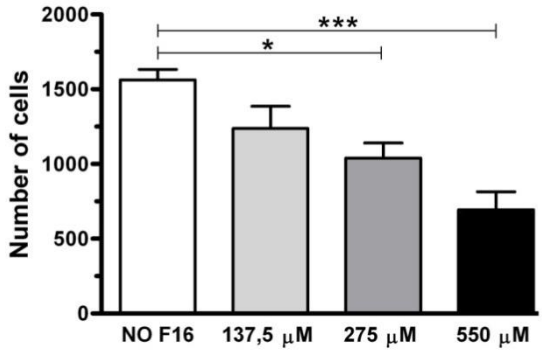

Figure 11. Effect of F16 on live cell number. F16 blocks normal mitochondrial function that eventually leads to cell death. Higher doses of F16 significantly reduce live cell number in a dose dependent manner.

We also found that F16 treatment reduces not only the live cell number, but also the mitochondrial MitoTracker red fluorescent signal in a dose dependent manner in the culture of H9c2 cells (Figure12.).

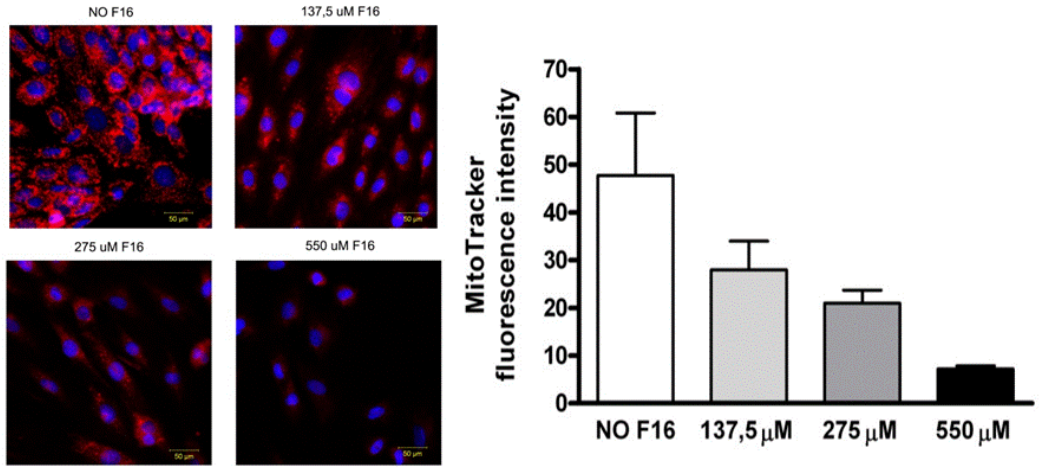

Figure 12. F16 decreases cell number and MitoTracker fluorescence signal in a dose dependent manner. Cells are labeled with Hoechst nuclear dye (blue) and MitoTracker Red mitochondrial dye (red). Cell number and also MitoTracker Red fluorescence intensity decreases with F16 treatment.

We determined the optimal concentration of F16 for our experiments, and pretreated H9c2 cells for 48 h with 200 μM F16 in the cell culture media. OGD treated H9c2 cells were co-cultured with healthy H9c2 cells or with F16 treated H9c2 cells and confocal microscopic images were taken after 24 h. The addition of healthy H9c2 cells significantly increased the number of surviving cells compared to the OGD treated control group. However, the addition of F16 treated mitochondria-damaged H9c2 cells did not improve the cell surviving ratio (Figure 13).

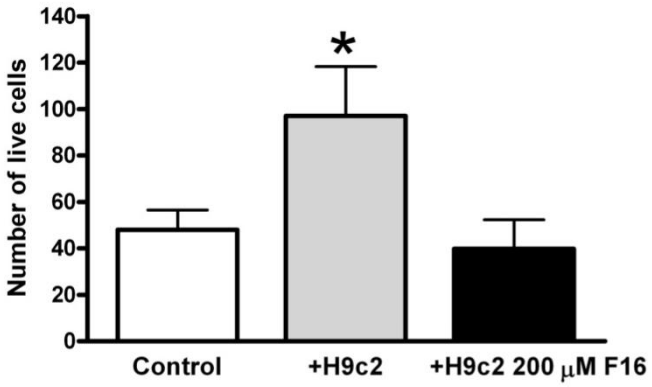

Figure 13. Mitochondria are essential for saving oxidatively injured cardiomyocytes. The diagram shows the live cell number in the control group of cells that received OGD treatment, but did not receive any additional cells. The addition of healthy H9c2 cells significantly increased the live cell number. F16 treatment of the additional H9c2 cells resulted in altered mitochondrial function, and these F16 treated H9c2 cells were not able to significantly increase the live cell number in the co-culture.

4.1.3. Mitochondrial transfer

4.1.3.1. Mitochondria movement in tunneling membrane tubes

To confirm the role of mitochondria in saving oxidatively damaged cardiomyocytes high resolution time lapse images were taken overnight with a confocal microscope. We detected the movement of cells towards each other and the formation of membrane bridges between OGD treated and healthy cells. The width of these membrane bridges was in the micrometer range, so we named them microtubes. We were also able to detect some nanotubes between the cells, but far less in number then microtubes. Healthy cells also formed microtubes among themselves, and similarly, we were able to detect microtubes between OGD treated cells. We labeled the mitochondria of the cells with MitoTracker, and we were able to follow mitochondrial movement. Our results show that mitochondria-like particles are drifting through these membrane bridges between neighboring cells (Figure 14.).

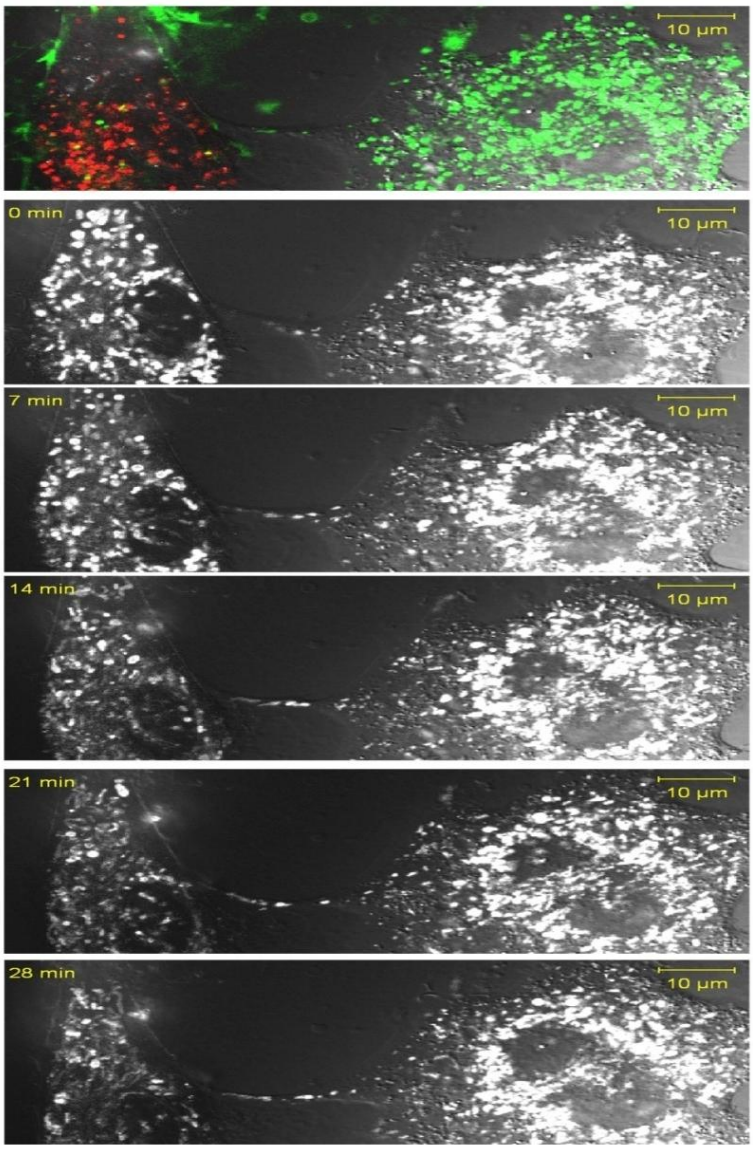

Figure 14. Mitochondrial movement between OGD treated and healthy cardiomyocytes. OGD treated Vybrant DiO labeled cardiomyocytes (red) and healthy Vibrant DiD labeled cardiomyocytes (green) develop connecting membrane bridges. MitoTracker labeled mitochondria (white) are traveling through these tunneling membrane tubes from one cell to another.

4.1.3.2. GFP and RFP labeled mitochondria exchange

Depending on these observations using MitoTracker to visualize mitochondria, it was not possible to determine the direction of mitochondrial transport. We applied another approach to track mitochondrial movement, we transfected H9c2 cells with green

fluorescent and red fluorescent proteins. The transfection of H9c2 cells with GFP and RFP targeted to mitochondria was considered successful, as about 50 % of the cells expressed the fluorescent signals as shown on Figure 15., panel A. Cells did not exchange their mitochondria in the first 24 hours of co-culture, however, after one day of co-culturing we found GFP-labeled mitochondria in the RFP labeled cells, as shown in Figure 15., panel B. We observed mitochondria exchange between healthy and OGD treated cells, as well as between healthy and healthy cells. The Z-stack images showed the position of the GFP-labeled mitochondria in the RFP-labeled cells, but the 3 dimensional structures, constructed from the Z-stack images, could not exactly locate the GFP-labeled mitochondria inside the RFP-labeled cells. These cells might overlap, climbing on top of each other on the surface of the culture dish, thus we could not surely conclude that these cells exchange whole mitochondria, but we could detect intensive mitochondrial traffic, as recorded on video files over several hours of observation (Figure 15.).

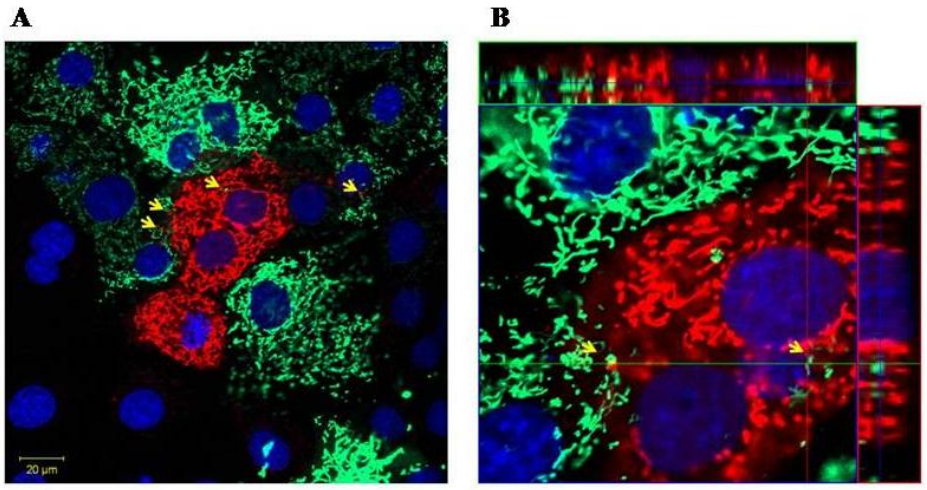

Figure 15. Co-culture of GFP and RFP labeled H9c2 cells. Transfection successfully labeled about 50% of the cells (panel A). Cells seem to lend their GFP-labeled (green) mitochondria to their RFP-labeled (red) neighbors indicated by yellow arrows. Panel B is a Z-stack picture from the same area, showing the location of the GFP-labeled mitochondria in the RFP-labeled cells. Nuclei are stained with Hoechst (blue).

4.1.4. Effects of the addition of different cell types to oxidatively damaged H9c2 cells

Tunneling nanotubes were observed between many different cell types, such as dendritic cells, macrophages or Jurkat T cells. A study by Gurke and Barroso states that normal rat kidney cells and human embryonic kidney cells are also able to form nanotubes (178). We hypothesized that kidney cells may also be capable of helping OGD treated H9c2 cells to survive. In search for easily accessible and more suitable cells in the regeneration process, we screened cell types at various stages of differentiation. OGD treated H9c2 cells were co-cultured with healthy MSCs, H9c2 cells, or with human embryonic kidney cells, or with adult Madin-Darby canine kidney cells. Our results show that the highest number of live cells is in the healthy H9c2 treated group. Human embryonic kidney cells also helped the survival of OGD treated H9c2 cells, but adult canine kidney cells were not able to improve the cell survival ratio in this experiment (Figure 16.).

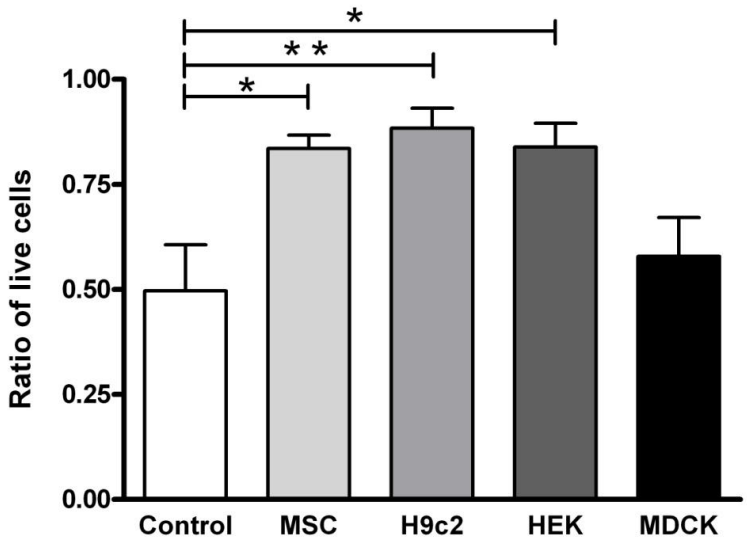

Figure 16. The effect of different types of rescue cells on the survival ratio of OGD treated cardiomyocytes. MSCs, H9c2 cells and HEK cells significantly improve the cell survival of OGD treated cardiomyocytes, while the addition of MDCK cells do not have a significant effect on the number of surviving cardiomyocytes.

4.2. Proteomic analysis experiments

4.2.1. H_2O_2 treatment results in extensive PARylation of rat liver and isolated mitochondria

We treated rat liver homogenate and isolated rat liver mitochondria with H_2O_2 to induce oxidative stress. PARylation was extensive in the liver homogenate compared to the control group and even stronger in the isolated mitochondria samples (Figure 17.).

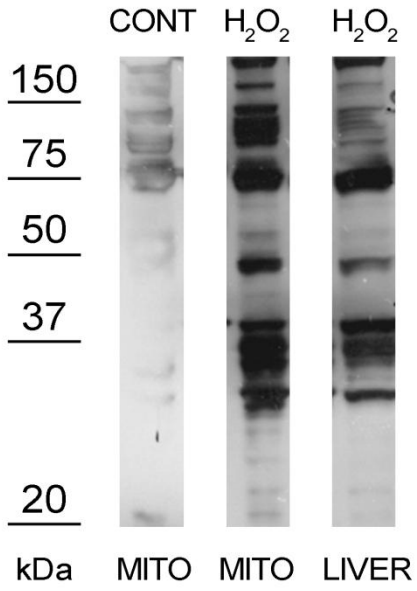

Figure 17. H_2O_2 treatment induces PARylation in rat liver and isolated mitochondria. Oxidative stress leads to the PARylation of various proteins in H_2O_2 treated liver and mitochondria samples. PAR positive bands are stronger in the isolated mitochondria samples than in the liver homogenate.

Two-dimensional gel electrophoresis separates the proteins with better resolution than the conventional one dimensional gel electrophoresis. In order to find and isolate the PARylated proteins from our samples we carried out 2D gel electrophoresis. 2D gel electrophoresis coupled with Western blot analysis confirmed the difference in the number of PARylated proteins between the control and the H_2O_2 treated mitochondria samples (Figure 18.).

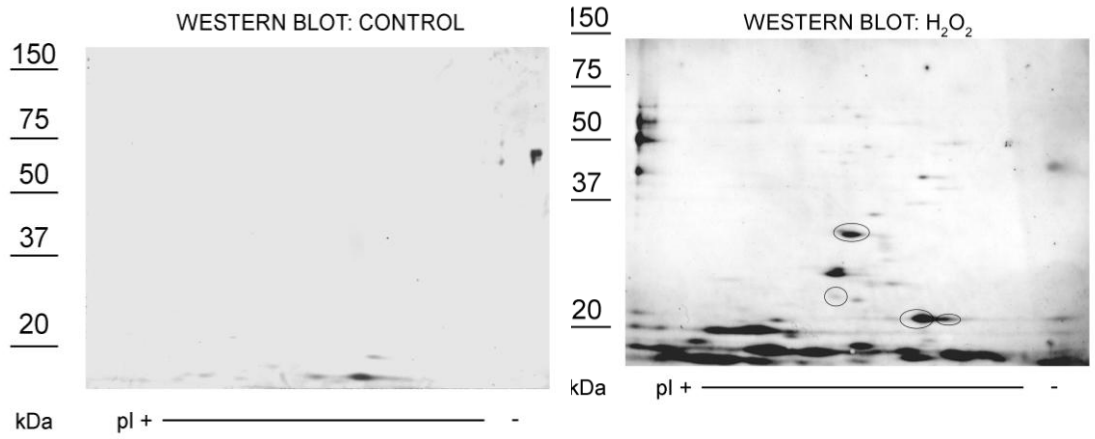

Figure 18. 2D gel electrophoresis coupled with Western blot shows numerous PARylated proteins in the H_2O_2 treated mitochondria. PAR positive protein dots are stronger in the H_2O_2 treated mitochondria than in the control. Circles indicate the PARylated proteins identified also on the silver stained gel, and analyzed with mass spectrometry.

Comparing the silver stained gel with the anti-PAR Western blot of the two-dimensional gel we identified 4 PARylated proteins with mass spectrometry. These proteins are: mitochondrial aldehyde dehydrogenase (gi|16073616, MW: 48271 Da, pI: 6.1, mtALDH), H^+-transporting two-sector ATPase, beta chain, mitochondrial (gi|92350 ,MW: 50771 Da, pI: 4.9, ATPase), ornithine transcarbamylase (gi|56789151, MW: 39574 Da, pI: 9.2, Otc) and carbamoyl-phosphate synthase 1, mitochondrial (gi|8393186, MW: 164581 Da, pI: 6.3, CPS1). The identity of the proteins was confirmed by post source decay data of peptides VVGNPFDSR and TFVQEDVYDEFVER for mtALDH, peptides IGLFGGAGVGK and VLDSGAPIKIPVGPETLGR for ATPase, peptide SLVFPEAENR for Otc, and peptide FLEEATR for CPS1 (Figure 19.). Protein masses in the database differ from the masses on the gel, but we expected a wide range of protein masses because of the different poly-ADP-ribosylation rate of the proteins. We have to mention also, that in some samples there might be more than one protein in the analyzed spots, but in questionable cases we determined the protein with post source decay analyses. Several other small molecular weight PARylated protein spots were also seen on the 2D blots but we were not able to match them with the silver stained gel.

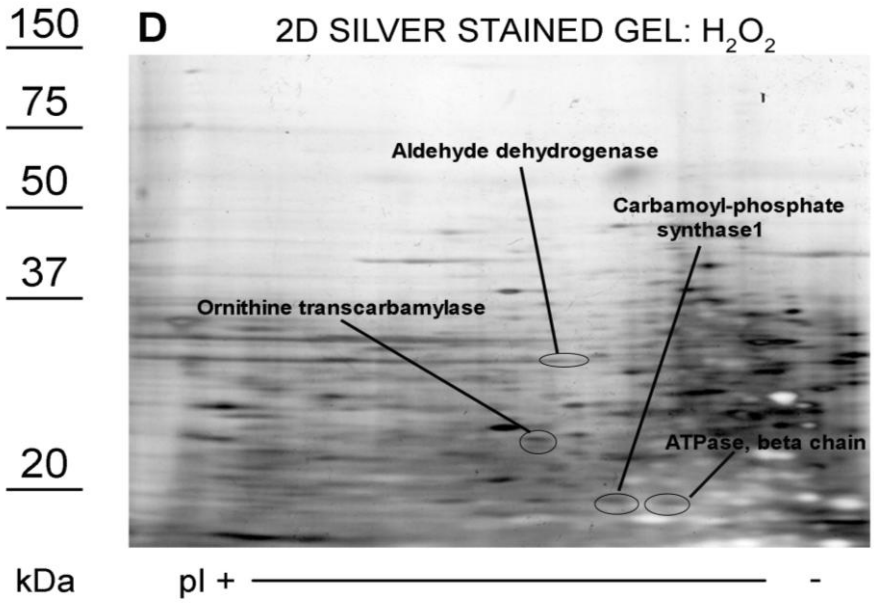

Figure 19. 2D silver stained gel of the H_2O_2 treated mitochondria. For protein dots were excised from the gel and identified by mass spectrometry. Several other PAR-positive proteins with smaller molecular weight are visible, and yet to be identified.

Mass spectrometry data for each identified proteins:

gi|92350 H^+-transporting two-sector ATPase, beta chain, mitochondrial
MW: 50771 Da pI: 4.9

49 masses were detected in the spectra out of which 10 corresponded to this protein.

1 TATGQIVAVI GAVVDVQFDE GLPPILNALE VQGRESRLVL EVAQHLGEST
51 VRTIAMDGTE GLVRGQKVLD SGAPIKIPVG PETLGRIMNV IGEPIDERGP
101 IKTKQFAPIH AEAPEFIEMS VEQEILVTGI KVVDLLAPYA KGGKIGLFGG
151 AGVGKTVLIM ELINNVAKAH GGYSVFAGVG ERTREGNDLY HEMIESGVIN
201 LKDATSKVAL VYGQMNEPPG ARARVALTGL TVAEYFRDQE GQDVLLFIDN
251 IFRFTQAGSE VSALLGRIPS AVGYQPTLAT DMGTMQERIT TTKKGSITSV
301 QAIYVPADDL TDPAPATTFA HLDATTVLSR AIAELGIYPA VDPLDSTSRI
351 MDPNIVGSEH YDVARGVQKI LQDYKSLQDI IAILGMDELS EEDKLTVSRA
401 RKIQRFLSQP FQVAEVFTGH MGKLVPLKET IKGFQQILAG DYDHLPEQAF
451 YMVGPIEEAV AKADKLAEEH GS

The coverage is 22%.

Post source decay analyses of two masses:

m/z	range	sequence
975,6	145-155	(K) IGLFGGAGVGK (T)
1919,0	68-86	(K) VLDSGAPIKIPVGPETLGR (I)

gi|8393186 carbamoyl-phosphate synthase 1, mitochondrial
MW: 164581 Da, pI: 6.3

37 masses were detected in the spectra out of which 11 corresponded to this protein.

Post source decay analyses:

m/z	sequence
865,6	(R) **FLEEATR** (V)

This sequence is only present in one protein according to the NCBInr rat database (06/01/2005).

1 MTRILTACKV VKTLKSGFGL ANVTSKRQWD FSRPGIRLLS VKAQTAHIVL
51 EDGTKMKGYS FGHPSSVAGE VVFNTGLGGY SEALTDPAYK GQILTMANPI
101 IGNGGAPDTT ARDELGLNKY MESDGIKVAG LLVLNYSHDY NHWLATK**SLG**
151 **QWLQEEKVPA IYGVDTR**MLT KIIRDKGTML GKIEFEGQSV DFVDPNKQNL
201 IAEVSTKDVK VFGKGNPTKV VAVDCGIKNN VIRLLVKRGA EVHLVPWNHD
251 FTQMDYDGLL IAGGPGNPAL AQPLIQNVKK ILESDRKEPL FGISTGNIIT
301 GLAAGAKSYK MSMANRGQNQ PVLNITNRQA FITAQNHGYA LDNTLPAGWK
351 PLFVNVNDQT NEGIMHESKP FFAVQFHPEV SPGPTDTEYL FDSFFSLIKK
401 GKGTTITSVL PKPALVASRV EVSKVLILGS GGLSIGQAGE FDYSGSQAVK
451 AMKEENVKTV LMNPNIASVQ TNEVGLKQAD AVYFLPITPQ FVTEVIKAER
501 PDGLILGMGG QTALNCGVEL FKRGVLKEYG VKVLGTSVES IMATEDRQLF
551 SDKLNEINEK IAPSFAVESM EDALKAADTI GYPVMIRSAY ALGGLGSGIC
601 PNKETLMDLG TKAFAMTNQI LVER**SVTGWK EIEYEVVR**DA DDNCVTVCNM
651 ENVDAMGVHT GDSVVVAPAQ TLSNAEFQML RRTSINVVRH LGIVGECNIQ
701 FALHPTSMEY CIIEVNARLS RSSALASKAT GYPLAFIAAK IALGIPLPEI
751 KNVVSGKTSA CFEPSLDYMV TKIPRWDLDR FHGTSSRIGS SMKSVGEVMA
801 IGRTFEESFQ KALRMCHPSV DGFTPRLPMN KEWPANLDLR KELSEPSSTR
851 IYAIAKALEN NMSLDEIVKL TSIDKWFLYK MRDILNMDKT LKGLNSESVT
901 EETLRQAKEI GFSDKQISKC LGLTEAQTRE LR**LKKNIHPW VK**QIDTLAAE
951 YPSVTNYLYV TYNGQEHDIK FDEHGIMVLG CGPYHIGSSV EFDWCAVSSI
1001 RTLRQLGKKT VVVNCNPETV STDFDECDKL YFEELSLERI LDIYHQEACN
1051 GCIISVGGQI PNNLAVPLYK NGVK**IMGTSP LQIDR**AED**RS IFSAVLDELK**
1101 VAQAPWKAVN TLNEALEFAN SVGYPCLLRP SYVLSGSAMN VVFSEDEMKR
1151 **FLEEATRVSQ EHPVVLTK**FI EGA**REVEMDA VGKEGR**VISH AISEHVEDAG
1201 VHSGDATLML PTQTISQGAI EKVKDATRKI AK**AFAISGPF NVQFLVKGND**
1251 **VLVIECNLR**A SRSFPFVSK**T LGVDFIDVAT K**VMIGESVDE KHLPTLEQPI
1301 IPSDYVAIKA PMFSWPRLRD ADPILRCEMA STGEVACFGE GIHTAFLKAM
1351 LSTGFKIPQK GILIGIQQSF RPRFLGVAEQ LHNEGFKLFA TEATSDWLNA
1401 NNVPATPVAW PSQEGQNPSL SSIRKLIRDG SIDLVINLPN NNTKFVHDNY
1451 VIRRTAVDSG IALLTNFQVT KLFAEAVQKA RTVDSKSLFH YRQYSAGKAA

The coverage is 9%.

gi|56789151, Otc protein
MW: 39574 Da, pI: 9.2

40 masses were detected in the spectra out of which 11 corresponded to this protein.

1 MLSNLRILLN KAALRKAHTS MVRNFRYGKP VQSQVQLKGR DLLTLKNFTG

51 EEIQYMLWLS ADLKFRIKQK GEYLPLLQGK SLGMIFEKRS TRTRLSTETG
101 FALLGGHPSF LTTQDIHLGV NESLTDTARV LSSMTDAVLA RVYKQSDLDI
151 LAKEATIPIV NGLSDLYHPI QILADYLTLQ EHYGSLKGLT LSWIGDGNNI
201 LHSIMMSAAK FGMHLQAATP KGYEPDPNIV KLAEQYAKEN GTRLSMTNDP
251 LEAARGGNVL ITDTWISMGQ EDEKKKRLQA FQGYQVTMKT AKVAASDWTF
301 LHCLPRKPEE VDDEVFYSPR SLVFPEAENR KWTIMVRKKR AMEGLSWYPC
The coverage is 27%.

Post source decay analyses:

m/z	range	sequence
1161,8	321-330	(K) SLVFPEAENR (T)

gi|16073616, aldehyde dehydrogenase
MW: 48271 Da pI: 6.1

26 masses were detected in the spectra out of which 12 corresponded to this protein.

1 DVDKAVKAAQ AAFQLGSPWR RMDASDRGRL LYRLADLIER DRTYLAALET
51 LDNGKPYVIS YLVDLDMVLK CLRYYAGWAD KYHGKTIPID GDFFSYTRHE
101 PVGVCGQIIP WNFPLLMQAW KLGPALATGN VVVMKVAEQT PLTALYVANL
151 IKEAGFPPGV VNIVPGFGPT AGAAIASHED VDKVAFTGST EVGHLIQVAA
201 GSSNLKRVTL ELGGKSPNII MSDADMDWAV EQAHFALFFN QGQCCCAGSR
251 TFVQEDVYDE FVERSVARAK SRVVGNPFDS RTEQGPQVDE TQFKKILGYI
301 KSGQQEGAKL LCGGGAAADR GYFIQPTVFG DVKDGMTIAK EEIFGPVMQI
351 LKFKTIEEVV GRANNSKYGL AAAVFTKDLD KANYLSQALQ AGTVWINCYD
401 VFGAQSPFGG YKMSGSGREL GEYGLQAYTE VKTVTVKVPQ KNS

The coverage is 25%.

Post source decay analyses:

m/z	Range	sequence
990,5	273-281	(R) VVGNPFDSR (T)
1775,8	251-264	(R) TFVQEDVYDEFVER (S)

4.2.2. DLDH contributes to mitochondrial poly(ADP-ribosyl)ation

4.2.2.1. Western blot experiments

Mitochondria from rat liver were also treated with NO donors to induce nitrosative stress, and Western blot experiments with anti-PAR antibodies were carried out to check poly (ADP-ribosyl)ation of mitochondrial proteins. PARylation of proteins in

GSNO treated mitochondria was compared to control groups and revealed several PAR-positive protein bands in the isolated mitochondria samples (Figure 20.).

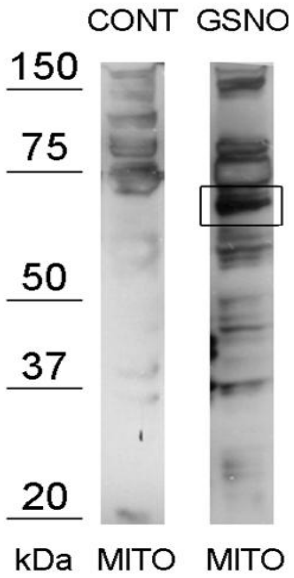

Figure 20. GSNO treatment of mitochondria results in extra PAR positive protein bands. A PARylated protein band at ~ 70 kDa was excised from the Comassie Blue stained gel of the GSNO treated mitochondria sample and was analyzed by mass spectrometry.

4.2.2.2. Mass spectrometry of DLDH

The protein in question was identified as mitochondrial dihydrolipoamide dehydrogenase (gi|38303871, MW: 54574 Da, pI: 7.96) a component of the alpha ketoglutarate dehydrogenase (KGDH) and pyruvate dehydrogenase (PDH) complexes (Figure 21.). The identity of the protein was confirmed by post source decay data of peptides ALTGGIAHLFK and GIEIPEVR.

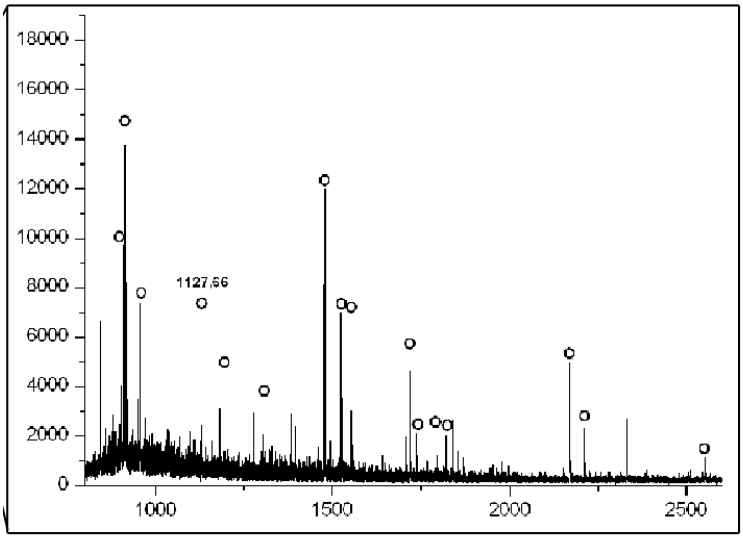

Figure 21. Positive protein mass fingerprint of DLDH. 37 masses were detected in the mass spectra, 15 of which corresponded to DLDH. The mass coverage was 36%. Post source decay analysis confirmed the identity of the protein.

Mass spectrometry data of DLDH:

gi|38303871 Dihydrolipoamide dehydrogenase [Rattus norvegicus]
(MW): 54574 Da, pI: 7.96

37 masses were detected in the spectra out of which 15 corresponded to this protein.

1 MQSWSRVYCS LAKKGHFNRL SHGLQGASSV PLRTYSDQPI DADVTVIGSG
51 PGGYVAAIKA AQLGFK**TVCI EKNETLGGTC LNVGCIPSKA LLNNSHYYHL**
101 **AHGK**DFASR**G IEIPEVR**LNL EKMMEQKRSA VK**ALTGGIAH LFK**QNK**VVHV**
151 **NGFGK**ITGK**N QVTATTADGS TQVIGTK**NIL IATGSEVTPF PGITIDEDTI
201 VSSTGALSLK KVPEKLVVIG AGVIGVELGS VWQRLGADVT AVEFLGHVGG
251 IGIDMEISKN FQRILQK**QGF KFKLNTKVTG ATK**KSDGKID VSVEAASGGK
301 **AEVITCDVLL VCIGRRPFTQ NLGLEELGIE LDPKGRIPVN TR**FQTKIPNI
351 FAIGDVVAGP MLAHKAEDEG IICVEGMAGG AVHIDYNCVP SVIYTHPEVA
401 WVGK**SEEQLK EEGVEFK**VGK **FPFAANSR**AK TNADTDGMVK ILGHKSTDRI
451 LGAHILGPGA GEMVNEAALA LEYGASCEDV AR**VCHAHPTL SEAFREANLA**
501 **ASFGKPINF**

The coverage is 36%.

Post source decay analyses of two masses:

m/z	tartomány	szekvencia
1127,8	133-143	(K) **ALTGGIAHLFK** (Q)
912,5	110-117	(R) **GIEIPEVR** (L)

4.2.2.3. DLDH causes extensive PARylation, but not increased PARP-1 presence

Incubation of the mitochondrial samples with excess recombinant DLDH protein resulted in strong PARylation of mitochondrial proteins that was concomitant with increased levels of PARP-1 presence, as confirmed by Western blot using anti-PAR and anti-PARP antibodies (Figure 22.).

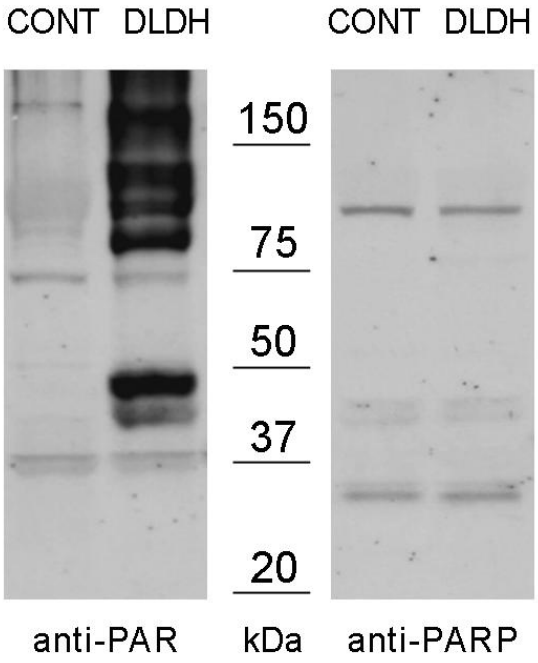

Figure 22. Excessive PARylation is not concurrent with excessive PARP-1 presence in rat liver mitochondria. Weak PARP-1 positive protein bands were detected in the mitochondria samples, however; the number and intensity of PAR-positive proteins were much higher.

4.2.3. PARP-like activity of the recombinant DLDH and KGDH enzymes

DLDH uses the same substrate as PARP, and shows strong PARylation in response to nitrosative agents just like PARP, we hypothesized that DLDH may have an intrinsic PARP-like enzymatic activity.

4.2.3.1. Modified protocol of Igamberdiev

In order to measure the intrinsic PARP-like activity of the recombinant DLDH and KGDH enzymes, we carried out Western blot analyses of the recombinant enzymes with anti-PAR antibody, as described earlier in Chapter 3.2.5.1. The enzymes were preincubated with their cofactors NADH and FAD^+ and optimal pH for their proper function was attained by $NaHPO_4$ in the incubation buffer mix. To mimic oxidative stress H_2O_2 was added to the same buffer mix. H_2O_2 treatment revealed one extra PARylated band at ~ 70 kDa in the DLDH group, and three major PAR positive bands in the KGDH group compared to the control (Figure 23.).

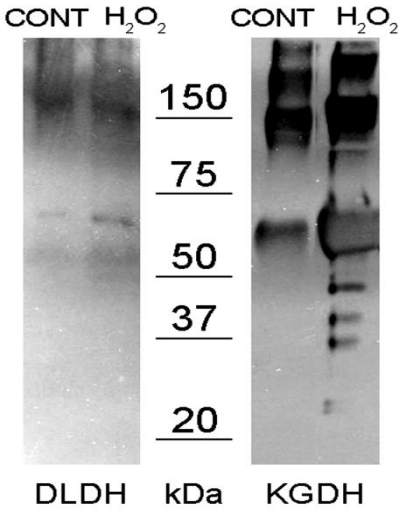

Figure 23. PARP-like enzymatic activity of the DLDH and KGDH enzymes. Western blot was carried out using anti-PAR antibody. H_2O_2 treatment of DLDH resulted in one weak PAR-positive protein band at ~ 70 kDa, which corresponds well with the known mass of DLDH. H_2O_2 treatment revealed three major and few smaller molecular weight PAR-positive protein bands in the KGDH group.

4.2.3.2. Colorimetric PARP assay

Using a colorimetric PARP enzyme activity assay kit, we were not able to detect significant PARP activity of DLDH compared to the 1U PARP positive control. However, KGDH showed significant PARP-like enzyme activity. The prototypical

PARP inhibitor 3-aminobenzamide inhibited PARP activity but did not affect the activity of KGDH (Figure 24.).

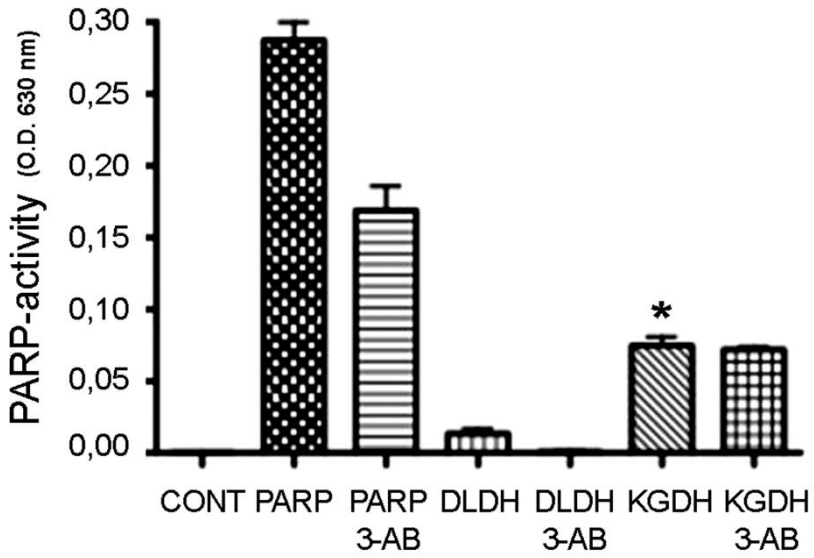

Figure 24. PARP-like enzymatic activity of the KGDH enzyme. 1 Unit PARP was used as positive control to measure PARP-like enzymatic activity of DLDH and KGDH. The PARP inhibitor 3-AB significantly decreased the activity of PARP. DLDH did not have a significant PARP-like activity, but KGDH showed significant PARP-like activity, which was not inhibitable by the PARP inhibitor 3-AB.

4.2.3.3. The inhibitor of DLDH diminishes PAR positive bands after nitrosative stress

Incubation of the mitochondrial samples with H_2O_2 or different NO donors, such as GSNO and SNAP (S-nitroso-N-acetylpenicillamine) resulted in extra PAR-positive bands on the Western blot. A specific inhibitor of dihydrolipoamide dehydrogenase (5-methoxyindole-2-carboxylic acid, MICA) diminished these extra PAR-positive bands (Figure 25.). The DLDH inhibitor MICA was added to the freshly isolated mitochondria samples 30 minutes prior to H_2O_2 or NO-donor treatment. Concentrations of MICA between 5-50 mM were tested in our previous studies, and the final concentration applied in the experiments was 5 mM, according to the available literature data (172), (179).

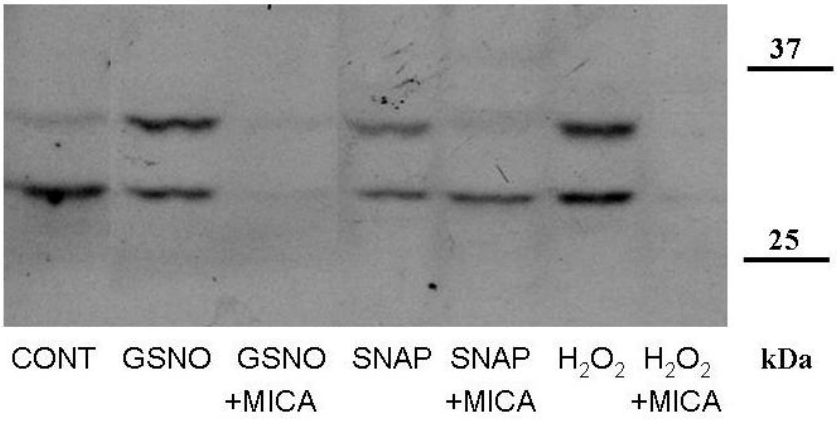

Figure 25. MICA inhibits the PARylation of proteins in the mitochondria. Treating mitochondria with H_2O_2 or different NO donors, such as GSNO and SNAP results in extra PAR – positive bands. MICA, the inhibitor of the DLDH enzyme inhibits the formation of these PAR positive bands.

4.3. NO measurement experiments

4.3.1. RNS production in mitochondria in an arginine-independent pathway

Isolated respiring mitochondria showed a similarly strong DAF fluorescence regardless of the presence or absence of the NOS substrate L-arginine or modulation of Ca^{2+} levels, the obligatory cofactor of NOS. Blockade of a potentially mitochondrial localized NOS by the competitive inhibitors L-NAME and L-NMMA failed to reduce mitochondrial DAF fluorescence. Prolonged in vivo application of L-NAME in the drinking water of the animals (10 mg/ml for 3 days) and supplementation of the mitochondria isolation buffers with L-NAME also failed to inhibit DAF fluorescence, making it very unlikely that the hypothetical mtNOS is responsible for the RNS production. Addition of $ONOO^-$ decomposition catalysts FeTPPS or FP15 to the mitochondria markedly decreased the fluorescence. Application of an SOD mimetic (M40401) or catalase or the co-application of both failed to affect the fluorescent signal, indicating that the DAF-FM fluorescence in mitochondria is not due to superoxide or hydrogen-peroxide but rather dependent on a nitrogen species such as $ONOO^-$. These experiments confirmed that mitochondria produce RNS independently from the L-arginine– NOS pathway or reactive oxygen species (Figure 26.).

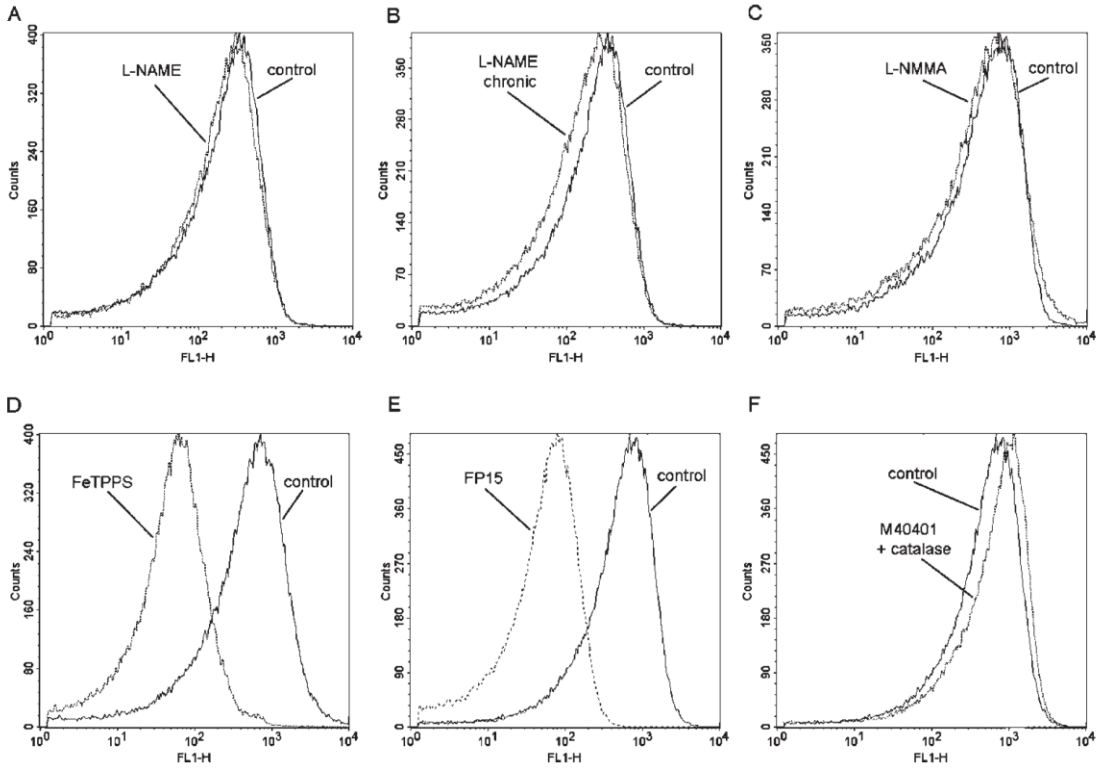

Figure 26. The role of reactive oxygen and nitrogen species in the generation of DAF fluorescence. The figure shows representative flow cytometric histograms of DAF-labeled freshly isolated mitochondria using the discontinuous Percoll gradient method. Control measurements were performed under conditions favorable for NOS activity, i.e. supplementation of the K^+ buffer with L-arginine (1mM) and $Ca2^+$ (1μM) and the omission of EGTA. The pharmacological substances were added to the heart mitochondria preparations before they were incubated with DAF. Panels A, B and C show that the NOS inhibitors L-NAME and L-NMMA in the absence of arginine and Ca^{2+} fail to prevent the occurrence of the mitochondrial DAF fluorescence signal. In case of L-NAME, even prolonged application for three days in the drinking water (Panel B, "chronic L-NAME") did not result in a reduced DAF signal. Panels D and E show that the presence of the ONOO decomposition catalysts FeTPPS and FP15 markedly inhibit DAF fluorescence. In contrast, Panel F shows that co-application of an SOD mimetic (MK40401) and catalase does not affect the RNS production. FL1-H: DAF-fluorescence, Counts: number of counted events.

Mitochondrial RNS production was also evaluated by the application of the spin trap CPH followed by electron spin resonance measurements. As seen on Figure 27, respiring mitochondria produced a significant amount of reactive species as shown using spin trapping technique. The generation of reactive species observed in this experiment was not sensitive to NO synthase inhibitors, complementing the data gathered by DAF fluorescence. Since the presence of SOD mimetics or $ONOO^-$

decomposition catalysts in the reaction mixture interferes with the ESR measurements, the following experiments were carried out by flow cytometric quantitation of DAF fluorescence.

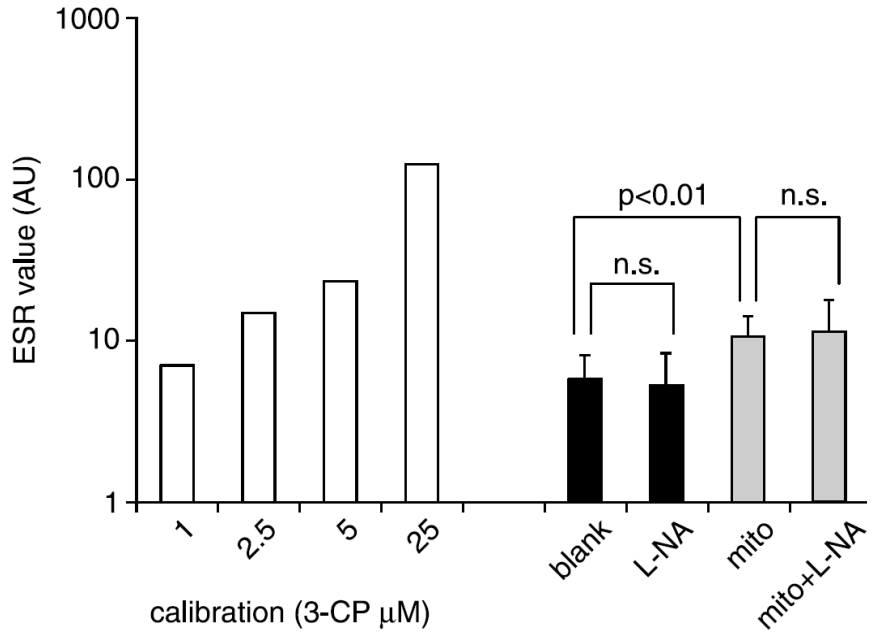

Figure 27. Measurement of mitochondrial reactive species production by EPR. Calibration data were obtained in mitochondria-free buffers containing increasing concentrations of the probe 3-CP. Live respiring heart mitochondria produced significant amounts of reactive species, which was not inhibitable by the presence of the NOS inhibitor N-nitro-L-arginine (L-NA).

Mitochondrial DAF fluorescence was markedly inhibited when the organelles were denatured by three cycles of freezing and thawing or heating the preparations to 95^0C for 5 min prior to the measurements. Similarly, DAF fluorescence was reduced when mitochondrial respiration was blocked by the application of rotenone or when respiratory substrates malate and glutamate (5mM each) were not supplemented in the medium. Inhibition of complex II by 3-NPA (100 μM) in the presence of complex I substrates malate and glutamate, or mitochondria respiring on succinate in the presence of the complex I inhibitor rotenone (5mM and 10μM, respectively) had similar fluorescence values, indicating that either complex I or complex II can supply electrons for the reaction. Inhibition of the ubiquinone oxidation site of complex III with myxothiazole (10 μM) slightly increased the fluorescence, supporting that the ubiquinone pool is necessary for the reaction. Inhibition of complex IV by cyanide (100

μM) or collapsing the proton gradient by FCCP (10 μM) had no effect on RNS production (Figure 28.).

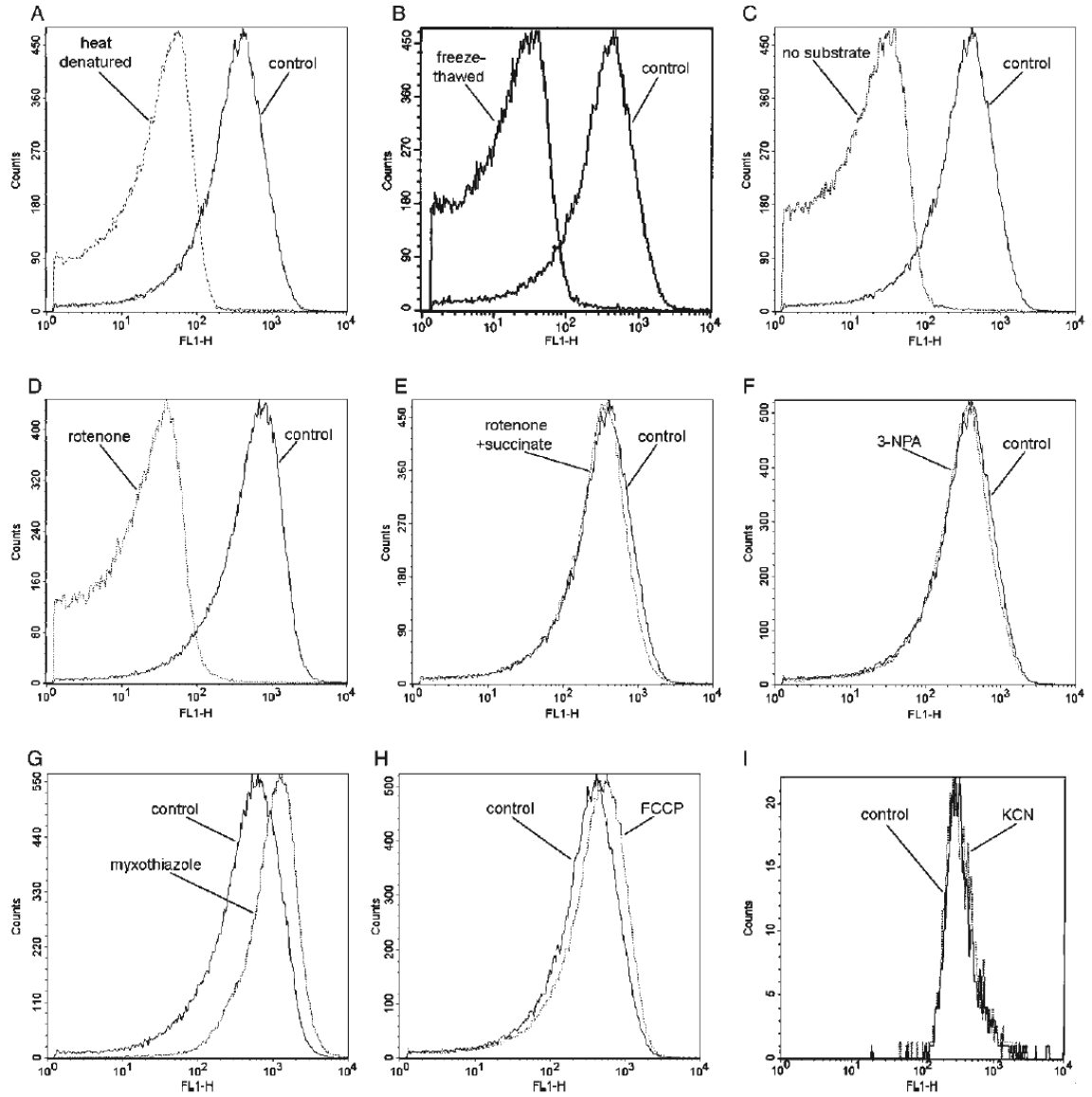

Figure 28. The role of the respiratory chain in generation of heart mitochondrial DAF fluorescence. The figure shows representative flow cytometric histograms of DAF-labeled freshly isolated mitochondria using the discontinuous Percoll gradient method. The pharmacological substances were added to the preparations before addition of the fluorescent probe. Panels A and B show that deenergizing the mitochondria by physical disruption (boiling for 5 min at 95 ^{0}C or three cycles of freezing and thawing) prevents the fluorescent conversion of DAF. Similar results can be obtained when the mitochondria do not receive any respiratory substrates (omission of malate and glutamate, Panel C) or when respiration is blocked by rotenone (Panel D). Panel E shows that respiration through complex I in the presence of glutamate and malate (control, Panel E) is equally effective as respiration through complex II in the presence of rotenone and succinate (Panel E). Panel F shows that the application of the succinate dehydrogenase inhibitor 3-NPA in the presence of glutamate and malate fails to

decrease the fluorescence. Disrupting the transmembrane proton gradient by FCCP or inhibiting cytochrome c oxidase by KCN also leaves RNS production unaffected (Panels H and I). However, myxothiazole, an inhibitor of the ubiquinone oxidation site of complex III slightly increases DAF fluorescence (Panel G). FL1-H: DAF-fluorescence, Counts: number of counted events.

4.3.2. Lack of mtNOS

First we attempted to locate a NOS-like protein in mouse heart mitochondria by Western blotting with a set of anti-NOS antibodies (data not shown). All of the antibodies reacted well with the positive controls but no specific mitochondrial bands were found at the expected molecular weights (144 kDa for eNOS, 150–160 kDa for nNOS and 125 kDa for iNOS). In addition, we confirmed these results in human tissues and did not find any NOS positive protein band in the mitochondria samples at the expected molecular weights (Fig. 29., Panel A). The physiological relevance of an enzyme is even more important than its quantity or localization, and the detection of its product, i.e. NO, is the first step in the determination of its role in a living organism. Therefore, we attempted to measure mitochondrial NO release by two independent methods. The gas-phase chemiluminescent technique is a direct and very sensitive method for the quantitation of NO in gas phase and it is routinely used in clinical settings to quantify the NO content of exhaled air. We detected as low as a few ppb NO in the headspace air of an NO donor, but in case of mitochondria the NO content was below the detection limit (Fig. 29., Panel B). Even though we could not detect mtNOS in mitochondria samples by Western blot, these results do not exclude the possibility that low levels of NO or other reactive nitrogen species are produced and metabolized in the mitochondrion without leaving the organelle.

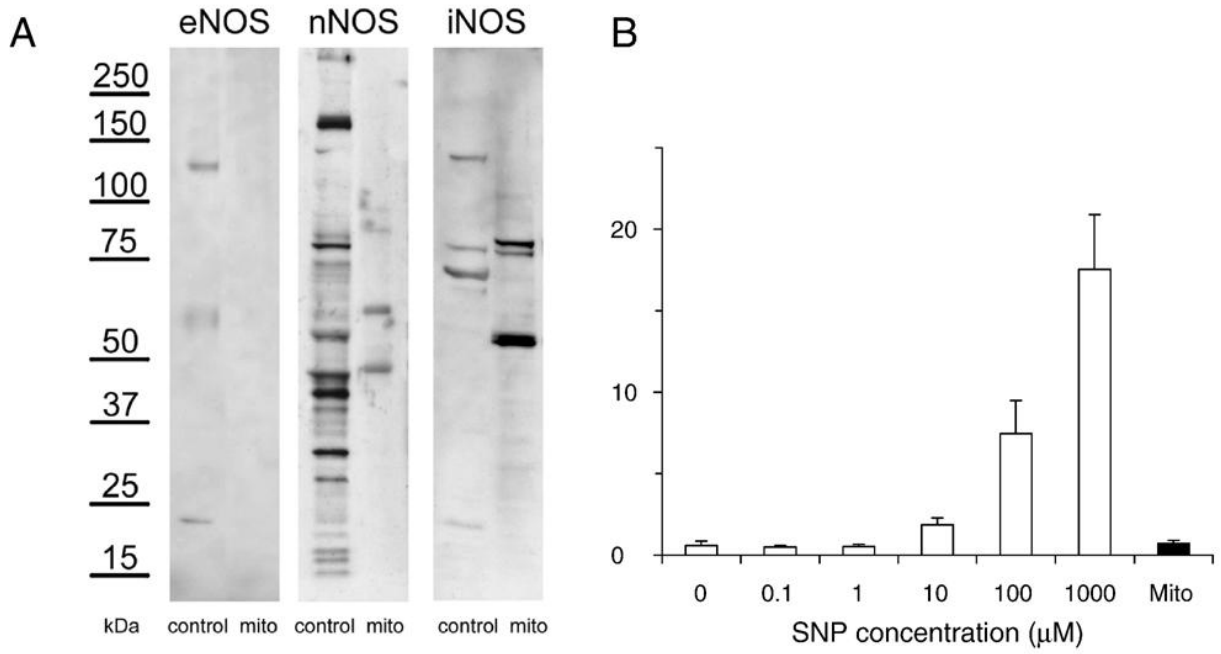

Figure 29. NOS isoforms and NO release in human heart mitochondria. Panel A shows Western blots with anti-NOS antibodies. Note that the positive controls contain a respective 140–160 kDa band and several unspecific lower molecular weight bands, while the mitochondria do not have a specific signal. Panel B shows gas-phase NO measurements after 45 - min incubation of mitochondria (n=6) in an air-tight container. Sodium nitroprusside (SNP) was used as a positive control.

5. DISCUSSION

Stem cell biology and regenerative medicine already have a great history, but scientists are still facing a problem of controlling the fate of transplanted cells. Although heart is one of the least regenerative organs, replacement of injured cardiac tissue gained great attention in the last decade, as heart diseases are the leading cause of hospitalization, morbidity and mortality of man in the Western world (180). Cell transplantation studies covered a wide range of potential cell types, including bone marrow cells, endothelial progenitor cells, mesenchymal stem cells, resident cardiac stem cells, embryonic stem cells, skeletal myoblasts and also cardiomyocytes. No agreement has been reached among scientific groups on the type of the most appropriate donor cells, on the techniques of cell application, and on the selection of the appropriate group of patients for cell therapy (181). Optimal timing of cell transplantation and long-term survival of implanted cells are still to be determined (16). Despite these controversies there is a general agreement that cell transplantation therapies of the injured heart reduce scar size and improve heart function. Abdel-Latif et al. carried out a meta-analysis with nearly a thousand patients and reported that bone marrow derived cell transplantation results in a modest 3.66% improvement of the left ventricular ejection fraction in patients with ischemic heart disease (182). Our earlier studies showed that mesenchymal stem cells can improve the survival of ischemic cardiomyocytes in co-culture. In this study we focused on the beneficial effects of healthy H9c2 cells on the survival of oxidatively damaged H9c2 cells in an *in vitro* ischemia model, and found that healthy H9c2 cells are able to increase the cell survival to the same extent as mesenchymal stem cells. Cells at various differentiation states had different effect on the cell survival ratio after oxygen-glucose deprivation. Up to date, many different hypotheses - such as transdifferentiation, cell fusion and direct cell-cell interactions - arose on the mode of action how neighboring cells can help each other to survive upon oxidative stress. There are various studies supporting each of these hypotheses. Some of them reported transdifferentiation of endothelial progenitor cells into cardiomyocytes without cell fusion but with cytoplasmic information transfer (183), while others described that cardiomyocytes are able to fuse with somatic and progenitor cell types (184), (185). The formation and importance of tunneling nanotubes

between different cell types has been also proved in many scientific articles (57), (58), (186). A study by Spees et al showed that mitochondrial transfer is possible in these tunneling membrane bridges. They found that mitochondria from stem cells can migrate to oxidative phosphorylation deficient cells, and can restore aerobic respiration (48). In our present study we found tunneling membrane tube formation between oxidatively damaged and healthy cardiomyocytes, and were also able to follow mitochondrial movement in these membrane bridges between cardiomyocytes. We found that healthy cardiomyocytes can save their oxidatively damaged neighbors from cell death in co-culture, but at the same time EtBr or F16 treated mitochondria–damaged cardiomyocytes were not able to save their neighbors from ischemic injury. We think that healthy mitochondria are necessary to achieve this 'rescue' effect and also showed that the presence of tunneling membrane bridges between cells enables mitochondrial traffic between OGD treated and healthy cardiomyocytes in cell culture. Although regenerating the heart is in the focus of research for the last ten years, it should be taken into consideration that there are still many gaps in our current knowledge. Cell-based cardiac therapies have the potential to improve heart function, but further research and long-term follow-up studies will be needed before safe clinical implications.

As we found an important role for mitochondria in our *in vitro* oxidative injury experiments, we were trying to find out what kind of molecular changes can occur in mitochondria following oxidative stress. Mitochondria are key performers both in oxidative and nitrosative stress. They are both sources and targets of ROS and RNS, and by releasing pro-apoptotic factors in hypoxic conditions, they also have a major role in cell death signaling. Oxidative and nitrosative injury leads to the post-translational modification of several proteins, including mitochondrial enzymes involved in respiration or energy metabolism. Stress induced post-translational modifications influence the activity of these enzymes, thus directly affecting cell signaling pathways. Poly (ADP-ribosyl)ation is a post-translational modification that occurs in the nucleus under normal conditions; however, overactivation of the nuclear PARP enzyme in hypoxia results in excess poly (ADP-ribose) polymer formation. PAR polymers were suggested as the moderator in the nuclear – to – mitochondrial crosstalk, transferring 'commit-suicide' signals and encouraging mitochondria to release AIF and cytochrome-c (141). How exactly PAR polymers communicate with mitochondria is not clear, but

experimental evidence showed that poly (ADP-ribosyl)ation is not the privilege of the PARP enzyme, and is not restricted to the nucleus. Some studies found PARP activity and poly (ADP-ribosyl)ation in the cytoplasm and also in the mitochondria (74), (142), (139). In this study we show that oxidative and nitrosative stress leads to the PARylation of several mitochondrial proteins, including the members of the Krebs cycle, urea cycle and the respiratory chain. ATPase and mtALDH are inhibited in oxidative stress, Otc has decreased level and CPS-1 releases from the mitochondria following oxidative or nitrosative stress (Table 5.), (150), (156), (187), (188), (189). Inhibition of ATPase leads to decreased ATP levels and finally to mitochondrial dysfunction. CPS-1 initiates the urea cycle and deficiency or decreased activity of the enzyme leads to hyperammonemia. Otc also has a role in the urea cycle and in arginine metabolism. In oxidative stress Otc preprotein does not translocate from the cytoplasm to the mitochondria causing decreased level of the mature protein. Oxidative stress results in lipid peroxidation and in the formation of toxic aldehydes such as, 4-hidroxy-2-nonenal (HNE), malondialdehyde (MDA). These toxic aldehydes inhibit mtALDH and also inhibit the mitochondrial respiration at complex II. and III. leading to changes in the mitochondrial transmembrane potential. Table 5. showes the effect of oxidative and nitrosative stress on the identified proteins and their role in mitochondrial energy maintenance and metabolism.

Name	Location	Subunit	Catalytic Activity	Function	During oxidative and nitrosative stress
mtALDH gi | 16073616	Mitochondrion matrix	Homotetramer	RCHO + NAD(P)+ + H2O = RCOOH + NAD(P)H + H+	Converts GTN to GDN, electron carrier activity, oxidoreductase activity	Inhibition of mtALDH, leads to nitrate tolerance, production of reactive lipid-derived aldehyde species, irreversible mitochondrial injury
ATPase gi | 92350	Inner mitochondrial membrane	F(1)- catalytic core F(0) – membrane proton channel	ATP + H2O + H+ (In) = ADP + Pi + H+ (Out)	Produces ATP from ADP in the presence of a proton gradient across the membrane	ATPase activity and ATP level decreases, leads to mitochondrial dysfunction
CPS1 gi | 8393186	Mitochondrion matrix	Small and large subunit	2ATP + HCO3- + NH3 = carbamoyl phosphate + 2ADP + Pi	Initiates the urea cycle and the biosynthesis of arginine and pyrimidines	CPS1 activity decreases, CPS1releases from mitochondria to plasma, leading to mitochondrial damage and depletion
Otc gi | 56789151	Mitochondrion matrix	Homotrimer	Carbamoyl phosphate + L-ornithine = phosphate + L-citrulline	Role in nitrogen metabolism and urea cycle	Oct activity decreases, mitochondrial import of the protein is inhibited, leading to mitochondrial dysfunction

Table 5. Structure and function of the identified poly (ADP-ribosyl)ated mitochondrial proteins. All of the identified proteins play an important role in mitochondrial homeostasis, energy maintenance and their inhibition leads to mitochondrial dysfunction. (Related references are cited in the text.)

DLDH, being a part of the PDH and KGDH enzymes plays an essential role in cell energy maintenance. DLDH has many different activities, which are influenced by the presence of free radicals, or by pH changes that occur in oxidative stress. In our experiments we showed by mass spectrometry that DLDH is PARylated in rat liver mitochondria following GSNO treatment and the incubation of mitochondria samples with the recombinant enzyme results in extensive PARylation of proteins that is not concomitant with increased PARP activity. The application of MICA – a specific DLDH inhibitor – have diminished or reduced the number of PAR-positive bands in isolated mitochondria samples following oxidative and nitrosative stress. In vitro enzyme activity assays showed PARP-like activity of KGDH in Western blot and spectrophotometric analysis. DLDH changes its oligomeric state under mitochondrial acidification in oxidative stress and has decreased activity. The inhibition of KGDH in oxidative stress is crucial for maintaining the energetic state of the cell. KGDH is inhibited or has decreased activity in oxidative or nitrosative stress (161), (162). KGDH is mainly inhibited by H_2O_2, but HNE, superoxide, peroxynitrite, and NO itself also decreases the activity of the enzyme. (164). PARylation of DLDH may be one of the factors responsible for the decreased activity of the KGDH enzyme in oxidative and nitrosative stress. Further studies are needed to determine whether KGDH is a physiological regulator of mitochondrial NAD and PAR metabolism, and whether it contributes to the pathological alterations in poly (ADP-ribosyl)ation in various diseases. Figure 30. shows the overall effect of oxidative and nitrosative stress on the identified five proteins.

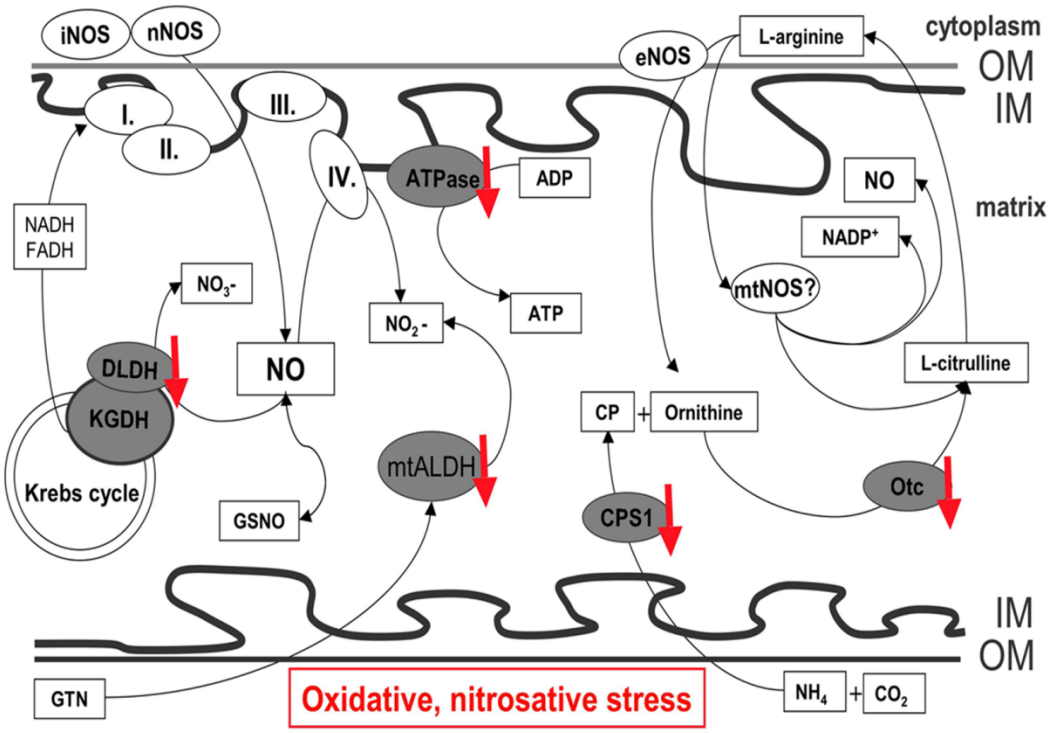

Figure 30. Mitochondrial proteomic changes following oxidative and nitrosative stress induced by H_2O_2 or NO-donors. The identified proteins are all important players in mitochondrial energy maintenance. Oxidative stress and nitrosative stress leads ti the inhibition or decreased activity of these enzymes. OM: outer membrane, IM: inner membrane, I., II., III., IV. : Respiratory chain complexes.

PARP is not the only enzyme that might have a mitochondrial counterpart. As it was mentioned earlier a putative mitochondrial nitric oxide synthase is believed to exist and believed to produce NO in the mitochondria, similarly to eNOS and nNOS. The first finding of mitochondrial NADPH diaphorase activity in basilar arteries, a marker of NO synthesis, was followed by several reports which suggested the presence of various NOS isoforms and also NO production within mitochondria (169), (96), (98), (92), (93). NO production in mitochondria was observed by several laboratories using diaminofluorescein fluorescent probes. However, in spite the strong DAF fluorescence signals in mitochondria, identification of any NOS-like protein in the mitochondria faces difficulties. Using several different antibodies against the known NOS isoforms we were not able to detect NOS-positive protein bands in human heart mitochondria samples; nor were we able to detect significant amounts of NO from the headspace air of mitochondria samples. DAF was also shown to be sensitive to peroxynitrite that is

readily formed from superoxide and NO in the mitochondria. In this study we tried to investigate if NO is produced by mtNOS in the arginine-to-citrulline conversion pathway in the mitochondria. It was shown in earlier studies that DAF fluorescence signals are unaffected by the genetic disruption of all known NOS isoforms (107), (108). Here we show that mitochondrial DAF fluorescence cannot be reduced even by rather high concentrations or prolonged application of NOS blockers (1mM L-NAME or L-NMMA, up to 3 days prior to the experiments in the drinking water of the animals). Withdrawal of L-arginine and Ca^{2+}, and the co-application of catalase and a SOD mimetic also failed to decrease DAF fluorescence in mitochondrial preparations, further supporting the idea that no arginine-dependent NOS is involved in the reaction. In contrast, the application of the $ONOO^-$ decomposition catalysts FP15 and FeTPPS, or denaturating the mitochondria, as well as the inhibition of mitochondrial respiration in the lack of substrates successfully prevented DAF fluorescence (190). Selective blockade of complex I. inhibits mitochondrial RNS production, which can be reversed by the addition of succinate, a complex II substrate. Conversely, inhibition of complex II in the presence of complex I substrates fails to prevent RNS production. Blocking the respiratory chain downstream of the ubiquinone pool did not affect DAF fluorescence. Myxothiazole, which inhibits the ubiquinone oxidation site of complex III even increases the mean DAF fluorescence to some extent, supporting the idea that the ubiquinone pool is necessary for RNS production. Unexpectedly, even the disruption of the membrane potential by the protonophore FCCP leaves mitochondrial DAF fluorescence intact in both isolated mitochondria as well as in the whole cell approach (190). Summarizing the experiments with respiratory chain inhibitors it is clear that electron transport through complexes I and II to the ubiquinone cycle is necessary for RNS production, however, the lack of a proton gradient or ATP production does not affect it. NO produced in different compartments of a cell or even in adjacent cells can easily diffuse into the mitochondria, finding superoxide readily there to form peroxynitrite that remains the main candidate responsible for the DAF fluorescence signals.

Controversies regarding the NO production by a putative mtNOS emerge mainly from the difficulties of reproducing experiments from various laboratories, because of the different mitochondria isolation protocols, contamination of the mitochondria

samples with other cellular components, such as the known eNOS isoform that was shown to be attached to the outer mitochondrial membrane. Henrich and colleagues located eNOS within sensory neurons and found that the enzyme is anchored to juxta-mitochondrial smooth endoplasmic reticulum (102). Gao et al. observed this phenomenon in endothelial cells and identified a pentabasic amino acid sequence in the autoinhibitory domain of eNOS, which is responsible for the mitochondrial docking of the enzyme (191). These findings indicate that mtNOS may indeed be a cellular NOS enzyme, which is loosely attached to the outer surface of mitochondria. Although there is not enough experimental evidence to prove it, one can hypothesize that mitochondrial attachment plays a role in the regulation of NOS activity, and thus docking of an active NOS on the outer membrane, with resultant NO production, regulates respiration. Genomic approaches were not able to detect a mitochondrial NOS gene in the genome, thus the putative NOS protein should be transported from the cytoplasm to the mitochondrial matrix via active transport. However, the known NOS isoforms do not possess the obligatory mitochondrial target sequence tag, required for the transportation of the protein to the mitochondria (174). In addition, the whole human heart mitochondrial proteome was described, but not any NOS isoforms were found among the mitochondrial proteins (192).

5. CONCLUSION

The ability of not only stem cells, but various cell types to improve cell survival after oxidative injury in our *in vitro* model suggest that it is not the differentiation state of the cells that mainly influence their beneficial effect, but more likely their intact energetic state. Mitochondria depletion forbid the rescue ability of cardiomyoblast co-cultured with oxidatively injured cells, pointing to the fact that healthy mitochondria play a crucial role in this process either by restoring energy levels in the dying cells or by inhibiting cell death signals of damaged mitochondria. The crosstalk between neighboring cells through tunneling membrane bridges, and the traffic of mitochondria-like particles along these membrane connections, highlights the importance of direct cell-to-cell contacts. Oxidative and nitrosative injury leads to the inhibition of several mitochondrial proteins, which can be partly explained by the poly (ADP-ribosyl)ation of these proteins. Inhibition of the Krebs cycle, urea cycle enzymes and respiratory chain complexes at the same time, leads to mitochondrial dysfunction, energy crisis and eventually cell death. α-ketoglutarate-dehydrogenase is a potential candidate that is responsible for the poly (ADP-ribosyl)ating events in mitochondria, as it uses similar cofactors as PARP, and serves as a target and generator of ROS and RNS in stress induced injuries. Nitric oxide alone can inhibit KGDH, but $ONOO^-$ - formed from NO and superoxide - is a more effective inhibitor of the enzyme. Although NO is present in the mitochondria we found no evidence for the existence of a mtNOS, but intense RNS production is possible on the respiratory chain, rather than on the arginine-dependent RNS production pathway.

6. ABSTRACT

Cell transplantation therapies are widely used treating several diseases – including stroke and myocardial infarction –, but in spite the completed clinical studies our understanding of the molecular mechanisms behind the regeneration process is still incomplete. The aim of the present study was to investigate the role of mitochondria in an in vitro model of cell transplantation after oxidative injury, and to follow molecular changes in the mitochondria as a source and target of reactive oxygen and reactive nitrogen species in oxidative injury. In our experiments we attempted to investigate the possible positive effects of the addition of healthy cells on the cell survival ratio of oxidatively injured cardiomyoblasts; and tried to outline the role of mitochondria in this beneficial effect. We found that the addition of healthy cells to oxidatively injured cardiomyoblasts can increase the number of surviving cells; while, on the contrary, mitochondria-depleted cells failed to improve the cell survival ratio. Our observation of the development of tunneling membrane bridges between healthy and oxidatively injured cells, and the finding of the traffic of mitochondria-like particles along these membrane connections between the cells, further points to the important role of mitochondria in this 'rescue' process. Mitochondria are not only important as energy sources of the cells, but also have major role in cell death signaling in oxidative and nitrosative stress. H_2O_2 and NO-donor treatment of isolated mitochondria samples resulted in the poly (ADP-ribosyl)ation of several mitochondrial proteins, including important members of the Krebs cycle, urea cycle and the respiratory chain. Concomitant inhibition of these proteins in oxidative injury leads to ATP depletion, membrane potential alteration, mitochondrial dysfunction, and finally cell death. We found a central role for α–ketoglutarate dehydrogenase in the poly (ADP-ribosyl)ating processes in the mitochondria. α–ketoglutarate dehydrogenase is inhibited by reactive oxygen and nitrogen species – such as H_2O_2, NO and $ONOO^-$ - , but it is also a source of free radicals. In search for possible NO and RNS sources in the mitochondria we could not identify the putative mtNOS, but found that mitochondria produce RNS mainly through the respiratory chain, rather than in an arginine-dependent pathway. These results indicate the important role of mitochondria in oxidative and nitrosative

injury, and highlight these organelles as a source of potential candidate molecules – such as KGDH – in combat with free radicals.

ÖSSZEFOGLALÁS

A sejtalapú terápiát számos betegség - mint például az iszkémiás stroke, vagy iszkémiás szívbetegségek - kezelésében egyre gyakrabban alkalmazzák a konvencionális kezelési módszerek mellett. A már lezajlott klinikai tanulmányok ellenére még mindig keveset tudunk a megfelelő sejttípus kiválasztásáról, a sejtek beadásának optimális módjáról és időpontjáról; és még kevesebbet a beültetett és a host sejtek között zajló molekuláris mechanizmusokról. Célunk a kívülről adott sejtek és a fogadó sejtek közötti direkt sejt-sejt kölcsönhatás vizsgálata volt egy *in vitro* iszkémia modellben, illetve a mitokondriumok szerepének leírása oxidatív és nitrozatív stresszel járó folyamatokban. Kísérleteinkben az oxidatív stresszen átesett kardiomioblasztok túlélési arányát szignifikánsan javította egészséges kardiomioblasztok jelenléte a sejtkultúrában, ezzel ellentétben, károsodott mitokondriummal rendelkező sejtek nem voltak képesek javítani az oxidatív stresszen átesett kardiomioblasztok túlélési arányát. A mitokondriumok szerepét emeli ki az a megfigyelésünk, hogy az egészséges és az oxidatív stresszen átesett sejtek egymás között membránfolyosókat alakítottak ki, amelyekben intenzív mitokondrium mozgást figyeltünk meg. Az oxidatív és nitrozatív stresszben a mitokondriumban bekövetkező molekuláris változások megfigyelésekor számos poly (ADP-ribozil)ált fehérjét találtunk, amelyek fontos szereplői a Krebs ciklusnak, urea ciklusnak vagy az elektron transzport láncnak. Ezeknek az enzimeknek oxidatív streszzben bekövetkező egyidejű gátlása az ATP raktárak kiürüléséhez, a membránpotenciál nagymértékű megváltozásához, mitokondriális diszfunkcióhoz és végül a sejt halálához vezethet. A Krebs ciklus egyik enzime, az α-ketoglutarát dehidrogenáz komplex, poly (ADP-ribozil)áló hatást mutatott színreakción alapuló enzim assay-ben és Western blot analízissel is. A KGDH-t a NO, H_2O_2 és a $ONOO^-$ is gátolja, de ez az enzim akár a szabadgyökök forrásaként is szolgálhat. Lehetséges NO forrásokat keresve a mitokondriumban nem találtunk mtNOS aktivitást, de megfigyeléseink alapján a reaktív nitrogén származékok termelése a mitokondriumban főként a légzési láncon zajlik, nem pedig egy arginin-függő útvonalon. Ezek az eredmények a mitokondriumok központi szerepét mutatják oxidatív és nitrozatív sejtkárosodáskor, és felhivják a figyelmet arra, hogy a mitokondriumok tartogatnak potenciális célpontokat – mint például a KGDH – a szabadgyökök elleni küzdelemre.

REFERENCE LIST

(1) Beltrami, A.P. et al. (2001). Evidence that human cardiac myocytes divide after myocardial infarction. N Engl J Med 344, 1750-7.

(2) Kim, B.O. et al. (2005). Cell transplantation improves ventricular function after a myocardial infarction: a preclinical study of human unrestricted somatic stem cells in a porcine model. Circulation 112, I96-104.

(3) Hiasa, K. et al. (2004). Bone marrow mononuclear cell therapy limits myocardial infarct size through vascular endothelial growth factor. Basic Res Cardiol 99, 165-72.

(4) Thompson, R.B., Emani, S.M., Davis, B.H., van den Bos, E.J., Morimoto, Y., Craig, D., Glower, D. and Taylor, D.A. (2003). Comparison of intracardiac cell transplantation: autologous skeletal myoblasts versus bone marrow cells. Circulation 108 Suppl 1, II264-71.

(5) Reffelmann, T., Leor, J., Muller-Ehmsen, J., Kedes, L. and Kloner, R.A. (2003). Cardiomyocyte transplantation into the failing heart-new therapeutic approach for heart failure? Heart Fail Rev 8, 201-11.

(6) Kim, S.U. and de Vellis, J. (2009). Stem cell-based cell therapy in neurological diseases: a review. J Neurosci Res 87, 2183-200.

(7) Peault, B. et al. (2007). Stem and progenitor cells in skeletal muscle development, maintenance, and therapy. Mol Ther 15, 867-77.

(8) Hipp, J. and Atala, A. (2008). Sources of stem cells for regenerative medicine. Stem Cell Rev 4, 3-11.

(9) Wei, H.M., Wong, P., Hsu, L.F. and Shim, W. (2009). Human bone marrow-derived adult stem cells for post-myocardial infarction cardiac repair: current status and future directions. Singapore Med J 50, 935-42.

(10) Limbourg, A., Limbourg, F. and Drexler, H. (2009). Cell-based therapies for ischemic heart disease--"trick and treat". Circ J 73, 2179-82.

(11) Mathiasen, A.B., Haack-Sorensen, M. and Kastrup, J. (2009). Mesenchymal stromal cells for cardiovascular repair: current status and future challenges. Future Cardiol 5, 605-17.

(12) George, J.C. Stem cell therapy in acute myocardial infarction: a review of clinical trials. Transl Res 155, 10-9.

(13) Roell, W. et al. (2002). Cellular cardiomyoplasty improves survival after myocardial injury. Circulation 105, 2435-41.

(14) Li, R.K., Jia, Z.Q., Weisel, R.D., Mickle, D.A., Zhang, J., Mohabeer, M.K., Rao, V. and Ivanov, J. (1996). Cardiomyocyte transplantation improves heart function. Ann Thorac Surg 62, 654-60; discussion 660-1.

(15) Sakai, T., Li, R.K., Weisel, R.D., Mickle, D.A., Kim, E.J., Tomita, S., Jia, Z.Q. and Yau, T.M. (1999). Autologous heart cell transplantation improves cardiac function after myocardial injury. Ann Thorac Surg 68, 2074-80; discussion 2080-1.

(16) Jawad, H., Lyon, A.R., Harding, S.E., Ali, N.N. and Boccaccini, A.R. (2008). Myocardial tissue engineering. Br Med Bull 87, 31-47.

(17) Strauer, B.E., Brehm, M., Zeus, T., Kostering, M., Hernandez, A., Sorg, R.V., Kogler, G. and Wernet, P. (2002). Repair of infarcted myocardium by autologous intracoronary mononuclear bone marrow cell transplantation in humans. Circulation 106, 1913-8.

(18) Hamano, K. et al. (2001). Local implantation of autologous bone marrow cells for therapeutic angiogenesis in patients with ischemic heart disease: clinical trial and preliminary results. Jpn Circ J 65, 845-7.

(19) Qian, H., Yang, Y., Huang, J., Dou, K. and Yang, G. (2006). Cellular cardiomyoplasty by catheter-based infusion of stem cells in clinical settings. Transpl Immunol 16, 135-47.

(20) Perin, E.C. and Lopez, J. (2006). Methods of stem cell delivery in cardiac diseases. Nat Clin Pract Cardiovasc Med 3 Suppl 1, S110-3.

(21) Haider, H. and Ashraf, M. (2005). Bone marrow stem cell transplantation for cardiac repair. Am J Physiol Heart Circ Physiol 288, H2557-67.

(22) Collins, S.D., Baffour, R. and Waksman, R. (2007). Cell therapy in myocardial infarction. Cardiovasc Revasc Med 8, 43-51.

(23) Beeres, S.L., Atsma, D.E., van Ramshorst, J., Schalij, M.J. and Bax, J.J. (2008). Cell therapy for ischaemic heart disease. Heart 94, 1214-26.

(24) Thompson, C.A. et al. (2003). Percutaneous transvenous cellular cardiomyoplasty. A novel nonsurgical approach for myocardial cell transplantation. J Am Coll Cardiol 41, 1964-71.

(25) Larose, E., Proulx, G., Voisine, P., Rodes-Cabau, J., De Larochelliere, R., Rossignol, G., Bertrand, O.F. and Tremblay, J.P. Percutaneous versus surgical delivery of autologous myoblasts after chronic myocardial infarction: an in vivo cardiovascular magnetic resonance study. Catheter Cardiovasc Interv 75, 120-7.

(26) Herreros, J. et al. (2003). Autologous intramyocardial injection of cultured skeletal muscle-derived stem cells in patients with non-acute myocardial infarction. Eur Heart J 24, 2012-20.

(27) Dib, N. et al. (2005). Safety and feasibility of autologous myoblast transplantation in patients with ischemic cardiomyopathy: four-year follow-up. Circulation 112, 1748-55.

(28) van Laake, L.W. et al. Extracellular matrix formation after transplantation of human embryonic stem cell-derived cardiomyocytes. Cell Mol Life Sci 67, 277-90.

(29) Deb, A., Wang, S., Skelding, K.A., Miller, D., Simper, D. and Caplice, N.M. (2003). Bone marrow-derived cardiomyocytes are present in adult human heart: A study of gender-mismatched bone marrow transplantation patients. Circulation 107, 1247-9.

(30) Jackson, K.A. et al. (2001). Regeneration of ischemic cardiac muscle and vascular endothelium by adult stem cells. J Clin Invest 107, 1395-402.

(31) Messina, E. et al. (2004). Isolation and expansion of adult cardiac stem cells from human and murine heart. Circ Res 95, 911-21.

(32) Oh, H. et al. (2003). Cardiac progenitor cells from adult myocardium: homing, differentiation, and fusion after infarction. Proc Natl Acad Sci U S A 100, 12313-8.

(33) Tomita, S., Li, R.K., Weisel, R.D., Mickle, D.A., Kim, E.J., Sakai, T. and Jia, Z.Q. (1999). Autologous transplantation of bone marrow cells improves damaged heart function. Circulation 100, II247-56.

(34) Pittenger, M.F. and Martin, B.J. (2004). Mesenchymal stem cells and their potential as cardiac therapeutics. Circ Res 95, 9-20.

(35) Caplan, A.I. and Dennis, J.E. (2006). Mesenchymal stem cells as trophic mediators. J Cell Biochem 98, 1076-84.

(36) Kinnaird, T., Stabile, E., Burnett, M.S., Lee, C.W., Barr, S., Fuchs, S. and Epstein, S.E. (2004). Marrow-derived stromal cells express genes encoding a broad spectrum of arteriogenic cytokines and promote in vitro and in vivo arteriogenesis through paracrine mechanisms. Circ Res 94, 678-85.

(37) Singla, D.K., Singla, R.D. and McDonald, D.E. (2008). Factors released from embryonic stem cells inhibit apoptosis in H9c2 cells through PI3K/Akt but not ERK pathway. Am J Physiol Heart Circ Physiol 295, H907-13.

(38) Koyanagi, M., Brandes, R.P., Haendeler, J., Zeiher, A.M. and Dimmeler, S. (2005). Cell-to-cell connection of endothelial progenitor cells with cardiac myocytes by nanotubes: a novel mechanism for cell fate changes? Circ Res 96, 1039-41.

(39) Rangappa, S., Entwistle, J.W., Wechsler, A.S. and Kresh, J.Y. (2003). Cardiomyocyte-mediated contact programs human mesenchymal stem cells to express cardiogenic phenotype. J Thorac Cardiovasc Surg 126, 124-32.

(40) Xu, M., Wani, M., Dai, Y.S., Wang, J., Yan, M., Ayub, A. and Ashraf, M. (2004). Differentiation of bone marrow stromal cells into the cardiac phenotype requires intercellular communication with myocytes. Circulation 110, 2658-65.

(41) Fukuhara, S., Tomita, S., Yamashiro, S., Morisaki, T., Yutani, C., Kitamura, S. and Nakatani, T. (2003). Direct cell-cell interaction of cardiomyocytes is key for bone marrow stromal cells to go into cardiac lineage in vitro. J Thorac Cardiovasc Surg 125, 1470-80.

(42) Wang, T., Xu, Z., Jiang, W. and Ma, A. (2006). Cell-to-cell contact induces mesenchymal stem cell to differentiate into cardiomyocyte and smooth muscle cell. Int J Cardiol 109, 74-81.

(43) Cselenyak, A., Pankotai, E., Horvath, E.M., Kiss, L. and Lacza, Z. Mesenchymal stem cells rescue cardiomyoblasts from cell death in an in vitro ischemia model via direct cell-to-cell connections. BMC Cell Biol 11, 29.

(44) Plotnikov, E.Y. et al. (2008). Cell-to-cell cross-talk between mesenchymal stem cells and cardiomyocytes in co-culture. J Cell Mol Med 12, 1622-31.

(45) Driesen, R.B. et al. (2005). Partial cell fusion: a newly recognized type of communication between dedifferentiating cardiomyocytes and fibroblasts. Cardiovasc Res 68, 37-46.

(46) Wallace, D.C. (1994). Mitochondrial DNA sequence variation in human evolution and disease. Proc Natl Acad Sci U S A 91, 8739-46.

(47) Dyall, S.D., Brown, M.T. and Johnson, P.J. (2004). Ancient invasions: from endosymbionts to organelles. Science 304, 253-7.

(48) Spees, J.L., Olson, S.D., Whitney, M.J. and Prockop, D.J. (2006). Mitochondrial transfer between cells can rescue aerobic respiration. Proc Natl Acad Sci U S A 103, 1283-8.

(49) King, M.P. and Attardi, G. (1989). Human cells lacking mtDNA: repopulation with exogenous mitochondria by complementation. Science 246, 500-3.

(50) Bodnar, A.G., Cooper, J.M., Holt, I.J., Leonard, J.V. and Schapira, A.H. (1993). Nuclear complementation restores mtDNA levels in cultured cells from a patient with mtDNA depletion. Am J Hum Genet 53, 663-9.

(51) Kumar, N.M. and Gilula, N.B. (1996). The gap junction communication channel. Cell 84, 381-8.

(52) Yeager, M. and Harris, A.L. (2007). Gap junction channel structure in the early 21st century: facts and fantasies. Curr Opin Cell Biol 19, 521-8.

(53) Kresh, J.Y. (2006). Cell replacement therapy: the functional importance of myocardial architecture and intercellular gap-junction distribution. J Thorac Cardiovasc Surg 131, 1310-3.

(54) Fevrier, B. and Raposo, G. (2004). Exosomes: endosomal-derived vesicles shipping extracellular messages. Curr Opin Cell Biol 16, 415-21.

(55) Rustom, A., Saffrich, R., Markovic, I., Walther, P. and Gerdes, H.H. (2004). Nanotubular highways for intercellular organelle transport. Science 303, 1007-10.

(56) Gerdes, H.H., Bukoreshtliev, N.V. and Barroso, J.F. (2007). Tunneling nanotubes: a new route for the exchange of components between animal cells. FEBS Lett 581, 2194-201.

(57) Gurke, S., Barroso, J.F. and Gerdes, H.H. (2008). The art of cellular communication: tunneling nanotubes bridge the divide. Histochem Cell Biol 129, 539-50.

(58) Gerdes, H.H. and Carvalho, R.N. (2008). Intercellular transfer mediated by tunneling nanotubes. Curr Opin Cell Biol 20, 470-5.

(59) Assmus, B. et al. (2002). Transplantation of Progenitor Cells and Regeneration Enhancement in Acute Myocardial Infarction (TOPCARE-AMI). Circulation 106, 3009-17.

(60) Schachinger, V., Assmus, B., Honold, J., Lehmann, R., Hofmann, W.K., Martin, H., Dimmeler, S. and Zeiher, A.M. (2006). Normalization of coronary blood flow in the infarct-related artery after intracoronary progenitor cell therapy: intracoronary Doppler substudy of the TOPCARE-AMI trial. Clin Res Cardiol 95, 13-22.

(61) Assmus, B. et al. (2010). Clinical outcome 2 years after intracoronary administration of bone marrow-derived progenitor cells in acute myocardial infarction. Circ Heart Fail 3, 89-96.

(62) Kang, H.J. et al. (2004). Effects of intracoronary infusion of peripheral blood stem-cells mobilised with granulocyte-colony stimulating factor on left ventricular systolic function and restenosis after coronary stenting in myocardial infarction: the MAGIC cell randomised clinical trial. Lancet 363, 751-6.

(63) Wollert, K.C. et al. (2004). Intracoronary autologous bone-marrow cell transfer after myocardial infarction: the BOOST randomised controlled clinical trial. Lancet 364, 141-8.

(64) Balogh, L., Czuriga, I., Hunyadi, J., Galuska, L., Kristof, E. and Edes, I. (2007). [Effects of autologous bone marrow derived CD34+ stem cells on the left ventricular function following myocardial infarction]. Orv Hetil 148, 243-9.

(65) Dimmeler, S. and Zeiher, A.M. (2009). Cell therapy of acute myocardial infarction: open questions. Cardiology 113, 155-60.

(66) Thiele, H., Schuster, A., Erbs, S., Linke, A., Lenk, K., Adams, V., Hambrecht, R. and Schuler, G. (2009). Cardiac magnetic resonance imaging at 3 and 15 months after application of circulating progenitor cells in recanalised chronic total occlusions. Int J Cardiol 135, 287-95.

(67) Barouch, L.A. et al. (2002). Nitric oxide regulates the heart by spatial confinement of nitric oxide synthase isoforms. Nature 416, 337-9.

(68) Giulivi, C. (2003). Characterization and function of mitochondrial nitric-oxide synthase. Free Radic Biol Med 34, 397-408.

(69) Brookes, P.S. (2004). Mitochondrial nitric oxide synthase. Mitochondrion 3, 187-204.

(70) Lacza, Z. et al. (2006). Mitochondrial NO and reactive nitrogen species production: does mtNOS exist? Nitric Oxide 14, 162-8.

(71) van Wijk, S.J. and Hageman, G.J. (2005). Poly(ADP-ribose) polymerase-1 mediated caspase-independent cell death after ischemia/reperfusion. Free Radic Biol Med 39, 81-90.

(72) Jorcke, D., Ziegler, M., Herrero-Yraola, A. and Schweiger, M. (1998). Enzymic, cysteine-specific ADP-ribosylation in bovine liver mitochondria. Biochem J 332 (Pt 1), 189-93.

(73) Ziegler, M., Jorcke, D. and Schweiger, M. (1997). Identification of bovine liver mitochondrial NAD+ glycohydrolase as ADP-ribosyl cyclase. Biochem J 326 (Pt 2), 401-5.

(74) Du, L. et al. (2003). Intra-mitochondrial poly(ADP-ribosylation) contributes to NAD+ depletion and cell death induced by oxidative stress. J Biol Chem 278, 18426-33.

(75) Yu, S.W. et al. (2002). Mediation of poly(ADP-ribose) polymerase-1-dependent cell death by apoptosis-inducing factor. Science 297, 259-63.

(76) Turrens, J.F., Alexandre, A. and Lehninger, A.L. (1985). Ubisemiquinone is the electron donor for superoxide formation by complex III of heart mitochondria. Arch Biochem Biophys 237, 408-14.

(77) Fiskum, G. (1985). Mitochondrial damage during cerebral ischemia. Ann Emerg Med 14, 810-5.

(78) Radi, R., Beckman, J.S., Bush, K.M. and Freeman, B.A. (1991). Peroxynitrite-induced membrane lipid peroxidation: the cytotoxic potential of superoxide and nitric oxide. Arch Biochem Biophys 288, 481-7.

(79) Chan, P.H. (1996). Role of oxidants in ischemic brain damage. Stroke 27, 1124-9.

(80) Stridh, H., Kimland, M., Jones, D.P., Orrenius, S. and Hampton, M.B. (1998). Cytochrome c release and caspase activation in hydrogen peroxide- and tributyltin-induced apoptosis. FEBS Lett 429, 351-5.

(81) Uberti, D., Yavin, E., Gil, S., Ayasola, K.R., Goldfinger, N. and Rotter, V. (1999). Hydrogen peroxide induces nuclear translocation of p53 and apoptosis in cells of oligodendroglia origin. Brain Res Mol Brain Res 65, 167-75.

(82) Hampton, M.B. and Orrenius, S. (1997). Dual regulation of caspase activity by hydrogen peroxide: implications for apoptosis. FEBS Lett 414, 552-6.

(83) Halliwell, B. and Gutteridge, J.M. (1990). Role of free radicals and catalytic metal ions in human disease: an overview. Methods Enzymol 186, 1-85.

(84) Sies, H. (1991). Oxidative stress: from basic research to clinical application. Am J Med 91, 31S-38S.

(85) Batty, E., Jensen, K. and Freemont, P. (2009). PML nuclear bodies and their spatial relationships in the mammalian cell nucleus. Front Biosci 14, 1182-96.

(86) Cleeter, M.W., Cooper, J.M., Darley-Usmar, V.M., Moncada, S. and Schapira, A.H. (1994). Reversible inhibition of cytochrome c oxidase, the terminal enzyme of the mitochondrial respiratory chain, by nitric oxide. Implications for neurodegenerative diseases. FEBS Lett 345, 50-4.

(87) Mason, M.G., Nicholls, P., Wilson, M.T. and Cooper, C.E. (2006). Nitric oxide inhibition of respiration involves both competitive (heme) and noncompetitive (copper) binding to cytochrome c oxidase. Proc Natl Acad Sci U S A 103, 708-13.

(88) Brown, G.C. and Borutaite, V. (2002). Nitric oxide inhibition of mitochondrial respiration and its role in cell death. Free Radic Biol Med 33, 1440-50.

(89) Brown, G.C. and Borutaite, V. (2007). Nitric oxide and mitochondrial respiration in the heart. Cardiovasc Res 75, 283-90.

(90) Zoratti, M. and Szabo, I. (1995). The mitochondrial permeability transition. Biochim Biophys Acta 1241, 139-76.

(91) Skulachev, V.P. (1998). Cytochrome c in the apoptotic and antioxidant cascades. FEBS Lett 423, 275-80.

(92) Bates, T.E., Loesch, A., Burnstock, G. and Clark, J.B. (1996). Mitochondrial nitric oxide synthase: a ubiquitous regulator of oxidative phosphorylation? Biochem Biophys Res Commun 218, 40-4.

(93) Bates, T.E., Loesch, A., Burnstock, G. and Clark, J.B. (1995). Immunocytochemical evidence for a mitochondrially located nitric oxide synthase in brain and liver. Biochem Biophys Res Commun 213, 896-900.

(94) Lacza, Z., Puskar, M., Figueroa, J.P., Zhang, J., Rajapakse, N. and Busija, D.W. (2001). Mitochondrial nitric oxide synthase is constitutively active and is functionally upregulated in hypoxia. Free Radic Biol Med 31, 1609-15.

(95) Hotta, Y. et al. (1999). Protective role of nitric oxide synthase against ischemia-reperfusion injury in guinea pig myocardial mitochondria. Eur J Pharmacol 380, 37-48.

(96) Loesch, A., Belai, A. and Burnstock, G. (1994). An ultrastructural study of NADPH-diaphorase and nitric oxide synthase in the perivascular nerves and vascular endothelium of the rat basilar artery. J Neurocytol 23, 49-59.

(97) Tatoyan, A. and Giulivi, C. (1998). Purification and characterization of a nitric-oxide synthase from rat liver mitochondria. J Biol Chem 273, 11044-8.

(98) Ghafourifar, P. and Richter, C. (1997). Nitric oxide synthase activity in mitochondria. FEBS Lett 418, 291-6.

(99) Navarro, A. and Boveris, A. (2008). Mitochondrial nitric oxide synthase, mitochondrial brain dysfunction in aging, and mitochondria-targeted antioxidants. Adv Drug Deliv Rev 60, 1534-44.

(100) Frandsen, U., Lopez-Figueroa, M. and Hellsten, Y. (1996). Localization of nitric oxide synthase in human skeletal muscle. Biochem Biophys Res Commun 227, 88-93.

(101) Rothe, F., Huang, P.L. and Wolf, G. (1999). Ultrastructural localization of neuronal nitric oxide synthase in the laterodorsal tegmental nucleus of wild-type and knockout mice. Neuroscience 94, 193-201.

(102) Henrich, M., Hoffmann, K., Konig, P., Gruss, M., Fischbach, T., Godecke, A., Hempelmann, G. and Kummer, W. (2002). Sensory neurons respond to hypoxia with NO production associated with mitochondria. Mol Cell Neurosci 20, 307-22.

(103) Li, G., Regunathan, S. and Reis, D.J. (1995). Agmatine is synthesized by a mitochondrial arginine decarboxylase in rat brain. Ann N Y Acad Sci 763, 325-9.

(104) Galea, E., Regunathan, S., Eliopoulos, V., Feinstein, D.L. and Reis, D.J. (1996). Inhibition of mammalian nitric oxide synthases by agmatine, an endogenous polyamine formed by decarboxylation of arginine. Biochem J 316 (Pt 1), 247-9.

(105) Lacza, Z., Pankotai, E. and Busija, D.W. (2009). Mitochondrial nitric oxide synthase: current concepts and controversies. Front Biosci 14, 4436-43.

(106) Venkatakrishnan, P., Nakayasu, E.S., Almeida, I.C. and Miller, R.T. (2009). Absence of nitric-oxide synthase in sequentially purified rat liver mitochondria. J Biol Chem 284, 19843-55.

(107) Lacza, Z., Snipes, J.A., Zhang, J., Horvath, E.M., Figueroa, J.P., Szabo, C. and Busija, D.W. (2003). Mitochondrial nitric oxide synthase is not eNOS, nNOS or iNOS. Free Radic Biol Med 35, 1217-28.

(108) Lacza, Z. et al. (2004). Lack of mitochondrial nitric oxide production in the mouse brain. J Neurochem 90, 942-51.

(109) French, S., Giulivi, C. and Balaban, R.S. (2001). Nitric oxide synthase in porcine heart mitochondria: evidence for low physiological activity. Am J Physiol Heart Circ Physiol 280, H2863-7.

(110) Tanuma, S., Yagi, T. and Johnson, G.S. (1985). Endogenous ADP ribosylation of high mobility group proteins 1 and 2 and histone H1 following DNA damage in intact cells. Arch Biochem Biophys 237, 38-42.

(111) Whitacre, C.M., Hashimoto, H., Tsai, M.L., Chatterjee, S., Berger, S.J. and Berger, N.A. (1995). Involvement of NAD-poly(ADP-ribose) metabolism in p53 regulation and its consequences. Cancer Res 55, 3697-701.

(112) Virag, L. and Szabo, C. (2002). The therapeutic potential of poly(ADP-ribose) polymerase inhibitors. Pharmacol Rev 54, 375-429.

(113) Kawaichi, M., Ueda, K. and Hayaishi, O. (1981). Multiple autopoly(ADP-ribosyl)ation of rat liver poly(ADP-ribose) synthetase. Mode of modification and properties of automodified synthetase. J Biol Chem 256, 9483-9.

(114) Oei, S.L. and Ziegler, M. (2000). ATP for the DNA ligation step in base excision repair is generated from poly(ADP-ribose). J Biol Chem 275, 23234-9.

(115) Ullrich, O., Ciftci, O. and Hass, R. (2000). Proteasome activation by poly-ADP-ribose-polymerase in human myelomonocytic cells after oxidative stress. Free Radic Biol Med 29, 995-1004.

(116) Germain, M., Affar, E.B., D'Amours, D., Dixit, V.M., Salvesen, G.S. and Poirier, G.G. (1999). Cleavage of automodified poly(ADP-ribose) polymerase during apoptosis. Evidence for involvement of caspase-7. J Biol Chem 274, 28379-84.

(117) Rosenthal, D.S., Simbulan, C.M. and Smulson, M.E. (1995). Model systems for the study of the role of PADPRP in essential biological processes. Biochimie 77, 439-43.

(118) Cregan, S.P., Dawson, V.L. and Slack, R.S. (2004). Role of AIF in caspase-dependent and caspase-independent cell death. Oncogene 23, 2785-96.

(119) Crowley, C.L., Payne, C.M., Bernstein, H., Bernstein, C. and Roe, D. (2000). The NAD+ precursors, nicotinic acid and nicotinamide protect cells against apoptosis induced by a multiple stress inducer, deoxycholate. Cell Death Differ 7, 314-26.

(120) Herceg, Z. and Wang, Z.Q. (1999). Failure of poly(ADP-ribose) polymerase cleavage by caspases leads to induction of necrosis and enhanced apoptosis. Mol Cell Biol 19, 5124-33.

(121) Ha, H.C. and Snyder, S.H. (1999). Poly(ADP-ribose) polymerase is a mediator of necrotic cell death by ATP depletion. Proc Natl Acad Sci U S A 96, 13978-82.

(122) Filipovic, D.M., Meng, X. and Reeves, W.B. (1999). Inhibition of PARP prevents oxidant-induced necrosis but not apoptosis in LLC-PK1 cells. Am J Physiol 277, F428-36.

(123) Palomba, L., Sestili, P., Columbaro, M., Falcieri, E. and Cantoni, O. (1999). Apoptosis and necrosis following exposure of U937 cells to increasing concentrations of hydrogen peroxide: the effect of the poly(ADP-ribose)polymerase inhibitor 3-aminobenzamide. Biochem Pharmacol 58, 1743-50.

(124) Moroni, F. et al. (2001). Poly(ADP-ribose) polymerase inhibitors attenuate necrotic but not apoptotic neuronal death in experimental models of cerebral ischemia. Cell Death Differ 8, 921-32.

(125) Thiemermann, C., Bowes, J., Myint, F.P. and Vane, J.R. (1997). Inhibition of the activity of poly(ADP ribose) synthetase reduces ischemia-reperfusion injury in the heart and skeletal muscle. Proc Natl Acad Sci U S A 94, 679-83.

(126) Zingarelli, B., Salzman, A.L. and Szabo, C. (1998). Genetic disruption of poly (ADP-ribose) synthetase inhibits the expression of P-selectin and intercellular adhesion molecule-1 in myocardial ischemia/reperfusion injury. Circ Res 83, 85-94.

(127) Weinberg, J.M. (1991). The cell biology of ischemic renal injury. Kidney Int 39, 476-500.

(128) Ferdinandy, P. and Schulz, R. (2003). Nitric oxide, superoxide, and peroxynitrite in myocardial ischaemia-reperfusion injury and preconditioning. Br J Pharmacol 138, 532-43.

(129) Pacher, P., Schulz, R., Liaudet, L. and Szabo, C. (2005). Nitrosative stress and pharmacological modulation of heart failure. Trends Pharmacol Sci 26, 302-10.

(130) Pacher, P., Liaudet, L., Mabley, J.G., Cziraki, A., Hasko, G. and Szabo, C. (2006). Beneficial effects of a novel ultrapotent poly(ADP-ribose) polymerase inhibitor in murine models of heart failure. Int J Mol Med 17, 369-75.

(131) Sun, A.Y. and Cheng, J.S. (1998). Neuroprotective effects of poly (ADP-ribose) polymerase inhibitors in transient focal cerebral ischemia of rats. Zhongguo Yao Li Xue Bao 19, 104-8.

(132) Fiorillo, C. et al. (2003). Beneficial effects of poly (ADP-ribose) polymerase inhibition against the reperfusion injury in heart transplantation. Free Radic Res 37, 331-9.

(133) Bartha, E. et al. (2009). PARP inhibition delays transition of hypertensive cardiopathy to heart failure in spontaneously hypertensive rats. Cardiovasc Res 83, 501-10.

(134) Bartha, E. et al. (2008). Effect of L-2286, a poly(ADP-ribose)polymerase inhibitor and enalapril on myocardial remodeling and heart failure. J Cardiovasc Pharmacol 52, 253-61.

(135) Chen, M., Zsengeller, Z., Xiao, C.Y. and Szabo, C. (2004). Mitochondrial-to-nuclear translocation of apoptosis-inducing factor in cardiac myocytes during oxidant stress: potential role of poly(ADP-ribose) polymerase-1. Cardiovasc Res 63, 682-8.

(136) Kun, E., Zimber, P.H., Chang, A.C., Puschendorf, B. and Grunicke, H. (1975). Macromolecular enzymatic product of NAD+ in liver mitochondria. Proc Natl Acad Sci U S A 72, 1436-40.

(137) Richter, C., Winterhalter, K.H., Baumhuter, S., Lotscher, H.R. and Moser, B. (1983). ADP-ribosylation in inner membrane of rat liver mitochondria. Proc Natl Acad Sci U S A 80, 3188-92.

(138) Masmoudi, A. and Mandel, P. (1987). ADP-ribosyl transferase and NAD glycohydrolase activities in rat liver mitochondria. Biochemistry 26, 1965-9.

(139) Druzhyna, N., Smulson, M.E., LeDoux, S.P. and Wilson, G.L. (2000). Poly(ADP-ribose) polymerase facilitates the repair of N-methylpurines in mitochondrial DNA. Diabetes 49, 1849-55.

(140) Masmoudi, A., el-Fetouaki, J., Weltin, D., Belhadj, O. and Mandel, P. (1993). Association of mitochondrial ADP-ribosyl transferase activity with the DNA-protein complex. Biochem Mol Biol Int 29, 77-83.

(141) Andrabi, S.A. et al. (2006). Poly(ADP-ribose) (PAR) polymer is a death signal. Proc Natl Acad Sci U S A 103, 18308-13.

(142) Lai, Y. et al. (2008). Identification of poly-ADP-ribosylated mitochondrial proteins after traumatic brain injury. J Neurochem 104, 1700-11.

(143) Poitras, M.F., Koh, D.W., Yu, S.W., Andrabi, S.A., Mandir, A.S., Poirier, G.G., Dawson, V.L. and Dawson, T.M. (2007). Spatial and functional relationship between poly(ADP-ribose) polymerase-1 and poly(ADP-ribose) glycohydrolase in the brain. Neuroscience 148, 198-211.

(144) Scovassi, A.I. (2004). Mitochondrial poly(ADP-ribosylation): from old data to new perspectives. Faseb J 18, 1487-8.

(145) Tretter, L. and Adam-Vizi, V. (2000). Inhibition of Krebs cycle enzymes by hydrogen peroxide: A key role of [alpha]-ketoglutarate dehydrogenase in limiting NADH production under oxidative stress. J Neurosci 20, 8972-9.

(146) Straub, F.B. (1939). Isolation and properties of a flavoprotein from heart muscle tissue. Biochem J 33, 787-92.

(147) Perham, R.N. (2000). Swinging arms and swinging domains in multifunctional enzymes: catalytic machines for multistep reactions. Annu Rev Biochem 69, 961-1004.

(148) Argyrou, A., Sun, G., Palfey, B.A. and Blanchard, J.S. (2003). Catalysis of diaphorase reactions by Mycobacterium tuberculosis lipoamide dehydrogenase occurs at the EH4 level. Biochemistry 42, 2218-28.

(149) Youn, H. and Kang, S.O. (2000). Enhanced sensitivity of Streptomyces seoulensis to menadione by superfluous lipoamide dehydrogenase. FEBS Lett 472, 57-61.

(150) Tretter, L. and Adam-Vizi, V. (2005). Alpha-ketoglutarate dehydrogenase: a target and generator of oxidative stress. Philos Trans R Soc Lond B Biol Sci 360, 2335-45.

(151) Igamberdiev, A.U., Bykova, N.V., Ens, W. and Hill, R.D. (2004). Dihydrolipoamide dehydrogenase from porcine heart catalyzes NADH-dependent scavenging of nitric oxide. FEBS Lett 568, 146-50.

(152) Bryk, R., Lima, C.D., Erdjument-Bromage, H., Tempst, P. and Nathan, C. (2002). Metabolic enzymes of mycobacteria linked to antioxidant defense by a thioredoxin-like protein. Science 295, 1073-7.

(153) Chen, L., Xie, Q.W. and Nathan, C. (1998). Alkyl hydroperoxide reductase subunit C (AhpC) protects bacterial and human cells against reactive nitrogen intermediates. Mol Cell 1, 795-805.

(154) Matsuyama, S., Llopis, J., Deveraux, Q.L., Tsien, R.Y. and Reed, J.C. (2000). Changes in intramitochondrial and cytosolic pH: early events that modulate caspase activation during apoptosis. Nat Cell Biol 2, 318-25.

(155) Klyachko, N.L., Shchedrina, V.A., Efimov, A.V., Kazakov, S.V., Gazaryan, I.G., Kristal, B.S. and Brown, A.M. (2005). pH-dependent substrate preference of pig heart lipoamide dehydrogenase varies with oligomeric state: response to mitochondrial matrix acidification. J Biol Chem 280, 16106-14.

(156) Opii, W.O. et al. (2007). Proteomic identification of oxidized mitochondrial proteins following experimental traumatic brain injury. J Neurotrauma 24, 772-89.

(157) Tretter, L. and Adam-Vizi, V. (2004). Generation of reactive oxygen species in the reaction catalyzed by alpha-ketoglutarate dehydrogenase. J Neurosci 24, 7771-8.

(158) Koh, J.Y., Suh, S.W., Gwag, B.J., He, Y.Y., Hsu, C.Y. and Choi, D.W. (1996). The role of zinc in selective neuronal death after transient global cerebral ischemia. Science 272, 1013-6.

(159) Choi, D.W. and Koh, J.Y. (1998). Zinc and brain injury. Annu Rev Neurosci 21, 347-75.

(160) Gazaryan, I.G., Krasnikov, B.F., Ashby, G.A., Thorneley, R.N., Kristal, B.S. and Brown, A.M. (2002). Zinc is a potent inhibitor of thiol oxidoreductase activity and stimulates reactive oxygen species production by lipoamide dehydrogenase. J Biol Chem 277, 10064-72.

(161) Humphries, K.M., Yoo, Y. and Szweda, L.I. (1998). Inhibition of NADH-linked mitochondrial respiration by 4-hydroxy-2-nonenal. Biochemistry 37, 552-7.

(162) Casley, C.S., Canevari, L., Land, J.M., Clark, J.B. and Sharpe, M.A. (2002). Beta-amyloid inhibits integrated mitochondrial respiration and key enzyme activities. J Neurochem 80, 91-100.

(163) Andersson, U., Leighton, B., Young, M.E., Blomstrand, E. and Newsholme, E.A. (1998). Inactivation of aconitase and oxoglutarate dehydrogenase in skeletal muscle in vitro by superoxide anions and/or nitric oxide. Biochem Biophys Res Commun 249, 512-6.

(164) Park, L.C., Zhang, H., Sheu, K.F., Calingasan, N.Y., Kristal, B.S., Lindsay, J.G. and Gibson, G.E. (1999). Metabolic impairment induces oxidative stress, compromises inflammatory responses, and inactivates a key mitochondrial enzyme in microglia. J Neurochem 72, 1948-58.

(165) Szabo, C. and Dawson, V.L. (1998). Role of poly(ADP-ribose) synthetase in inflammation and ischaemia-reperfusion. Trends Pharmacol Sci 19, 287-98.

(166) Ying, W., Chen, Y., Alano, C.C. and Swanson, R.A. (2002). Tricarboxylic acid cycle substrates prevent PARP-mediated death of neurons and astrocytes. J Cereb Blood Flow Metab 22, 774-9.

(167) Sardao, V.A., Oliveira, P.J., Holy, J., Oliveira, C.R. and Wallace, K.B. (2007). Vital imaging of H9c2 myoblasts exposed to tert-butylhydroperoxide--characterization of morphological features of cell death. BMC Cell Biol 8, 11.

(168) Desjardins, P., Frost, E. and Morais, R. (1985). Ethidium bromide-induced loss of mitochondrial DNA from primary chicken embryo fibroblasts. Mol Cell Biol 5, 1163-9.

(169) Kozlov, A.V., Staniek, K. and Nohl, H. (1999). Nitrite reductase activity is a novel function of mammalian mitochondria. FEBS Lett 454, 127-30.

(170) Romero, J.M. and Bizzozero, O.A. (2006). Extracellular S-nitrosoglutathione, but not S-nitrosocysteine or N(2)O(3), mediates protein S-nitrosation in rat spinal cord slices. J Neurochem 99, 1299-310.

(171) Casadei, M., Persichini, T., Polticelli, F., Musci, G. and Colasanti, M. (2008). S-glutathionylation of metallothioneins by nitrosative/oxidative stress. Exp Gerontol 43, 415-22.

(172) Mitra, K. and Shivaji, S. (2004). Novel tyrosine-phosphorylated post-pyruvate metabolic enzyme, dihydrolipoamide dehydrogenase, involved in capacitation of hamster spermatozoa. Biol Reprod 70, 887-99.

(173) Witze, E.S., Old, W.M., Resing, K.A. and Ahn, N.G. (2007). Mapping protein post-translational modifications with mass spectrometry. Nat Methods 4, 798-806.

(174) Lacza, Z., Snipes, J.A., Miller, A.W., Szabo, C., Grover, G. and Busija, D.W. (2003). Heart mitochondria contain functional ATP-dependent K+ channels. J Mol Cell Cardiol 35, 1339-47.

(175) Broillet, M., Randin, O. and Chatton, J. (2001). Photoactivation and calcium sensitivity of the fluorescent NO indicator 4,5-diaminofluorescein (DAF-2): implications for cellular NO imaging. FEBS Lett 491, 227-32.

(176) Pacher, P. et al. (2003). Potent metalloporphyrin peroxynitrite decomposition catalyst protects against the development of doxorubicin-induced cardiac dysfunction. Circulation 107, 896-904.

(177) Kozlov, A.V., Szalay, L., Umar, F., Kropik, K., Staniek, K., Niedermuller, H., Bahrami, S. and Nohl, H. (2005). Skeletal muscles, heart, and lung are the main sources of oxygen radicals in old rats. Biochim Biophys Acta 1740, 382-9.

(178) Gurke, S., Barroso, J.F., Hodneland, E., Bukoreshtliev, N.V., Schlicker, O. and Gerdes, H.H. (2008). Tunneling nanotube (TNT)-like structures facilitate a constitutive, actomyosin-dependent exchange of endocytic organelles between normal rat kidney cells. Exp Cell Res 314, 3669-83.

(179) Kumar, V., Kota, V. and Shivaji, S. (2008). Hamster sperm capacitation: role of pyruvate dehydrogenase A and dihydrolipoamide dehydrogenase. Biol Reprod 79, 190-9.

(180) Laflamme, M.A. and Murry, C.E. (2005). Regenerating the heart. Nat Biotechnol 23, 845-56.

(181) Singla, D.K. (2009). Embryonic stem cells in cardiac repair and regeneration. Antioxid Redox Signal 11, 1857-63.

(182) Abdel-Latif, A. et al. (2007). Adult bone marrow-derived cells for cardiac repair: a systematic review and meta-analysis. Arch Intern Med 167, 989-97.

(183) Badorff, C. et al. (2003). Transdifferentiation of blood-derived human adult endothelial progenitor cells into functionally active cardiomyocytes. Circulation 107, 1024-32.

(184) Matsuura, K. et al. (2004). Cardiomyocytes fuse with surrounding noncardiomyocytes and reenter the cell cycle. J Cell Biol 167, 351-63.

(185) Ishikawa, F. et al. (2006). Purified human hematopoietic stem cells contribute to the generation of cardiomyocytes through cell fusion. Faseb J 20, 950-2.

(186) Pontes, B., Viana, N.B., Campanati, L., Farina, M., Neto, V.M. and Nussenzveig, H.M. (2008). Structure and elastic properties of tunneling nanotubes. Eur Biophys J 37, 121-9.

(187) Wenzel, P. et al. (2007). Role of reduced lipoic acid in the redox regulation of mitochondrial aldehyde dehydrogenase (ALDH-2) activity. Implications for mitochondrial oxidative stress and nitrate tolerance. J Biol Chem 282, 792-9.

(188) Comelli, M., Di Pancrazio, F. and Mavelli, I. (2003). Apoptosis is induced by decline of mitochondrial ATP synthesis in erythroleukemia cells. Free Radic Biol Med 34, 1190-9.

(189) Wright, G., Terada, K., Yano, M., Sergeev, I. and Mori, M. (2001). Oxidative stress inhibits the mitochondrial import of preproteins and leads to their degradation. Exp Cell Res 263, 107-17.

(190) Lacza, Z. et al. (2006). Mitochondria produce reactive nitrogen species via an arginine-independent pathway. Free Radic Res 40, 369-78.

(191) Gao, S. et al. (2004). Docking of endothelial nitric oxide synthase (eNOS) to the mitochondrial outer membrane: a pentabasic amino acid sequence in the autoinhibitory domain of eNOS targets a proteinase K-cleavable peptide on the cytoplasmic face of mitochondria. J Biol Chem 279, 15968-74.

(192) Lopez, M.F., Kristal, B.S., Chernokalskaya, E., Lazarev, A., Shestopalov, A.I., Bogdanova, A. and Robinson, M. (2000). High-throughput profiling of the mitochondrial proteome using affinity fractionation and automation. Electrophoresis 21, 3427-40.

9. PUBLICATION LIST

9.1. Publications related to the present thesis

Cselenyak A, **Pankotai E**, Horvath EM, Kiss L, Lacza Z. Mesenchymal stem cells rescue cardiomyoblasts from cell death in an in vitro ischemia model via direct cell-to-cell connections. BMC Cell Biol. 2010 Apr 20;11(1):29.

IF:3,16

Pankotai E, Lacza Z, Murányi M, Szabó C. Intra-mitochondrial poly(ADP-ribosyl)ation: potential role for alpha-ketoglutarate dehydrogenase. Mitochondrion. 2009 Apr;9(2):159-64.

IF:4,262

Csordás A, **Pankotai E**, Snipes JA, Cselenyák A, Sárszegi Z, Cziráki A, Gaszner B, Papp L, Benko R, Kiss L, Kovács E, Kollai M, Szabó C, Busija DW, Lacza Z. Human heart mitochondria do not produce physiologically relevant quantities of nitric oxide. Life Sci. 2007 Jan 23;80(7):633-7.

IF: 2,389

Lacza Z, Kozlov AV, **Pankotai E**, Csordás A, Wolf G, Redl H, Kollai M, Szabó C, Busija DW, Horn TF. Mitochondria produce reactive nitrogen species via an arginine-independent pathway. Free Radic Res. 2006 Apr;40(4):369-78

IF: 5,44

Lacza Z, **Pankotai E**, Busija DW. Mitochondrial nitric oxide synthase: current concepts and controversies. Front Biosci. 2009 Jan 1;14:4436-43. Review. PubMed PMID: 19273361.

IF: 3,308

9.2. Publications not related to the present thesis

Cao T, Racz P, Szauter KM, Groma G, Nakamatsu GY, Fogelgren B, **Pankotai E**, He QP, Csiszar K. Mutation in Mpzl3, a novel gene encoding a predicted adhesion protein, in the rough coat (rc) mice with severe skin and hair abnormalities. J Invest Dermatol. 2007 Jun;127(6):1375-86.

IF: 4,829

Seabra AB, **Pankotai E**, Fehér M, Somlai A, Kiss L, Bíró L, Szabó C, Kollai M, de Oliveira MG, Lacza Z. S-nitrosoglutathione-containing hydrogel increases dermal blood flow in streptozotocin-induced diabetic rats. Br J Dermatol. 2007 May;156(5):814-8.

IF: 3,503

Tóth-Zsámboki E, Horváth E, Vargova K, **Pankotai E**, Murthy K, Zsengellér Z, Bárány T, Pék T, Fekete K, Kiss RG, Préda I, Lacza Z, Gerö D, Szabó C. Activation of poly(ADP-ribose) polymerase by myocardial ischemia and coronary reperfusion in human circulating leukocytes. Mol Med. 2006 Sep-Oct;12(9-10):221-8.

IF: 2,708

Lacza Z, Horváth EM, **Pankotai E**, Csordás A, Kollai M, Szabó C, Busija DW. The novel red-fluorescent probe DAR-4M measures reactive nitrogen species rather than NO. J Pharmacol Toxicol Methods. 2005 Nov Dec;52(3):335-40.

Lacza Z, **Pankotai E**, Csordás A, Gero D, Kiss L, Horváth EM, Kollai M, Busija DW, Szabó C. Mitochondrial NO and reactive nitrogen species production: does mtNOS exist? Nitric Oxide. 2006 Mar;14(2):162-8.

IF: 2,509

Horváth S, Prandovszky E, **Pankotai E**, Kis Z, Farkas T, Boldogköi Z, Boda K, Janka Z, Toldi J. Use of a recombinant pseudorabies virus to analyze motor cortical reorganization after unilateral facial denervation. Cereb Cortex. 2005 Apr;15(4):378-84.

IF: 6,187

10. ACKNOWLEDGEMENTS

I would like to express my sincere gratitude to Dr. Zsombor Lacza, my supervisor, for his scientific guidance, for his driving ideas and questions throughout the years I spent in his laboratory. I also thank Professor Márk Kollai for providing me the opportunity to work at the Institute of Human Physiology and Clinical Experimental Research, where I always received friendly and supporting advice from all the members of the Institute. I am thankful to Professor Csaba Szabó for giving me the chance to work at the University of Medicine and Dentistry of New Jersey. I also would like to thank to all contributors, co-authors, my collegues in the laboratory and my friends for their help throughout my studies. Finally, I thank my parents and my sister, for their love, encouragement and support.

11. APPENDIX (Paper I-V)